


6-1-1975

Movement of Pesticides in the Soil Water Fertilizer System

H. Don Scott

University of Arkansas, Fayetteville

Follow this and additional works at: <https://scholarworks.uark.edu/awrcctr>

 Part of the [Fresh Water Studies Commons](#), and the [Water Resource Management Commons](#)

Recommended Citation

Scott, H. Don. 1975. Movement of Pesticides in the Soil Water Fertilizer System. Arkansas Water Resources Center, Fayetteville, AR. PUB035. 112

This Technical Report is brought to you for free and open access by the Arkansas Water Resources Center at ScholarWorks@UARK. It has been accepted for inclusion in Technical Reports by an authorized administrator of ScholarWorks@UARK. For more information, please contact scholar@uark.edu, ccmiddle@uark.edu.

PUB 35

WATER RESOURCES RESEARCH CENTER

• 113 Ozark Hall



UNIVERSITY OF ARKANSAS • Fayetteville, Arkansas 72701

MOVEMENT OF PESTICIDES IN THE SOIL WATER
FERTILIZER SYSTEM

by

H. Don Scott

UNIVERSITY OF ARKANSAS

#35

**MOVEMENT OF PESTICIDES IN THE SOIL WATER
FERTILIZER SYSTEM**

by

H. Don Scott



WATER RESOURCES RESEARCH CENTER

Publication No. 35

**In Cooperation With the
AGRICULTURAL EXPERIMENT STATION
UNIVERSITY OF ARKANSAS
Fayetteville**

1975

PROJECT COMPLETION REPORT

PROJECT NO: A-021-ARK

AGREEMENT NO: 14-31-0001-3804

STARTING DATE: JULY 1972

COMPLETION DATE: JUNE, 1975

MOVEMENT OF PESTICIDES IN THE SOIL WATER
FERTILIZER SYSTEM

By

H. Don Scott

WATER RESOURCES RESEARCH CENTER

UNIVERSITY OF ARKANSAS

Fayetteville, Arkansas

July, 1975

ABSTRACT

A theoretical and experimental study of the transport of pesticides was conducted in several Arkansas soils with metribuzin, a herbicide. In a field study, chloride and metribuzin were applied to a Captina silt loam under maximum leaching conditions and their redistribution was compared with that of soil water. Metribuzin was found in significantly detectable quantities to a depth of 61 cm; the largest concentrations were detected in the surface 23 cm and particularly in the 0-5 cm increment. Two days after application 72.6 and 33.6% could be detected in the vegetation and no-vegetation plots. The metribuzin half life was 7.88 and 5.13 days in the no-vegetation and vegetation plots, respectively. Chloride was found throughout the profile. Metribuzin and chloride generally were observed to move in the same direction as soil water, but at a considerably slower rate. Persistence of metribuzin within the soil was influenced greatly by microbial degradation.

The laboratory studies centered on further quantifying the transport and adsorption-desorption parameters of metribuzin under controlled environmental conditions. Diffusion coefficients of ^{14}C -metribuzin, ^{36}Cl , and ^3HOH were shown to be influenced by soil type, soil water content, and soil temperature. The magnitude of the diffusivities were in the order $^3\text{HOH} > ^{36}\text{Cl} > ^{14}\text{C}$ -metribuzin; however, the ratios varied. The rates of adsorption of metribuzin were found to be dependent on shaking time and soil type. For the most part linear adsorption isotherms were observed. Desorption rates were found to be influenced by solution concentration, shaking time and soil type.

It was concluded from these studies that the potential polluting effects of metribuzin leaching through the soil and subsequently moving into the water table or underground streams are minimal. Metribuzin will redistribute within the soil profile, but will be degraded by microorganisms before it becomes a potential pollution hazard.

ACKNOWLEDGEMENTS

The research performed during this contract period was supported in part with funds provided by the Office of Water Resources Research, U. S. Department of the Interior, under Grant No. A-021-ARK, as authorized under the Water Resources Research Act of 1964, P. L. 88-379, as amended by P.L. 89-404 and P.L. 92-175.

The research program was performed under the direction of H. D. Scott, Assistant Professor, Department of Agronomy, and was conducted by R. F. Paetzold, Graduate Research Assistant, Department of Agronomy. The assistance of Ms. Nora Harrison and Ms. Cindy Benton is also acknowledged.

TABLE OF CONTENTS

TITLE PAGE	i
ABSTRACT	iii
ACKNOWLEDGEMENTS	v
TABLE OF CONTENTS	vi
LIST OF FIGURES	vii
LIST OF TABLES	x
INTRODUCTION	1
LITERATURE REVIEW	3
Diffusion of Pesticides	4
Mass Flow of Pesticides	6
Adsorption-Desorption of Pesticides	13
METHODS AND MATERIALS	16
Field Transport Study	16
Laboratory Transport Characterization	23
RESULTS AND DISCUSSION	27
Field Study	27
<u>In Situ</u> Hydraulic Conductivity	27
Solute Transport	37
Comparison of Water and Solute Fluxes	55
Laboratory Study	62
Adsorption of Metribuzin	62
Self-Diffusion of ^3HOH , ^{36}Cl , and ^{14}C -metribuzin	75
Dispersion	87
APPENDIX TABLE 1	97
APPENDIX TABLE 2	98
LITERATURE CITED	99

LIST OF FIGURES

- FIGURE 1. Bulk density and clay percentages of Captina soil at study site.
- FIGURE 2. Water retention curves for Ap and B2t horizons of Captina soil at study site.
- FIGURE 3. Soil water content distributions in Captina soil at study site.
- FIGURE 4. Drainage rate of soil water from Captina profile.
- FIGURE 5. Soil water tension distribution in Captina soil at study site.
- FIGURE 6. Hydraulic conductivity as a function of soil water content at 15 cm intervals of Captina soil (in situ data).
- FIGURE 7. Hydraulic conductivity as a function of soil water content of the horizons in Captina soil (in situ data).
- FIGURE 8. Hydraulic conductivity as a function of soil water content of the Ap and B2t horizons of Captina soil (predicted data).
- FIGURE 9. Soil water tensions of Captina soil profile in solute transport plots during the monitoring period.
- FIGURE 10. Soil water contents of Captina soil profile in solute transport plots during the monitoring period.
- FIGURE 11. Relation between the logarithm of metribuzin concentration and time for vegetation and non-vegetation plots.
- FIGURE 12. Fluxes of water and Cl^- across 15 cm depth in solute transport plot.
- FIGURE 13. Fluxes of water and Cl^- across 45 cm depth in solute transport plot.
- FIGURE 14. Fluxes of water and Cl^- across 122 cm depth in solute transport plot.
- FIGURE 15. Adsorption of ^{14}C -metribuzin by Ap horizon of the Dubbs soil.
- FIGURE 16. Adsorption-desorption of ^{14}C -metribuzin by Ap horizon of Captina soil.
- FIGURE 17. Adsorption-desorption of ^{14}C -metribuzin by B2t horizon of Captina soil.

LIST OF FIGURES
(Continued)

- FIGURE 18. Freundlich plot of adsorption-desorption of ^{14}C -metribuzin by Ap horizon of Captina soil.
- FIGURE 19. Freundlich plot of adsorption-desorption of ^{14}C -metribuzin by B2t horizon of Captina soil.
- FIGURE 20. Freundlich model of adsorption-desorption of ^{14}C -metribuzin by Ap horizon of Captina soil.
- FIGURE 21. Freundlich model of adsorption-desorption of ^{14}C -metribuzin by B2t horizon of Captina soil.
- FIGURE 22. First order adsorption plot of adsorption of ^{14}C -metribuzin by Ap horizon of Captina soil.
- FIGURE 23. Relation between distribution coefficient (K_d) and the logarithm of shaking time.
- FIGURE 24. Relation between amount of metribuzin adsorbed and the $t^{1/2}$ for Captina silt loam.
- FIGURE 25. Relation between adsorption of metribuzin and shaking time for the Dubbs soil.
- FIGURE 26. Relation between amount of metribuzin adsorbed and number of extractions for Captina Ap.
- FIGURE 27. Relation between amount of metribuzin adsorbed and number of extractions for Captina B2t.
- FIGURE 28. Relation between self-diffusion of ^3HOH and soil water contents of selected soils.
- FIGURE 29. Relation between self-diffusion coefficients of ^3HOH , ^{36}Cl , and ^{14}C -metribuzin and soil water content of the Ap horizon of Captina soil.
- FIGURE 30. Relation between self-diffusion coefficient of ^3HOH , ^{36}Cl , and ^{14}C -metribuzin and soil water content of B2t horizon of Captina soil.
- FIGURE 31. Relation between self-diffusion coefficient of ^3HOH , ^{36}Cl , and ^{14}C -metribuzin and soil water content of Ap horizon of Dubbs soil.
- FIGURE 32. Arrhenius plot of diffusivity versus $1/T$.
- FIGURE 33. Activation energy values of radioactive isotopes as a function of soil water content.

LIST OF FIGURES
(Continued)

- FIGURE 34. Dispersion break-through curve for metribuzin and water in Captina Ap. Moisture contents of half cells equal 20 and 25 percent. Two hour diffusion time.
- FIGURE 35. Dispersion break-through curve for metribuzin and water in Dubbs Ap. Moisture contents of half cells equal 15 and 20 percent. One and one half hour diffusion time.
- FIGURE 36. Dispersion break-through curve for metribuzin and water in Dubbs Ap. Moisture contents of half cells equal 15 and 20 percent. Metribuzin added to low moisture side. Two and one half hour diffusion time.

LIST OF TABLES

- TABLE 1. On-site morphological description of Captina soil.
- TABLE 2. Particle size distribution of Captina soil at study site.
- TABLE 3. Chemical properties of Captina soil at study site.
- TABLE 4. Depth of water (cm) in surface 107 cm of soil in solute transport plots.
- TABLE 5. Changes in moisture, rainfall, and total moisture lost from soil profile during several measurement periods.
- TABLE 6. Chloride concentration (ppm) as a function of soil depth during the field experiment.
- TABLE 7. Chloride concentration ($\mu\text{g Cl/cm}^3$ soil) as a function of soil depth during the field experiment.
- TABLE 8. Chloride concentration ($\mu\text{g Cl/cm}^2$ soil) as a function of soil depth during the field experiment.
- TABLE 9. Amount and percentage recovery of chloride in the solute transport plot.
- TABLE 10. Metribuzin concentration (ppm) as a function of soil depth during the field experiment.
- TABLE 11. Metribuzin concentration ($\mu\text{g/cm}^3$) as a function of soil depth during the field experiment.
- TABLE 12. Metribuzin concentration ($\mu\text{g/cm}^2$) as a function of soil depth during the field experiment.
- TABLE 13. Amount and percentage recovery of metribuzin in the solute transport plot.
- TABLE 14. Freundlich adsorption and desorption constants for metribuzin on a Captina silt loam.
- TABLE 15. Physical and chemical properties of Ap horizon of three soils used in the laboratory studies.
- TABLE 16. Thermodynamic constants for self-diffusion in Captina silt loam.
- APPENDIX TABLE 1. Water retention data for three depths of Captina soil.
- APPENDIX TABLE 2. Self-diffusion of ^3HOH in selected soils.

INTRODUCTION

The preservation of a high quality environment requires, among other things, an ability to predict the fate of pesticides in soil and water systems. The fate of any pesticide in these systems depends upon certain biological, chemical, and physical processes which govern the concentration of "active" pesticide. Mechanisms that reduce the "active" concentration of a pesticide in the soil environment include leaching, microbial degradation, adsorption-desorption, volatilization, photodecomposition, and plant uptake. All of these processes are influenced by water and soil in one way or another, and, because portions of all pesticidal sprays reach the soil, the fate of these chemicals in the soil and water systems has received considerable research attention. In addition the degree to which these processes affect the fate of a pesticide is influenced by the transport rates within the environment and the properties of the soil-water system. This report is concerned primarily with those physical-chemical mechanisms affecting the transport of pesticides in selected Arkansas soils.

Solutes such as pesticides move in soil primarily as a result of two physical processes, molecular diffusion and mass flow with the soil water. Often one process will dominate the other; over short distances, as in the transport of molecules to plant surfaces, molecular diffusion is commonly the dominant process. Under static water flow conditions diffusion would be the only transport process operating. Under conditions of rapid water movement, such as immediately after large amounts of rainfall and irrigation, mass flow is the dominant process. Solutes

moving with the water, however, do not always move at the same rate as the water. The rate of solute movement depends on many factors including the velocity of soil water flow, soil moisture content, and the degree of interaction, if any, of the solute with soil surfaces. Thus, in order to characterize and predict the fate of pesticides in the environment, one must have some knowledge of soil water transfer rates, pesticide interaction rates with soil surfaces, and microbial degradation rates.

The objectives of this project were (1) to evaluate the effects of water and soluble salts on the transport of pesticides in soil, (2) to determine the importance of diffusion and mass flow as transport mechanisms in soil to certain agronomic crops important to Arkansas, (3) to determine the importance of degradation of the pesticide and its influence on the transport, persistence, and absorption by plants, and (4) to predict the potential effects of the results found under objectives 1-3 on the quality of water that may be used as domestic, recreational and agricultural water supplies. The study was conducted under both field and laboratory conditions.

LITERATURE REVIEW

The general one dimensional transport equation for pesticides in soil can be written as

$$\frac{\partial C}{\partial t} = D \frac{\partial^2 C}{\partial x^2} - v \frac{\partial C}{\partial x} - \frac{\rho}{\theta} \frac{\partial S}{\partial t} - \alpha C \quad [1]$$

where C is the solute concentration ($\mu\text{g}/\text{cm}^3$), t is the time (sec), D is the solute dispersion coefficient (cm^2/sec), v is the average pore water flow velocity (cm/sec), x is the spatial coordinate (cm), ρ is the soil bulk density (g/cm^3), θ is the volumetric soil water content (cm^3/cm^3), S is the concentration of adsorbed solute ($\mu\text{g}/\text{g}$), and α is the degradation coefficient (sec^{-1}). The value of D includes both molecular diffusion and dispersion processes and varies with the flow velocity of water. Values of v can be obtained from Darcy's law for steady state soil water flow and require a knowledge of the magnitude of the hydraulic conductivity and potential gradient. Parts of equation [1] have been solved analytically for several boundary and initial conditions (Bresler, 1973; van Genuchten and Wierenga, 1974; Warrick et al., 1971); however, numerical techniques are needed to solve the complete equation. Leistra (1973) and Boast (1973) have published excellent review articles on modeling soil water-solute movement and have illustrated many of the parameters needed to solve equations similar to [1].

A knowledge of the magnitude of the parameters required for the solution of equation [1] would provide the information needed to meet the objectives of this project. These parameters include self-diffusion

coefficients of the solutes, the hydraulic conductivity of the soil, and the interaction of the solute with soil surfaces (adsorption-desorption relations). The factors affecting each of these parameters are discussed in detail.

Diffusion of Pesticides

Transport of pesticides by diffusion is an important mechanism by which these chemicals redistribute in soil and water. Molecular diffusion of pesticides is the process of dissipation of any inequality of concentration or activity by the random thermal movement of molecules or ions. Movement by diffusion is a slow process in comparison with transport by mass flow, but over short distances may become very important. The mathematics describing diffusion processes is well advanced (Carslaw and Jaeger, 1959; Crank, 1956), and most pesticide diffusion problems have been solved by use of classical diffusion theory. The modern theoretical treatment of diffusion processes is credited to Fick (1855), who recognized an analogy with the conduction of heat in solids. Under steady-state conditions Fick's first law can be stated as

$$J = - D \frac{dC}{dx} \quad [2]$$

where J is the pesticide flux ($\mu\text{g}/\text{cm}^2\text{sec}$), D is the diffusion coefficient (cm^2/sec), C is the pesticide concentration ($\mu\text{g}/\text{cm}^3$), and x is the spatial coordinate (cm). The negative sign in equation [2] indicates that diffusion of pesticides occurs in the direction of decreasing concentrations and is proportional to the concentration gradient.

The diffusion coefficient of a pesticide in soil is a measure of the various physical and chemical factors that affect the transport rate.

Olsen and Kemper (1968) showed that for ions or molecules restricted to the solution phase, the porous diffusion coefficient, D_p , can be related to the diffusion coefficient in aqueous solution D_o , by

$$D_p = D_o(L/Le)^2\theta\alpha\gamma \quad [3]$$

where $(L/Le)^2$ is the ratio of diffusion pathlength in soil to that in aqueous solution, α is the ratio of the mobility of the soil water where the pesticide is diffusing to that of pure water, θ is the volumetric soil water content, and γ is the electrical interaction of the ion or molecule. The quantities $(L/Le)^2$, θ , α , and γ can take on values between 0 and 1 and collectively are known as the transmission factor.

In porous materials such as soils, pesticides interact with soil surfaces. As a result, diffusion of pesticides can occur in the adsorbed, liquid, and vapor phases. Thus, the total flux through the soil would be the sum of the fluxes in each phase. The concentration and mobility of the pesticide in each of these soil phases will vary depending on the relative partitioning between these phases and the interaction between the physical and chemical properties of the pesticide and the soil. As shown by Scott et al. (1974), the apparent diffusion coefficient, D_e , of a pesticide in soil will depend on the sum of the rates of diffusion in each soil phase. Assuming that diffusion occurs only in the solution and vapor phases and a linear adsorption isotherm, D_e can be defined as

$$D_e = \frac{D_p}{(\theta + kd\rho_b)} = \frac{D_p}{B\theta} \quad [4]$$

where kd is the slope of the adsorption isotherm, ρ_b is the soil bulk

density, and B is the capacity factor or retardation factor. B can be further defined as

$$B = 1 + R \quad [5]$$

where R equals $k_d \rho_b$ divided by the water content, θ . The value of D_p is a measure of the ease with which pesticides diffuse through the pores of the medium.

For transient-state conditions the conservation equation

$$\frac{\partial C}{\partial t} = -\frac{\partial J}{\partial x} \quad [6]$$

is combined with equation [2] to give

$$\frac{\partial C}{\partial t} = \frac{\partial}{\partial x} \left[D_e \frac{\partial C}{\partial x} \right] \quad [7]$$

which is known as Fick's second law. If the pesticide diffusion coefficient is shown to be independent of concentration, equation [7] simplifies to

$$\frac{\partial C}{\partial t} = D_e \frac{\partial^2 C}{\partial x^2} \quad [8]$$

which can be solved analytically for several initial and boundary conditions. The diffusion of herbicides in soils was reviewed by Scott (1975).

Mass Flow of Pesticides

If water is flowing in a soil treated with a pesticide, then the pesticide is carried with and in the same direction as the water. The

flux of pesticide, J_p , due to the convective flow of water can be predicted from

$$J_p = J_w C \quad [9]$$

where J_w is the flow velocity of water (cm/sec) and C is the concentration of pesticide in the soil solution ($\mu\text{g}/\text{cm}^3$). Thus, information on the movement of water and the concentration in the soil-water system is required to describe the mass transport of a pesticide.

Mass transport by water flowing through a soil profile is dependent on the direction and rate of water flow and the sorption characteristics of the pesticide with soil. Soil water moves in response to various potentials including gravitational, thermal, and matric. Its transport in soils is generally divided into two classes, saturated and unsaturated flow. Saturated flow, however, is only a special case of unsaturated flow and occurs when the moisture content reaches its maximum value. The equation describing water flow through soil is known as Darcy's law and is expressed as

$$J_w = -k \nabla \phi \quad [10]$$

where J_w is the volume of water crossing per unit area perpendicular to the flow per unit time ($\text{cm}^3/\text{cm}^2\text{sec}$), k is the proportionality constant known as the hydraulic conductivity (cm/sec), and $\nabla \phi$ represents the driving force which is the hydraulic head gradient (cm/cm). Even though Darcy's law has been shown to have limitations under unsaturated flow conditions, in most instances the assumption of the validity of Darcy's law can be justified (Kirkham and Powers, 1972). The relationship between J , the flow velocity with respect to the total soil medium,

and V_o , the average pore flow velocity in equation [1] is given by

$$V_o = Jw/\theta \quad 0 < \theta < 1 \quad [11]$$

where θ is the water-filled porosity. Because θ is always less than one, the average pore velocity is always greater than the flux.

Equation [10] is valid for steady state conditions. However, transient state conditions predominate in the field. These can be described by combining Darcy's law [10] with the equation of continuity

$$\frac{\partial(\rho\theta)}{\partial t} = -\rho(V \cdot J) \quad [12]$$

where ρ is the density of the soil solution (g/cm^3), θ is the volumetric soil water content (cm^3/cm^3), t is the time (sec), and J is the flux (cm/sec). Assuming a constant fluid density and that the hydraulic potential, ϕ , is composed of a matrix potential, h , and a gravitational potential, z , equations [10] and [12] can be combined for one dimensional vertical flow as

$$\frac{\partial\theta}{\partial t} = \frac{\partial}{\partial z} \left[k \frac{\partial(h+z)}{\partial z} \right] \quad [13]$$

For horizontal flow [13] reduces to

$$\frac{\partial\theta}{\partial t} = \frac{\partial}{\partial x} \left[k \frac{\partial h}{\partial x} \right] \quad [14]$$

Because of the highly developed state of diffusion mathematics, it is sometimes desirable to replace k with a quantity defined as the soil water diffusivity, D .

$$D = k \frac{dh}{d\theta} \quad [15]$$

where $d\theta/dh$ is known as the specific water capacity. Assuming h is a unique function of θ , i.e., no hysteresis, the chain rule gives

$$\frac{\partial h}{\partial z} = \frac{\partial h}{\partial \theta} \frac{\partial \theta}{\partial z} \quad [16]$$

Substituting [15] and [16] into [14], the one-dimensional horizontal flow equation becomes

$$\frac{\partial \theta}{\partial t} = \frac{\partial}{\partial x} \left[D \frac{\partial \theta}{\partial x} \right] \quad [17]$$

This equation has many useful applications, especially under laboratory experimental conditions.

Many methods have been devised for determining hydraulic conductivity. These methods can be divided into three general categories, field methods, laboratory methods, and calculation from soil properties such as pore size distribution. Klute (1972) gives a comprehensive review of many of these methods.

All field methods for determining unsaturated hydraulic conductivities require determinations of volumetric soil moisture content and hydraulic potential as functions of depth and time. Although several investigators (Nielsen et al., 1964; Ogata and Richards, 1957; Richards et al., 1956) had determined unsaturated hydraulic conductivities in situ, Rose et al. (1965) were the first to present the theory of this method. Using a water balance approach, they presented the theory in the form of equation [18] based on Darcy's law.

$$\langle k_z(\theta) \rangle = \int_{t_1}^{t_2} (P+I-E - \int_0^z \frac{\partial \theta}{\partial t} dz) dt / (\langle \frac{\partial h}{\partial z} \rangle + 1)_z (t_2 - t_1) \quad [18]$$

where $k_z(\theta)$ is the time averaged hydraulic conductivity at the depth z and average moisture content θ , and t_1 and t_2 are the times of measurement. P is the precipitation rate, I is the irrigation rate, and E is the evaporation rate. P , I and E can be assumed equal to zero if the soil surface is covered. The total potential gradient at depth, z , is given by the average matric potential gradient $\frac{\partial h}{\partial z}$, plus one for the gravitational potential ($\frac{\partial z}{\partial z} = 1$).

Field methods, using undisturbed soil in situ, should yield the most accurate values of hydraulic conductivity. However, there are major disadvantages to these methods. One disadvantage common to field methods is the limited range of moisture contents over which the conductivities can be calculated. If tensiometers are used to measure hydraulic potential, the range of conductivity values is limited by the useful range (< 1 atm) of the tensiometer (Nielsen et al., 1964). If potentials are inferred from a soil moisture characteristic curve, excessive time may be required to obtain conductivity values at low soil moisture contents; this is especially true for greater depths in the soil profile. Another disadvantage of field methods is the inherent spatial variability of soils (Nielsen et al., 1973; van Bavel et al., 1968). For certain applications, such as irrigation scheduling, it is desirable to have an average conductivity curve for an entire field, which might require determination at several locations throughout the field. Another disadvantage is the length of time required to perform the analyses.

Although many techniques have been suggested for laboratory measurement of unsaturated hydraulic conductivity, there is no generally accepted satisfactory method (Klute, 1965). The methods used can be

divided into two classes, steady-state and transient state. With the steady-state methods, flow of water is established through the soil sample, usually an undisturbed core, in which flux, matrix potential and water content are constant; with the transient state methods these parameters may vary. Because of the variability of the results, it is desirable to use a large number of samples. When a soil is continually leached, as required by the steady-state methods, the magnitude of the hydraulic conductivity generally varies with time.

Soil scientists have long recognized the disadvantages of the field and laboratory methods for determining hydraulic conductivity and have attempted to find easily or routinely determined soil properties from which hydraulic conductivities can be calculated. Early attempts used particle size and total porosity in a Kozeny type of equation

$$J = \frac{P_O - P_L}{L} \frac{D_p^2}{150\mu} \frac{\epsilon^3}{(1-\epsilon)^2} \quad [19]$$

where L is the length of the packed column, D_p is the mean particle diameter, ϵ is the void fraction, μ is the viscosity of the fluid and $P_O - P_L$ is the pressure differential including gravity. This equation may be recognized as another form of Darcy's law where $\frac{P_O - P_L}{L}$ is the driving force and the remainder of the right side is constant, i.e., the hydraulic conductivity. Equations of this type can be applied in treatment of packed beds of uniform-size particles. They are not, however, suitable for natural soils. Childs and Collis-George (1950) developed a method for the calculation of hydraulic conductivity from pore size distribution data based on a capillary tube bundle model and Poiseuille's law

$$Q/t = \frac{\pi(P_0 - P_L)R^4}{8\mu L} \quad [20]$$

where Q is the quantity of water flowing past a given point in time, t , and R is the radius of the capillary. The equation developed by Childs and Collis-George is

$$k = M \int_{P=0}^{P=R} \int_{\sigma=0}^{\sigma=R} \sigma^2 f(\rho) \delta r f(\sigma) \delta \sigma \quad [21]$$

where $f(\rho)\delta r$ is the cross-sectional area associated with pores in the range of σ to $\sigma+\delta r$. The summation is stopped at the pore size R appropriate to the largest pore that remains full of water. The constant M is determined by matching calculated and experimental values at a single point. Equation [21] is the basis for all subsequent models attempting to calculate hydraulic conductivities from pore size distribution data. Much progress has been made in this area, but the best equations still require an experimentally determined matching point to yield satisfactory results (Green and Corey, 1971; Luxmoore, 1973).

The hydraulic conductivity of a soil is a measure of its ability to conduct water and is chiefly dependent upon the pore size distribution (Childs and Collis-George, 1950; Marshall, 1958) and the moisture content (Richards, 1936) of the soil. Together these factors determine the cross-sectional area available for water flow. The hydraulic conductivity decreases rapidly as the soil moisture decreases from its saturated value as a result of the decrease in total cross-sectional area. The largest soil pores are emptied first as the water content decreases and because the contribution to permeability per unit area varies roughly as the square of the pore radius, the conductivity can be expected to decrease much more rapidly than the moisture content

(Phillip, 1958). As the moisture content decreases, water may be trapped in pores or wedges isolated from the continuous network of the flowing water films. This trapped water is thus unavailable for liquid flow of water or the mass flow of pesticides.

Adsorption-Desorption of Pesticides

Pesticide molecules have a constant random motion because of their kinetic energy. Upon coming into contact with a clay or organic matter surface, these molecules normally remain on the surface for a period of time that depends on the nature of the colloid surface and pesticide molecule, the temperature, and the presence of competing molecules. This phenomenon is known as adsorption (de Boer, 1968). Adsorption of pesticides on solid surfaces in soils depends principally upon pesticide-water, pesticide-colloid, and colloid-water interactions, all operating simultaneously. Definition of these interactions is complicated by the wide range in physico-chemical properties of different pesticides, by the complexity of the colloid surface, and by the variable composition of the soil solution (Green, 1974). Reviews on pesticide adsorption have been published recently by Bailey and White (1970), Green (1974), Hamaker and Thompson (1972), and Weed and Weber (1974). These authors generally described the nature and properties of the soil surfaces and of the pesticide molecules that are important in adsorption reactions. For example, Bailey and White (1970) concluded that the following properties of the pesticide molecule determine its adsorption-desorption by soil colloids: chemical character, shape, and configuration; acidity or basicity of the molecule; solubility in water; charge distribution on the cation; polarity; molecular size; and

polarizability. The properties of the soil surfaces which influence pesticide adsorption are primarily related to the area and configuration of the surface, and to the magnitude, distribution, and intensity of the electrical field at the surface. Those properties are influenced by several soil physical, chemical, and mineralogical parameters.

Several mathematical models have been proposed to describe equilibrium adsorption of pesticides in soils, but the most commonly used are the Freundlich and the Langmuir equations. The Freundlich equation is purely empirical and can be expressed as

$$S = kC^{1/n} \quad [22]$$

where S is the amount of pesticide adsorbed ($\mu\text{g/g}$), C is the solution concentration ($\mu\text{g/ml}$), k is an equilibrium constant and $1/n$ is an exponent which usually has a magnitude of approximately 1. The Freundlich equation predicts that no limit exists to the amount of pesticide adsorbed by soil surfaces. This is an unreasonable conclusion because soil surfaces have a limited number of available adsorption sites. Fortunately, the Freundlich equation can be used to compare the adsorption behavior of many pesticides applied at field rates.

Assuming the exponent in equation [22] has a value of 1.0, equation [22] reduces to the linear form

$$S = K_d C \quad [23]$$

where K_d is the distribution coefficient. This equation predicts a linear relation between the amount of pesticide in solution and the amount adsorbed by the soil.

The second model is represented by the Langmuir equation and is

$$S = \frac{k_1 k_2 C}{1 + k_2 C} \quad [24]$$

where k_1 and k_2 are constants for the system. For low concentrations and low values of k_2 , this relation approaches the linear adsorption equation. The Langmuir equation has not been as successful in predicting adsorption of pesticides in aqueous solutions as it has been for gases. Boast (1973) gives a review of adsorption models used in several water-solute transport studies.

An important aspect of the sorption phenomenon is the rate of equilibrium establishment. The slurry technique has been used in most pesticide adsorption studies and the adsorption process is reported to be complete within a few hours. However, Leistra (1973) is of the opinion that the adsorption rate in soils under in situ conditions is controlled mainly by the pesticide diffusion rate in the water phase and the spatial arrangement of the adsorbing surfaces.

Several models of pesticide adsorption have emphasized nonequilibrium conditions. For example, Lindstrom and Boersma (1970) used the following equation

$$\frac{\partial S}{\partial t} = k_1 (S_{\max} - k_2 C) \sinh k_3 \left(1 - \frac{k_2 C}{S_{\max}}\right) \quad [25]$$

and Lindstrom et al. (1971) used

$$\frac{\partial S}{\partial t} = k_1 e^{k_2 S} k_3 C e^{-2k_2 S - S} \quad [26]$$

to predict adsorption of pesticides in miscible displacement equations.

METHODS AND MATERIALS

The study of pesticide movement was divided into two phases. The first phase was conducted in the field and centered on the transport of soil water, chloride, and a model pesticide under maximum leaching conditions. The second phase was concerned with further defining the transport coefficients of water, chloride, and the model pesticide under controlled conditions of soil moisture and temperature. In addition characterization studies were performed on the adsorption-desorption relations between the model pesticide and soil surfaces. This phase was conducted entirely within the laboratory.

Field Transport Study

The field study consisted of two parts, (1) the characterization of the in situ hydraulic conductivity of the various soil horizons, and (2) the comparison of the transport rates of soil water, chloride and the model pesticide under well characterized soil water flow regimes. The pesticide chosen was 4-amino-6-tert-butyl-3-(methylthio)-as-triazin-5-(4H)-one which has a common name of metribuzin. Metribuzin is one of the newer herbicides presently being marketed commercially with the name of SENCOR. It has a solubility in water of 1200 ppm and a molecular weight of 214.3. Preliminary observations of field trials have indicated that it is one of the more mobile herbicides presently being studied for soybean weed control and that, with relatively high rainfall frequency, it can cause residue problems.

The field study site selected is on the Agronomy farm of the Agricultural Experiment Station at Fayetteville in an area mapped as Captina silt loam, 1 to 3 percent slope. The Captina soil is classified as a Typic Fragiudalf in the fine-silty, mixed, mesic family. The soil is described as a deep, moderately well drained, slowly permeable soil commonly having a fragipan at a depth of 50 cm. A profile description taken at the study site is given in Table 1. The study site is nearly level (1 to 2% slope) and the surface runoff was estimated to be slow.

Soil samples were taken at 15 cm intervals to a depth of 150 cm for chemical analysis and particle size determination. The samples, composites of several cores, were air dried, ground, and passed through a 2 mm sieve. In addition, samples were taken at 15 cm intervals to a depth of 122 cm for determination of soil bulk density and moisture retention properties. Selected physical and chemical properties of the Captina soil are given in Tables 2 and 3.

The capillary conductivity as a function of soil water content and depth was determined at the study site by a method similar to that of Nielsen et al. (1964). A circular plot 6.1 m in diameter was constructed by removing the grass vegetation and constructing an earthen dike. Three seamless steel access tubes, 1.8 m long, were placed in the center of the plot at a 1 m spacing. Another access tube was placed adjacent to the perimeter of the plot to detect any lateral soil water movement. Two tensiometers were placed at each 15 cm increment to a depth of 152 cm. The plot was covered with a single layer of 3-mil plastic mylar sheet. Plastic tape was used to seal the plastic around the access tubes and tensiometers. The plastic prevented water loss from evaporation and addition of water from precipitation. Water was

Table 1. On site morphological description of Captina soil.

- Ap 0-22 cm Brown to dark brown (7.5YR4/4) silt loam with very weak medium subangular block (or massive) structure; very friable; common to many fine roots; common fine pores; few fine concretions; abrupt smooth boundary.
- B1 22-37 Strong brown (7.5YR5/6) silt loam with common to many fine brown to dark brown (7.5YR4/4) mottles which appear to be material from the Ap horizon and are mainly on ped faces and in pores; weak, medium subangular structure; friable; no clay films observed; common fine roots, common to many fine and medium roots; few fine concretions; gradual smooth boundary.
- B2t 37-74 Strong brown (7.5YR5/6) heavy silt loam with very weak medium prismatic break to moderate medium angular and subangular blocky structure; firm, thin, discontinuous (approx. 40% coverage) brown to dark brown clay films; few fine roots; common fine and medium and few coarse pores; few fine concretions; abrupt irregular boundary.
- Bx1 74-107 Dark red (2.5YR3/6) silty clay loam with many coarse light brownish gray (10YR6/2) and few to common fine strong brown (7.5YR5/6) mottles, weak coarse prismatic breaking to moderate medium and coarse angular blocky structure; very firm, very brittle; thin discontinuous clay films; approx. 50% of coarser pores have clay linings of about 1 mm thickness; few fine and medium pores and occasional coarse void; gray material (10YR6/2) which is mainly on ped faces has common fine and medium pores; few fine roots which are restricted primarily to ped faces and old channels of some nature; few to common black Fe-Mn stains on ped faces in some areas of the pedon (primarily redder areas) occasional (approx. 2% by volume) 2mm to 10mm rounded pebble, mainly sandstone or siltstone but also occasional chert; gradual smooth boundary.
- Bx2 107-157 Dark red (2.5YR3/6) silty clay loam with few fine strong brown (7.5YR5/6) mottles and common medium light brownish gray (10YR6/2) mottles which are primarily on ped faces; moderate medium angular blocky structure with gray outline of a few coarse prisms; very firm, very brittle; medium discontinuous (approx. 35% coverage clay films 2.5YR3/6); medium and thin clay linings in most pores, occasional fine root, few to common fine and medium pores few coarse pores, few voids 1-2 cm in diameter which have clay (gray and/or red) linings and occur primarily between 43 and 48 inches; horizon contains about 2% coarse material, 2m to 2 cm in diameter which is mainly rounded siltstone or sandstone but includes some chert; also one zone between 51 and 56 inches contains 20 to 30% coarse rounded stones which range from 2 mm to 6 inches in diameter, and are mainly sandstone and siltstone, but some are chert - this zone could represent a stone line, boundary not observed.

Table 2. Particle size distribution of Captina soil at study site.

Depth (cm)	clay	f. silt	m. silt	c. silt	Total silt	f. b. sand	f. sand	m. sand	c. sand	v. c. sand	Total sand	gravel*	Texture
0-5	9.3	2.7	21.8	43.4	67.9	10.7	8.7	2.0	1.1	0.4	22.9	2.69	silt loam
10-20	9.1	5.4	21.4	42.7	69.5	10.4	8.1	1.7	0.9	0.4	21.5	2.91	silt loam
25-36	18.0	5.7	22.7	39.0	67.4	6.1	6.1	1.4	0.8	0.3	14.7	0.90	silt loam
41-51	24.3	7.0	24.0	32.7	63.7	5.3	4.8	1.1	0.6	0.2	12.0	2.19	silt loam
56-66	26.3	7.7	23.8	30.2	61.7	4.8	4.5	1.1	0.9	0.7	12.0	1.86	silt loam
**56-66	30.0	6.2	19.4	32.3	57.9	5.4	4.9	1.0	0.5	0.3	12.1	3.07	silty clay loam
71-81	32.8	6.8	20.8	29.3	56.9	4.3	4.3	1.0	0.5	0.2	10.3	0.97	silty clay loam
**71-81	28.7	6.2	20.2	32.7	59.1	5.6	4.9	1.0	0.5	0.2	12.2	2.34	silty clay loam
86-97	32.7	6.1	18.8	32.9	57.8	4.3	3.7	0.8	0.5	0.3	9.6	3.57	silty clay loam
102-112	31.8	5.1	19.8	31.8	56.7	5.4	4.4	0.9	0.5	0.3	11.5	0.76	silty clay loam
117-127	33.5	5.8	19.0	30.9	55.7	5.2	3.8	0.8	0.6	0.4	10.8	2.84	silty clay loam
132-142	31.2	6.5	19.6	31.0	57.1	5.6	3.8	0.9	0.8	0.6	11.7	9.94	silty clay loam
147-157	30.3	5.6	18.5	29.7	53.8	7.1	4.5	1.1	1.3	2.0	16.0	43.30	gravelly silty clay loam

* All percentages with the exception of gravel are of the less than 2.0 mm fraction of the soil.

** These samples were taken in the fragipan; the other samples at these depths are from above the pan.

Table 3. Chemical properties of Captina soil at study site.

Depth (cm)	pH	% O.M	Kg/ha					Cond. Ec x 10 ³
			P	K	Ca	Na	Mg	
0-5	4.8	1.1	178+	341	880	137	64	0.18
5-10	5.0	0.9	77	99	1100	110	31	0.10
10-15	5.6	0.8	79	77	1320	110	44	0.10
15-30	5.9	0.6	11	88	1650	110	55	0.10
30-46	5.5	0.5	14	88	1540	137	71	0.10
46-61	4.8	0.4	7	99	1430	110	97	0.10
61-76	5.0	0.4	3	121	1980	137	253	0.10
76-91	5.2	0.3	1	121	2200	137	418	0.10
91-107	5.4	0.5	1	121	1760	137	440	0.10
107-122	5.6	0.5	1	132	2090	137	528	0.10
122-152	5.6	0.5	1	143	2200	165	660	0.10

ponded on the soil surface for approximately two weeks in an attempt to saturate the soil. The plastic surface then was covered with a layer of soil to hold the plastic in place and to minimize thermal fluctuations in the soil profile.

Neutron probe readings were made at 15 cm intervals to 1.5 m simultaneously with tensiometer readings. These data were analyzed with a program modified from that published by Popham and Ursic (1968). Hydraulic gradients at each depth were calculated by use of slopes of curves obtained from tensiometer data. Hydraulic conductivities were obtained by dividing the soil water flux by the hydraulic gradient according to Rose et al. (1965). The values of hydraulic conductivity were plotted against volumetric soil water content and a least squares line was fitted to the points for each depth.

Hydraulic conductivities were also calculated from pore size distribution data by the Green and Corey (1971) method as modified by Luxmoore (1973). The computer program determined matching factors from an experimentally determined value of k taken from the in situ data. This method of calculating hydraulic conductivity values was used only for the Ap and B2t horizons.

The experimental site for the metribuzin-water-chloride study was adjacent to the in situ hydraulic conductivity site. An earthen dike was placed around a 6.1 by 12.2 m area and the vegetation (primarily fescue and clover) on half of the plot area was killed chemically. Thus, two 6.1 m square plots and two soil moisture regimes were created. In each plot three 1.8 m seamless steel access tubes were placed in the center and were surrounded by two banks of tensiometers. Thus, each plot contained two tensiometers at depths of 15, 30, 45, 60, 90 and 120 cm.

Soil water contents and pressures were monitored at each measurement period and depth with the neutron probe and tensiometers, respectively.

Water was ponded initially on the soil surface of the solute transport plot for 10 days to saturate the profile. Before the solutes were applied, an additional 8 cm of water was ponded on the soil surface. Metribuzin and KCl then were dissolved in 1600 l of water and applied to the soil at a rate of 45.6 and 1140 kg/ha, respectively. An additional 1600 l of water was added to the soil before infiltration ceased.

Soil samples for solute concentration were taken gravimetrically in increments of 0-5, 5-10, 10-15, 15-23, 23-30, 30-46, 46-61, 61-91, 91-121 cm at selected times after the initiation of the experiment. Several composited cores were taken at random throughout each plot. The composited soil samples were stored in a freezer at -10°C until analyzed.

Before analysis each soil sample was air dried in a forced draft oven at 56°C , ground, passed through a 2 mm sieve, divided into two portions and refrozen. One set of samples was shipped to Chemagro for analysis of metribuzin content. The other set was analyzed for chloride content. The soil samples for chloride analyses were arranged in groups of 50 with two blanks in each group. Duplicate 10 g samples of soil were weighed; 50 ml of deionized water was added to each sample. The soil samples were filtered through Whatman number 2 filter paper and were washed with an additional 50 ml of deionized water. The filtrate was analyzed with a Beckman Expandomatic pH meter on the mv scale. A Corning specific ion electrode was used for the chloride analyses with a saturated calomel electrode as a reference.

Chloride and metribuzin fluxes were calculated by mass balance, assuming no addition or loss of chloride and metribuzin across the soil surface. These fluxes are, therefore, average fluxes over the time intervals involved. Water fluxes were calculated by use of the hydraulic conductivities obtained from the in situ plot and the hydraulic gradients calculated from tensiometer data. These fluxes were compared by soil depth over a period of two months.

Laboratory Transport Characterization

The second phase was conducted in the laboratory and consisted of determining (1) the self-diffusion coefficients of ^3HOH , ^{36}Cl and ^{14}C -metribuzin in several soils, (2) the adsorption-desorption of metribuzin from two soils, and (3) the transport of ^3HOH , ^{36}Cl and ^{14}C -metribuzin in soil as influenced by hydraulic gradient, water content, and placement position.

The self-diffusion coefficients of ^3HOH , ^{36}Cl and ^{14}C -metribuzin were determined in the Ap horizon of several soils in eastern Arkansas. These soils are very extensive in the Mississippi Delta and their physical and chemical properties are given in Table 15. The diffusion method used was developed by Phillips and Brown (1964) and consisted of filling two plexiglas half cells with soil at equal soil water contents. The soil on one side of the cell was tagged with either ^3HOH , ^{36}Cl or ^{14}C -metribuzin. The cells were taped together and the tagged molecules or ions were allowed to diffuse for a given time interval. After this time had elapsed the cells were broken apart and the concentrations of the tagged material was determined by liquid scintillation techniques. The self-diffusion coefficient was calculated from the equation

$$D_e = \frac{\pi h^2 F^2}{t} \quad [27]$$

where D_e is the apparent diffusion coefficient (cm^2/sec), h is the length of the half cell (cm), F is the fraction of the tagged molecules that moved across the interface, and t is the diffusion time (sec). This procedure was followed for all soil water and temperature treatments, the only variation being the amount of water added to the soil or the temperature at which the diffusion process occurred.

The adsorption and desorption studies were conducted with ^{14}C -metribuzin and the Dubbs and Captina soils. The soil:water ratio was 1:2. The initial experiment was a kinetic study designed to show the influence of equilibration time on the adsorption of metribuzin. Exactly 5.0 g of soil and 10 ml of aqueous solution containing a known rate of the herbicide were placed into each of four centrifuge tubes. The tubes were capped and placed on a rotary shaker (rotating at 33 rpm) for various equilibration times. After being shaken for a predetermined time, the tubes were removed and centrifuged for one hour. Two 500 λ aliquots were taken from the supernatant and the activity of ^{14}C -metribuzin was determined on a Packard Tricarb Liquid Scintillation spectrometer. The amount of herbicide adsorbed by the soil was determined by the difference between the amount applied and the average amount in solution. The second study was a determination of the metribuzin:soil adsorption isotherm. The procedure used was essentially the same as given above with three exceptions; the soil and water quantities were 2.5 g and 5 ml, respectively, various rates of metribuzin were applied to the soil in the aqueous solution, and each tube was

shaken for 168 hours. The third study was a kinetic study of the desorption process. The herbicide was adsorbed by the soil in the usual manner. From each centrifuge tube 2 - 250 λ aliquots were removed from the supernatant and placed in a liquid scintillation vial for counting. To keep the soil:water ratio constant, 500 λ of distilled deionized water were added to each centrifuge tube, then the adsorption process was repeated. After the equilibration period, two samples of 250 λ were removed from the supernatant in each tube, counted, and replaced with water. The adsorption process was repeated. The procedure was repeated five times, each time removing 500 λ more than the previous time. At each desorption step the amount of metribuzin remaining on the exchange complex was determined by the difference between the amount applied and the average amount in the soil solution.

The transport of ^3HOH , ^{36}Cl and ^{14}C -metribuzin in the Captina soil as influenced by hydraulic gradient, soil water content, and placement position was studied by techniques similar to those used in the self-diffusion studies. The soil was prepared by the above method. However, instead of equal soil water contents on both sides of the half cells as before, the water content of the soil on one side was reduced by 5% on a weight basis. The radioactive solutes were placed in the soil on either side and were allowed to redistribute for approximately two hours. The cells then were broken apart, frozen in liquid air, and sectioned in 500 μ sections with a refrigerated microtome. Ten of these sections of soil were placed in a liquid scintillation vial, weighed, and radioassayed by liquid scintillation techniques. A computer program was written which separates the radioactivity of ^3HOH , ^{36}Cl and/or ^{14}C -metribuzin when two of these isotopes are contained in an aqueous sample.

The distributions (C/Co) of $^3\text{H}\text{OH}$, ^{36}Cl and ^{14}C -metribuzin were determined as a function of distance along the half cell, and the diffusivity of each was determined at various points along the curves by the computer program developed by Fuqua et al. (1973). This process was repeated at gravimetric soil moisture contents ranging from 5 to 30%. Preliminary studies had shown that little if any impedance was observed at the interface.

RESULTS AND DISCUSSION

The results of the field and laboratory transport studies are given, and their application is discussed according to the objectives of the project.

Field Study

In Situ Hydraulic Conductivity

The study of water movement under field conditions included an on-site soil description as well as a laboratory characterization of the soil physical and chemical properties. The soil at the study site is classified as a Captina silt loam (Table 1). In textures, the Ap, B1 and B2t horizons are silt loams and the fragipan horizons are silty clay loams (Table 2). Soil structure ranges from very weak, medium, subangular blocky in the Ap horizon to moderate, medium, subangular blocky in the Bx2 horizon. An important characteristic of this soil which influences soil water movement is the abrupt, irregular boundary between the B2t and Bx1 horizons. The depth to this boundary which separates the fragipan from the B horizon above ranges from 50 to 100 cm. Fragipans are generally thought to retard the movement of water and solutes in the soils in which they are present. Soil bulk density and clay content variations with soil depth are given in Figure 1. These data represent the averages of five and two replicates, respectively. Two zones of relatively high bulk density were observed in the profile. The first peak is near the bottom of the Ap and may be due to a weak traffic pan; the second peak is in the Bx1 (fragipan) horizon. Clay

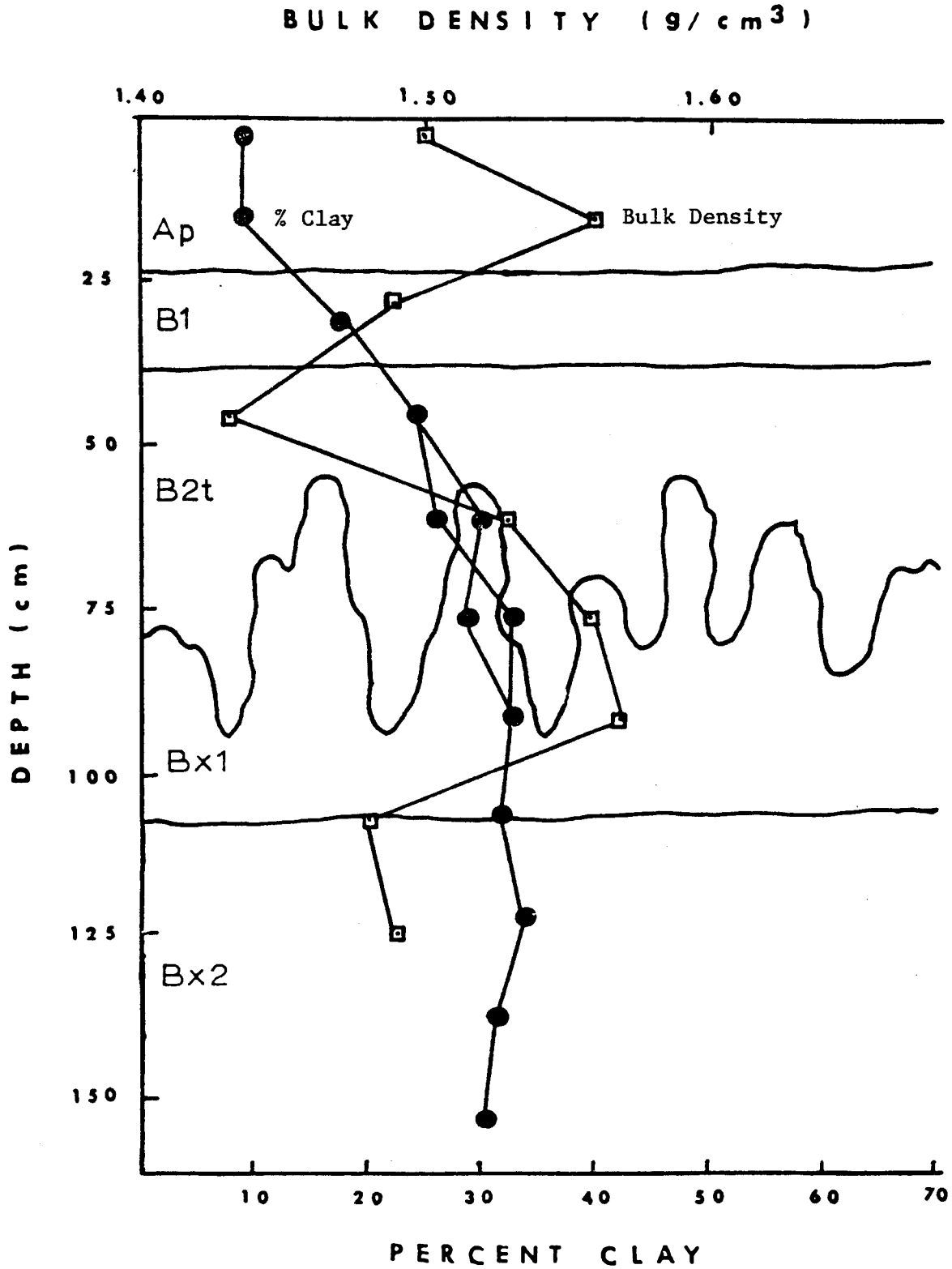


Figure 1. Bulk density and clay percentages of Captina soil at study site.

content increases with depth from 10% in the Ap to 32% in the fragipan horizons. These data indicate that there is little if any direct relationship between bulk density and clay content in this soil.

Soil moisture release curves for each horizon were determined by combining the field data (neutron probe and tensiometer measurements) with the laboratory data (pressure plate measurements). These data also were used in the calculation of the hydraulic conductivities by the computer program published by Luxmoore (1973). The water retention data for the Ap and B2t horizons are given in Figure 2; the water retention data for the other horizons are given in Appendix Table 1. The Ap horizon had a lower saturated water content (0.41 vs 0.44 cm^3/cm^3) and a greater number of large pores than the B2t horizon. As a result the Ap consistently retained less water than the B2t at all soil water tensions. This can be attributed to its higher bulk density and lower clay content. The chemical properties of the Captina soil are given in Table 3. They generally show that the soil has a moderate to low fertility status with respect to plant growth.

The soil was wet up and allowed to drain for approximately three months. The redistribution of soil water was monitored with the neutron probe and tensiometers for 53 days. Moisture content drainage profiles at various times after initiation of the study are shown in Figure 3. They show that the profile lost less than 3 cm of water during the 53 days and that less than 0.5 cm was lost from the fragipan horizons (76 to 150 cm). The Ap horizon lost the most water (8% by volume). The Bx2 horizon lost less than 1%. The greater moisture decrease in the Bx1 in comparison with the Bx2 horizon was probably due to the irregular boundary, i.e. about one-half of the soil from 50 to 100 cm

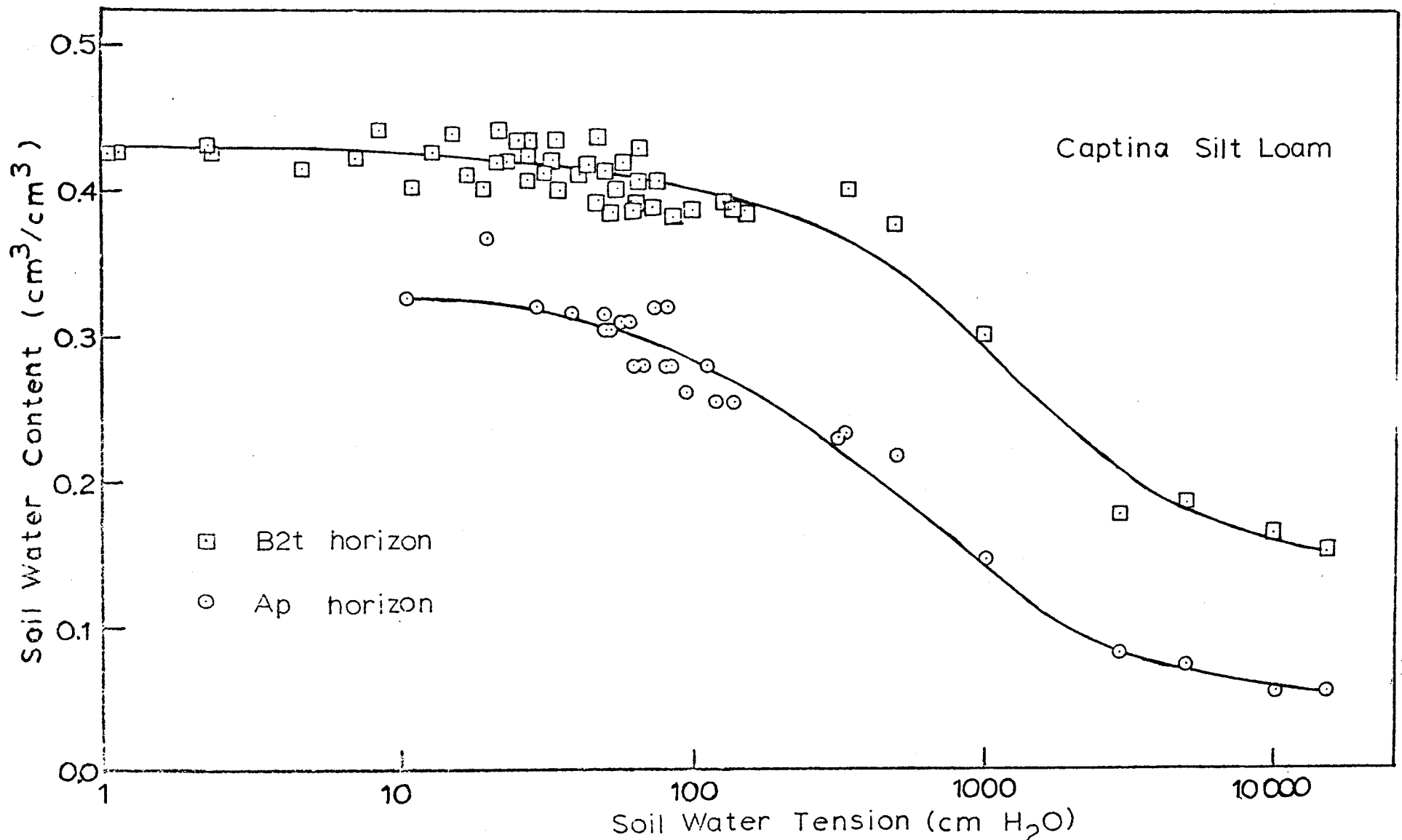


Figure 2. Water retention curves for Ap and B2t horizons of Captina soil at study site.

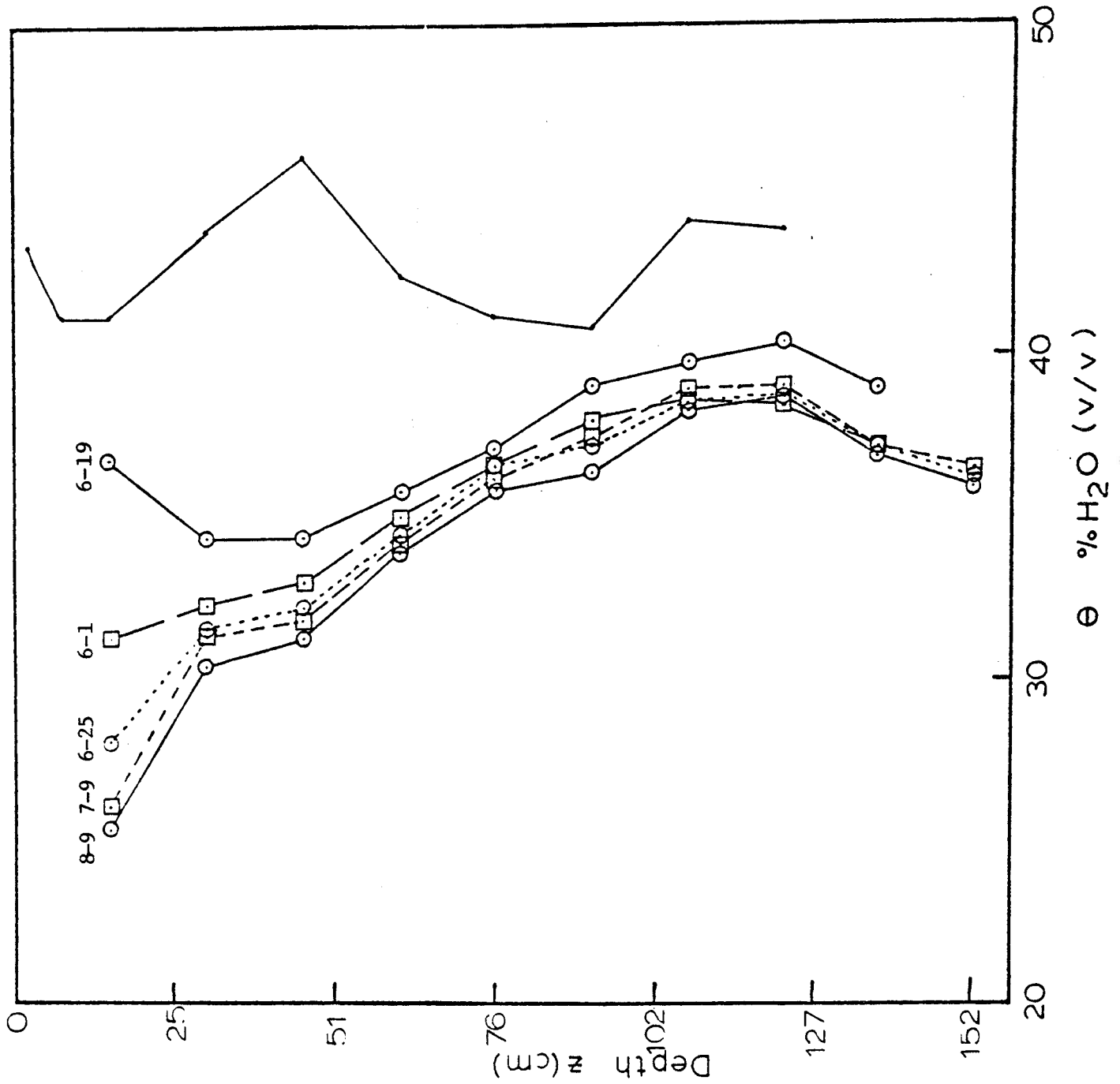


Figure 3. Soil water content distributions in Captina soil at study site.

was contained in the B2t horizon which lost more water than the Bx1. The drainage rate from the profile during the monitoring period is shown in Figure 4. Soil moisture tension profiles (Figure 5) indicate that the soil profile was near saturation initially. The largest increase in tension, corresponding to a decrease in soil moisture content, occurred in the Ap horizon, where the tension increased by more than 100 cm water. The tensions in the fragipan horizons showed little variation, and thus indicate relatively constant soil moisture contents.

The magnitude of the in situ hydraulic conductivities decreased with soil water content and soil depth (Figure 6). The slopes of the curves generally increase with depth and range from 0.003 for the 15 cm depth to 0.030 for the 137 cm depth. Thus, the largest slopes are in the fragipan horizons where the soil moisture contents changed the least. The least squares fit of the lines to the data points is excellent for most depths. However, the major disadvantage of this field method, as was noted previously, is the small range of soil moisture contents over which the hydraulic conductivities can be measured. This is especially true in soils of slow to moderate permeabilities such as the Captina.

If one assumes that there is little variation of hydraulic conductivity within a given soil horizon, the values measured at all depths within a horizon can be pooled to give conductivity curves for each horizon (Figure 7). Compared with the curves for individual depths (Figure 6), the points show considerable scatter about the least squares fitted curves. Further, slopes of the curves as functions of horizonation decrease in the deeper horizons in contrast to the slopes of the curves for the individual depths. Apparently, because of the small

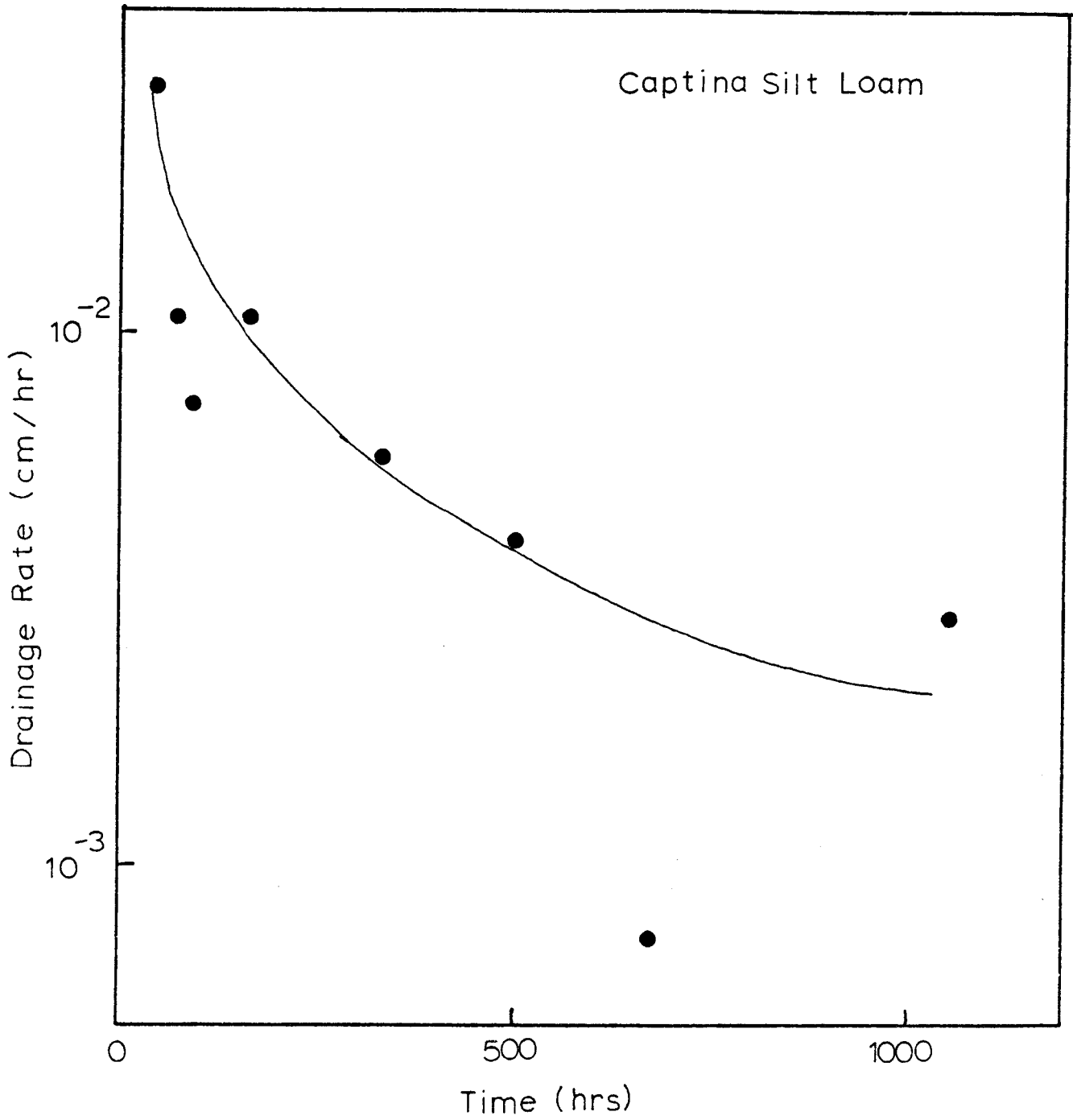


Figure 4. Drainage rate of soil water from Captina profile.

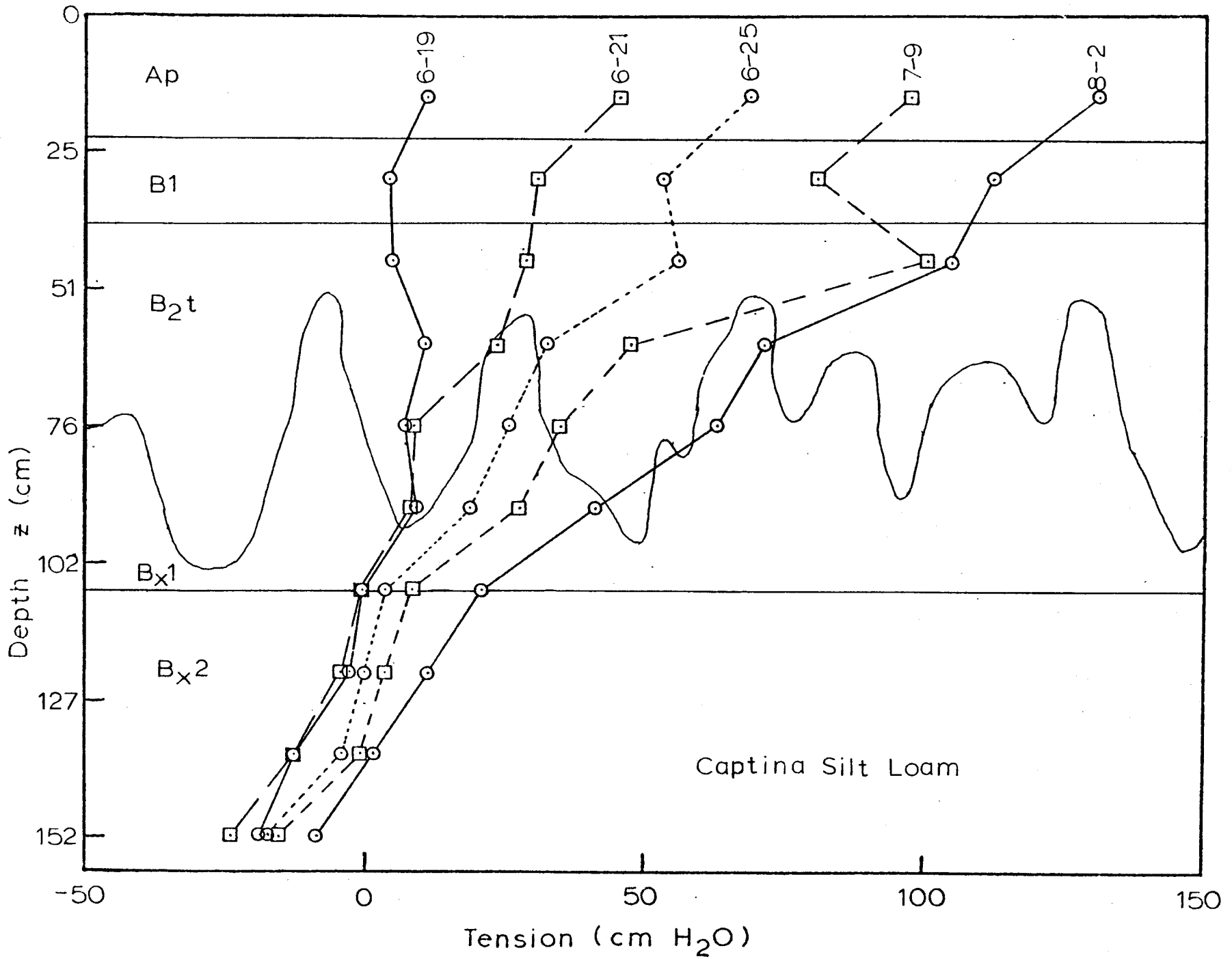


Figure 5. Soil water tension distribution in Captina soil at study site.

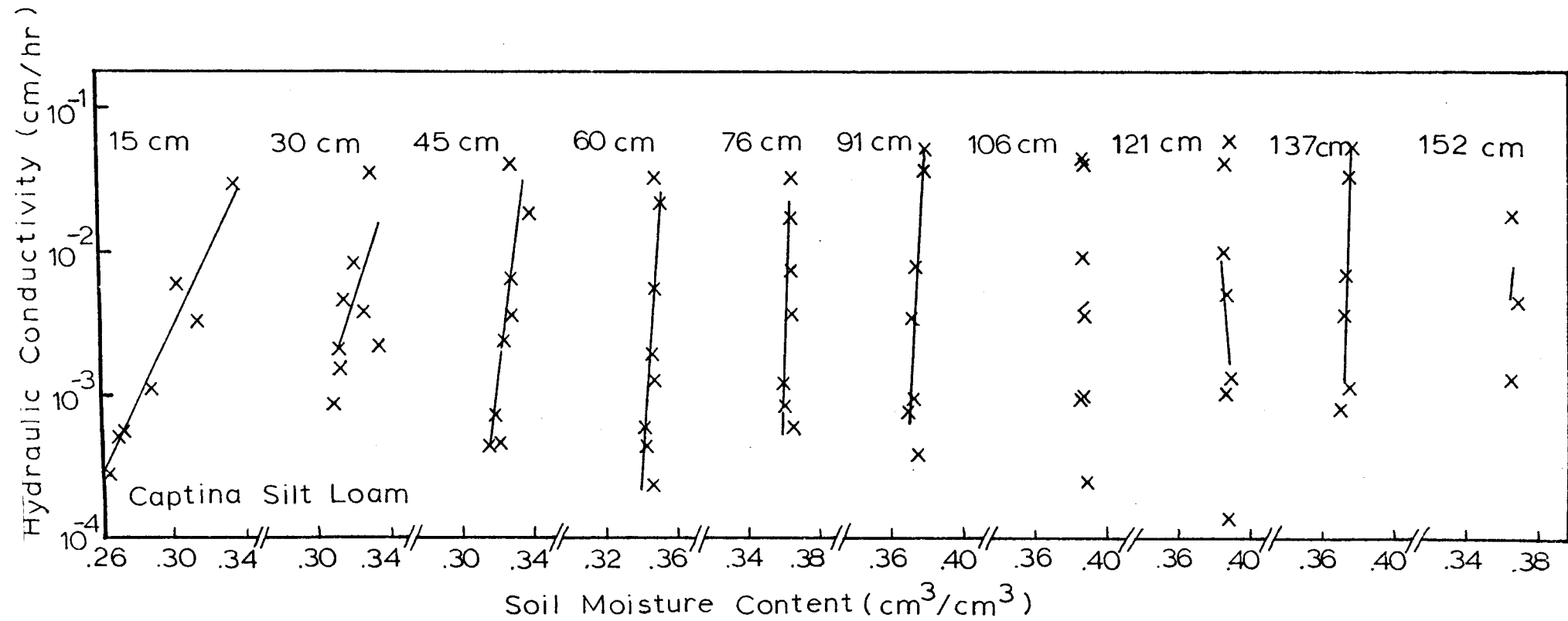


Figure 6. Hydraulic conductivity as a function of soil water content at 15 cm intervals of Captina soil (in situ data).

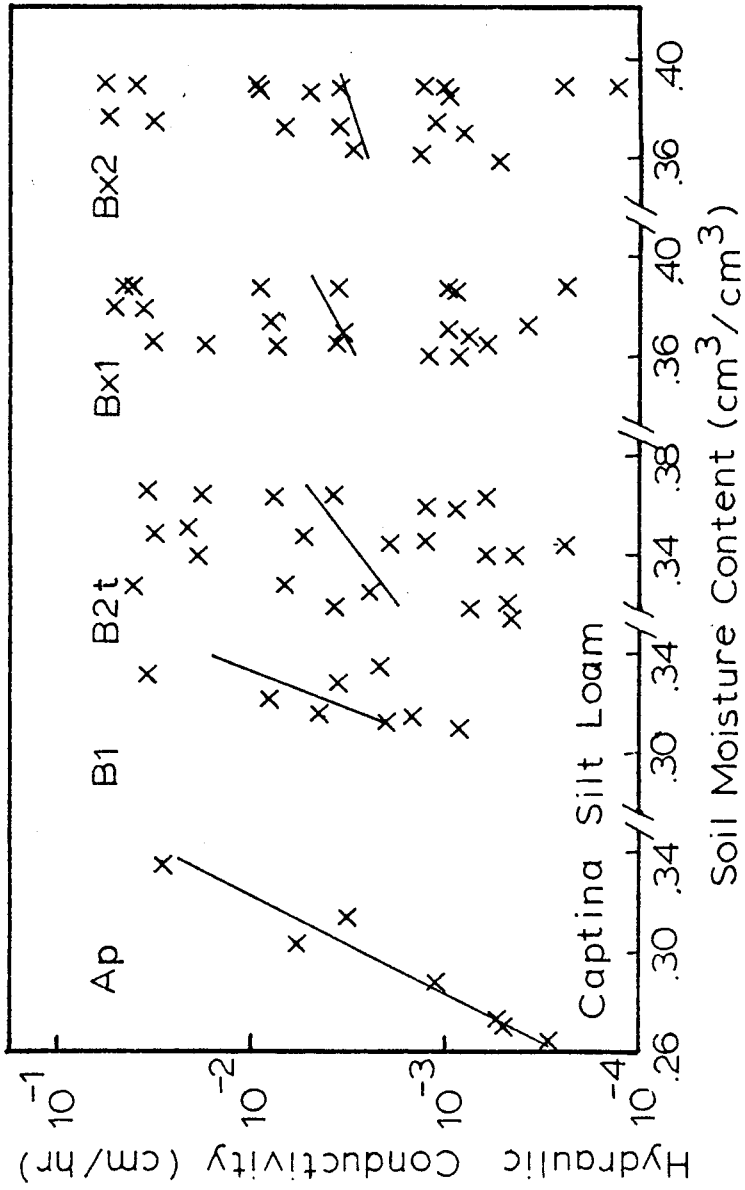


Figure 7. Hydraulic conductivity as a function of soil water content of the horizons in Captina soil (in situ data).

range of soil moisture contents over which the conductivity values were measured at the lower depths, the data for the individual depths represent experimental variation about a single value rather than a true curve. This would also explain the negative slope at the 121 cm depth in Figure 6. The calculated curves were matched at a single point by use of the experimentally determined values taken from the midpoints of the least squares curves. The calculated hydraulic conductivity curve for the Ap agrees well with the in situ determined values for the 15 cm depth (Figure 8). Because the in situ data for depths within and near the B2t show considerable scatter about the calculated curve for the horizon, curves fitted to the in situ data appear to have steep slopes. However, when all data are plotted the values seem to represent scatter about the true curve. In view of the spatial variability in soils, the calculated values should provide adequate data for most soil water transport studies.

Solute Transport

The addition of metribuzin and chloride at the relatively high rates to the plots killed the grass on the vegetation-covered plots in approximately one week. Even so the vegetation was living and transpiring for a short time, and thus created a moisture regime different from that of the adjacent bare plot. Later, the killed vegetation formed a greater mulch on the soil surface, thereby maintaining soil moisture differences between the two plots. These results are shown in Figures 9 and 10. The initial measurements of soil water tensions, made on July 13, indicate that water was moving downward at all depths within the no-vegetation plot except at the surface

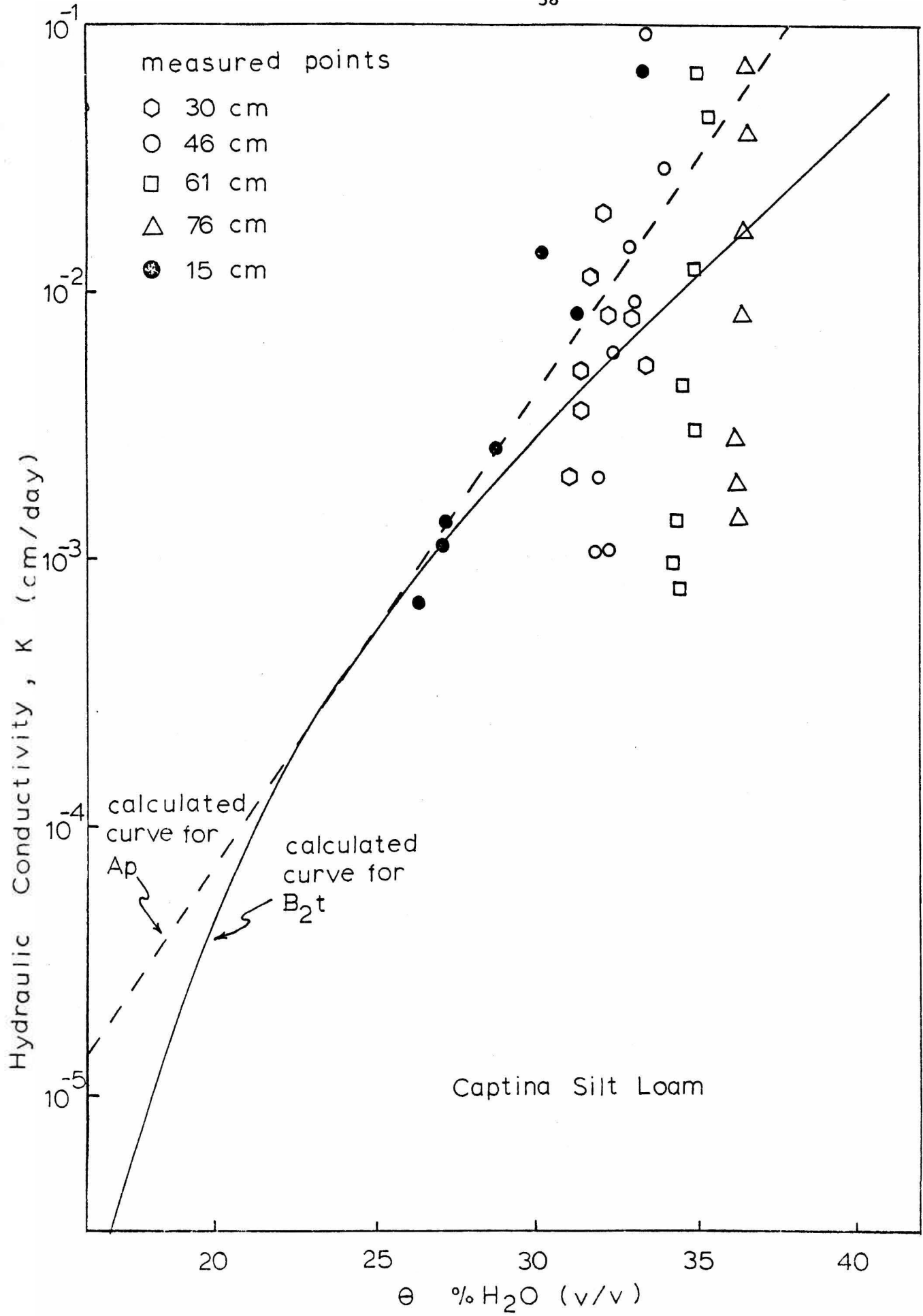


Figure 8. Hydraulic conductivity as a function of soil water content of the Ap and B₂t horizons of Captina soil (predicted data).

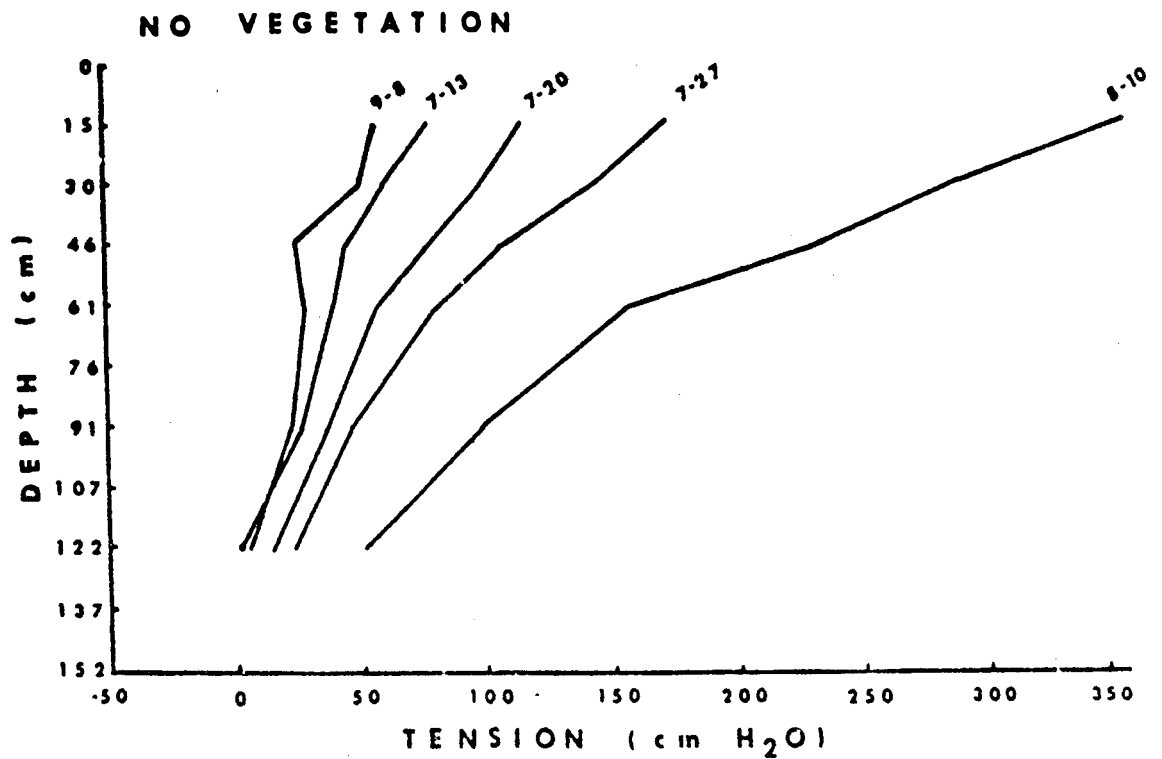
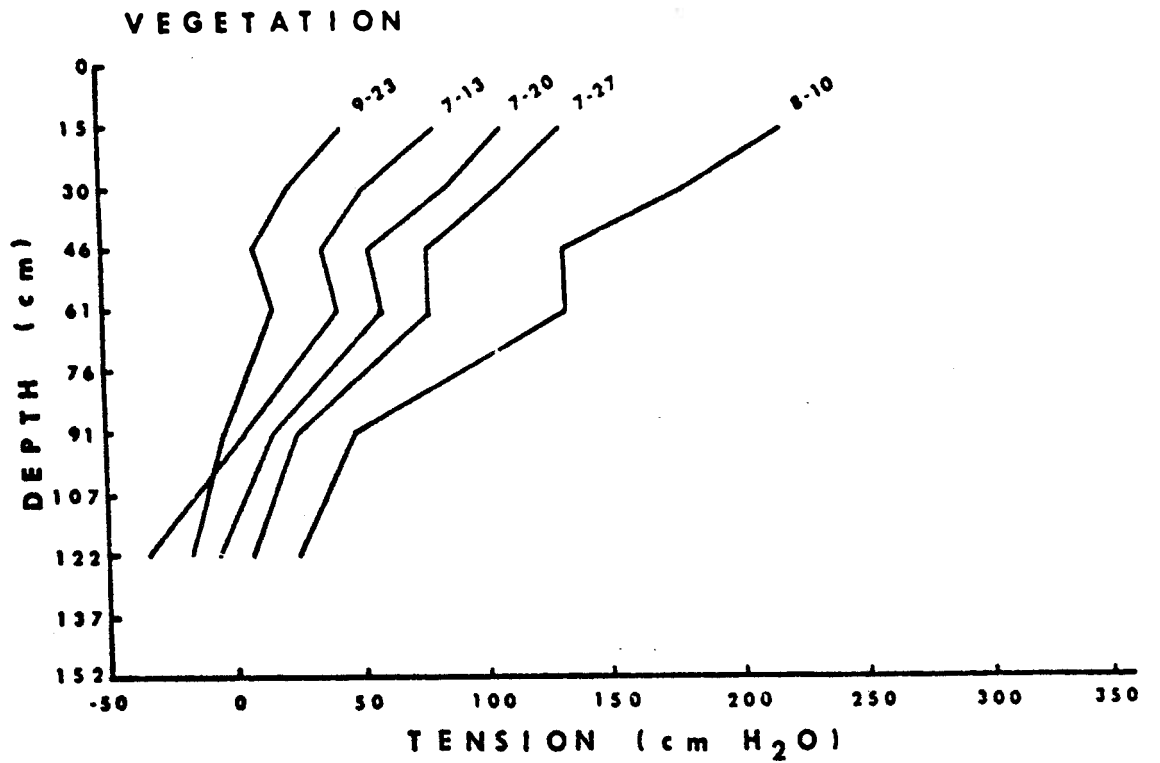


Figure 9. Soil water tensions of Captina soil profile in solute transport plots during the monitoring period.

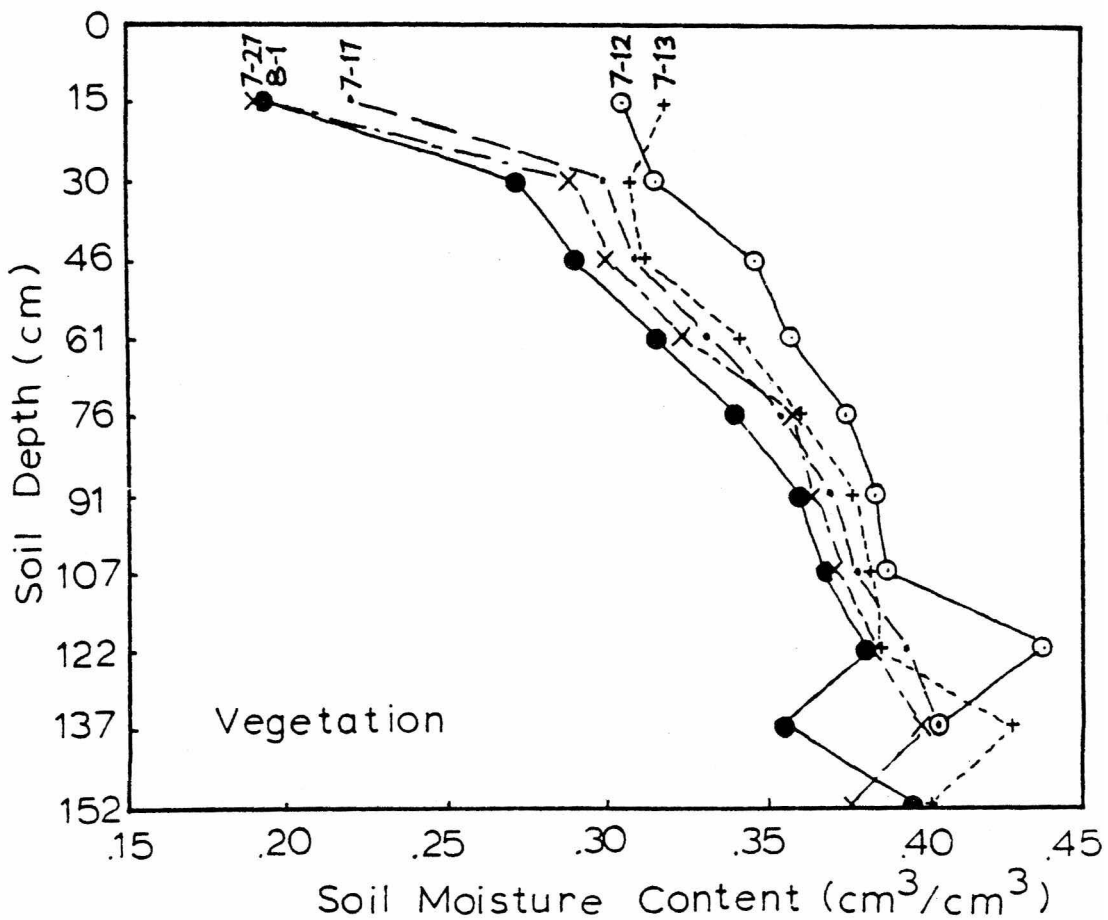
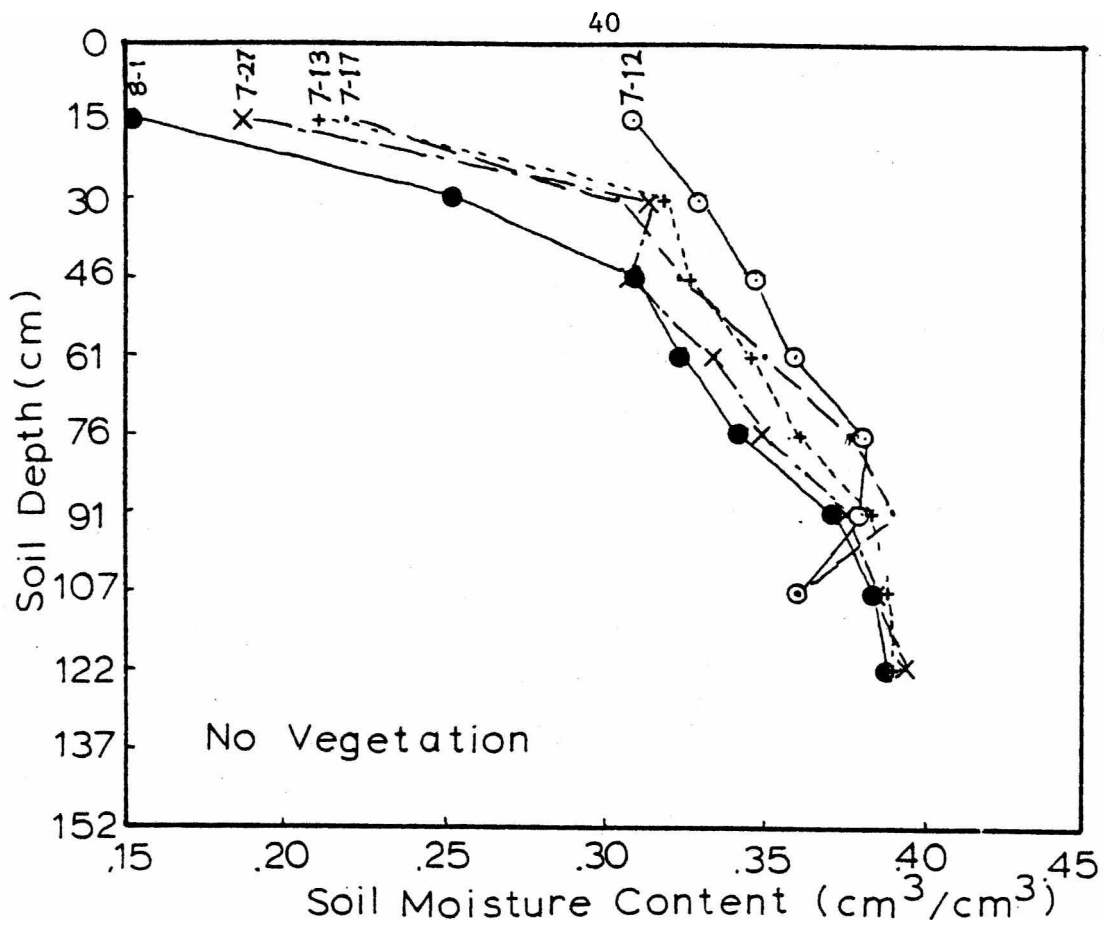


Figure 10. Soil water contents of Captina soil profile in solute transport plots during the monitoring period.

15 cm. Water was moving downward in the vegetation-covered plot below the 46 cm depth and upward above that depth. Two weeks after the water and solute application, water was moving upward from all depths in the no-vegetation plot, whereas water in the vegetation plot was moving downward only below the 46 cm depth. The surface horizons in the no-vegetation plot dried faster and to a greater extent than those of the vegetation-covered plot. This faster drying is evidenced by the higher soil water tensions and lower soil water contents in the surface horizons. The profiles of both plots were wet approximately to their initial water contents by late summer rains.

A soil water balance was computed on the water in the surface 107 cm in both transport plots assuming no loss from runoff. The computations were made on the initial 20 days of the experiment. As shown in Table 4, the soil profile in both plots lost approximately the same amount (5 cm) of water during the 20-day period. The changes in moisture, rainfall, and total moisture lost in both plots during several measurement intervals are given in Table 5. The total moisture lost from the profile is the sum of evapotranspiration (ET) and drainage beyond the 107 cm depth. Even though the same amounts of water were lost from both profiles at the end of the 20-day measurement period, the plots reacted differently with respect to the rate of moisture lost during any given interval. Because most of the water lost in the first time interval can be attributed to drainage, the amount drained in the no-vegetation plot was almost twice as great as that in the vegetation plot. However, the amount of water lost from the vegetation plot during the first 8 days was 0.72 cm greater than that lost from the no-vegetation plot (4.03 and 3.31 cm, respectively). Most of this difference in water lost can

Table 4. Depth of water (cm) in surface 107 cm of soil
in the solute transport plots.

Plot	Depth of Water (cm)					
	7/12	7/13	7/17	7/20	7/27	8/1
Vegetation	37.82	36.70	34.56	34.63	33.41	32.76
No Vegetation	37.62	35.53	35.29	35.15	34.41	32.53

Table 5. Change in moisture, rainfall, and total moisture lost from soil profile during several measurement periods.

Moisture Parameter	Measurement Interval				
	7/12-7/13	7/13-7/17	7/17-7/20	7/20-7/27	7/27-8/1
Moisture Change (cm)					
vegetation	-1.12	-2.12	+0.07	-1.22	-0.65
no vegetation	-2.09	-0.24	-0.14	-0.74	-1.38
Rainfall (cm)	0	0.51	0.33	0.71	0
Total Moisture Loss (cm)					
vegetation	-1.12	-2.65	-0.26	-1.93	-0.65
no vegetation	-2.09	-0.75	-0.47	-1.45	-1.88

be attributed to transpiration from the grass. The grass lived until approximately one week after application of the metribuzin and chloride. The greater amount of water lost by the no-vegetation plot after this period can be attributed to its greater evaporation rate. The dead grass of the "vegetation" plot created a mulch on the soil surface which reduced the evaporation rate below that of the no-vegetation plot. These data agree with those presented in Figures 9 and 10.

The profile distribution of chloride at several sampling times during the transport study is shown in Table 6. With the exception of those at the 10-15 and 30-46 cm depths, the initial chloride concentrations were relatively uniform with depth of soil. The magnitude of the initial values shows that considerable amounts of Cl^- were in the profile before the solute applications. Its presence probably was due to previous applications of fertilizer to the grasses in and around the plot area. During the monitoring period considerable changes in Cl^- concentration occurred at a given depth. Because Cl^- does not undergo microbial degradation, volatilization, or change in form, it was transferred from one soil depth to another by the movement of water. As water moved through the profile to the soil surface, it carried the soluble Cl^- to the surface where it accumulated as the water evaporated. Most of the increases in Cl^- concentration occurred in the surface 15 cm of soil particularly in the 0-5 cm increment. These increases were greater in the no-vegetation plot than in the vegetation plot and obviously were caused by the greater amount of water evaporated during the latter part of the monitoring period by the no-vegetation plot. The greatest Cl^- concentration was observed in the 0-5 cm increment of soil of the no-vegetation plot. A considerable amount of rain fell

Table 6. Chloride concentration (ppm) as a function of soil depth during the field experiment.

Depth (cm)	Chloride Concentration (ppm)							
	Initial	7/12	7/13	7/16	7/20	7/27	8/10	9/23
Vegetation								
0-5	3.60	6.40	7.80	7.85	9.40	21.25	35.15	13.50
5-10	3.10	4.90	4.80	8.30	4.60	6.95	2.85	4.45
10-15	9.85	8.65	5.05	5.35	2.85	4.00	4.80	9.15
15-23	1.30	5.80	2.20	1.85	4.35	2.25	3.00	4.00
23-30	2.90		6.65	9.25	5.15	3.45	2.50	5.00
30-46	9.35		1.60	2.50	1.55	2.00	2.15	2.70
46-61	2.05		1.40	1.85	1.10	2.60	1.70	5.35
61-91	5.20		3.90	4.60	4.60	4.85	4.45	5.50
91-122	4.50		4.10	5.85	3.00	4.65	4.25	5.45
No Vegetation								
0-5	3.60	6.70	6.40	6.40	12.10	23.20	52.95	34.00
5-10	3.10	2.60	2.15	3.10	3.10	4.25	1.70	7.20
10-15	9.85	3.95	2.85	3.00	2.85	6.85	2.45	4.40
15-23	1.30	4.30	3.50	4.77	4.05	2.00	1.60	3.60
23-30	2.90	4.25	2.80	2.90	2.55	3.45	3.15	5.40
30-46	9.35	1.55	1.20	2.00	2.50	2.35	3.45	5.75
46-61	2.05	2.50	2.70	4.50	3.75	3.55	5.29	5.85
61-91	5.20	3.70	5.00	5.90	5.15	7.45	9.00	6.70
91-122	4.50	5.40	5.10	4.20	5.40	5.25	6.95	4.50

during September and it leached some of the Cl^- from the surface deeper into the soil. The amount of Cl^- per unit volume of soil ($\mu\text{g}/\text{cm}^3$) and the amount of Cl^- per unit area of soil ($\mu\text{g}/\text{cm}^2$) are given in Tables 7 and 8, respectively.

A mass balance of Cl^- was computed for the 122 cm profile and is given in Table 9. Two days after the Cl^- application 62.4 and 65.7% could be accounted for in the vegetation and no-vegetation plots, respectively. These values indicate that a large amount of the Cl^- moved through the profile and out of the sampling zone with the leaching water initially added to the plots. For this movement to occur the soil profile had to contain several large and continuous pores which conducted the water and Cl^- rapidly through and out of the sampling zone. Evidently little interaction occurred between the Cl^- and soil surfaces, and the Cl^- recovered was in the dead end pores and/or small pores. Such pores do not transmit water at a rapid rate. These data also were verified by the length of time needed to wet the profile in the in situ hydraulic conductivity plot. Quisenberry (1974) observed a similar phenomenon in his soil water and Cl^- movement studies under field conditions in Kentucky. These results indicate that the infiltration models available do not apply to the Captina soil under in situ conditions.

The amount of Cl^- recovered in the profile generally increased as water moved upward toward the soil surface (Table 9). Maximum Cl^- concentrations were observed on 9/23 and 8/1 for the vegetation and no-vegetation plots, respectively. These findings indicate that some of the Cl^- that had moved past the lowest sampling point moved back into the profile as the water flowed upward. More Cl^- was recovered in

Table 7. Chloride concentration ($\mu\text{g Cl/cm}^3$ soil) as a function of soil depth during the field experiment.

Depth (cm)	Chloride Concentration ($\mu\text{g/cm}^3$)						
	7/12	7/13	7/16	7/20	7/27	8/1	9/23
Vegetation							
0-5	9.63	11.71	11.79	14.12	31.92	52.80	20.28
5-10	7.54	7.38	12.77	7.08	10.69	4.38	6.84
10-15	13.45	7.85	8.32	4.43	6.22	7.46	14.23
15-23	9.05	3.43	2.89	6.79	3.51	4.68	6.24
23-30		10.21	14.30	7.50	5.30	3.84	7.67
30-46		2.33	3.64	2.58	2.91	3.13	3.93
46-61		2.02	2.67	1.59	3.75	2.45	7.72
61-91		6.03	7.11	7.11	7.49	6.87	8.50
91-122		6.09	8.69	4.45	6.91	6.31	8.09
No Vegetation							
0-5	10.06	9.13	9.13	18.17	34.85	79.53	51.07
5-10	4.14	3.31	4.72	4.72	6.54	2.62	11.09
10-15	6.14	4.43	4.66	4.43	10.62	3.80	6.82
15-23	6.71	5.46	7.44	6.32	3.13	2.50	5.62
23-30	6.52	4.30	4.15	3.91	5.30	4.83	8.30
30-46	2.26	1.75	2.91	3.64	3.42	5.03	8.38
46-61	3.61	3.90	6.49	5.41	5.12	7.63	8.44
61-91	5.72	7.73	9.12	7.96	11.51	13.91	10.35
91-122	8.02	7.57	6.24	8.02	7.80	10.32	6.68

Table 8. Chloride concentration ($\mu\text{g Cl/cm}^2$ soil) as a function of soil depth during the field experiment.

Depth (cm)	Chloride Concentration ($\mu\text{g/cm}^2$)						
	7/12	7/13	7/16	7/20	7/27	8/1	9/23
Vegetation							
0-5	48.92	59.49	59.89	71.73	162.15	268.22	103.02
5-10	38.30	37.49	64.87	35.97	54.31	22.25	34.75
10-15	68.33	39.88	42.27	22.50	31.60	37.90	72.29
15-23	68.96	26.14	22.02	51.74	26.75	35.66	47.55
23-30		77.80	108.20	57.15	40.39	29.26	58.45
30-46		35.51	55.47	39.32	44.35	50.44	59.89
46-61		30.78	40.69	24.23	57.15	37.24	117.65
61-91		183.79	216.71	216.71	228.30	209.40	259.08
91-122		185.62	264.87	135.64	210.62	192.33	246.58
No Vegetation							
0-5	51.10	46.38	46.38	92.30	177.04	404.01	259.44
5-10	21.03	16.81	23.98	23.98	33.22	13.31	56.24
10-15	31.19	22.50	23.67	22.50	53.95	19.30	34.65
15-23	51.13	41.61	56.69	48.16	23.85	19.05	42.82
23-30	49.68	32.77	31.62	29.79	40.39	36.80	63.25
30-46	34.44	26.67	44.35	55.47	52.17	76.66	127.71
46-61	55.02	59.44	98.91	82.45	78.03	116.28	128.63
61-91	174.35	235.61	277.98	242.62	350.82	423.98	315.47
91-122	244.45	230.73	190.20	244.45	237.74	314.55	203.61

Table 9. Amount and percentage recovery of chloride in the solute transport plot.

Plot	Sampling Date					
	7/13	7/16	7/20	7/27	8/1	9/23
Vegetation						
Amount added (g)	403.4	403.4	403.4	403.4	403.4	403.4
Amount recovered (g)	251.7	325.6	243.7	318.4	328.5	371.8
% recovered	62.4	80.7	60.4	78.9	81.4	92.2
No Vegetation						
Amount added (g)	403.4	403.4	403.4	403.4	403.4	403.4
Amount recovered (g)	265.1	295.4	313.2	289.6	529.5	458.1
% recovered	65.7	73.2	77.6	96.6	131.3	113.5

the no-vegetation plot on these dates than was added. This may be attributed to Cl^- already present in the soil below the sampling zone moving up into the sampling zone along with the added Cl^- .

The profile distribution of metribuzin at several sampling times during the transport study is shown in Table 10. The metribuzin concentrations in the soil samples taken before application were negligible throughout the profile. The greatest concentrations of metribuzin were detected in the surface 23 cm, particularly in the 0-5 cm depth increment. The greatest concentration in this increment was recorded two days after application (7/13) and decreased thereafter. The data show that metribuzin was present in significantly detectable quantities to a depth of 61 cm for 9 days after application in both the vegetation and no-vegetation plots. However, the concentration of metribuzin decreased with time at all depths. Unfortunately, not all the residue data on the no-vegetation plot are available, and complete conclusions are impossible. However, the decrease in metribuzin concentration is attributed to microbial degradation because losses by volatilization, change in form, and photodecomposition are thought to be negligible under the conditions of the experiment. The amount of metribuzin per unit volume of soil ($\mu\text{g}/\text{cm}^3$) and the amount of metribuzin per unit area of soil ($\mu\text{g}/\text{cm}^2$) are given in Tables 11 and 12, respectively.

A mass balance of metribuzin was computed for the 122 cm profile and is given in Table 13. Two days after application 72.6 and 33.6% could be detected in the vegetation and no-vegetation plots, respectively. As with Cl^- , a large amount of the metribuzin moved through the profile and out of the sampling zone with the leaching water. Because the metribuzin was dissolved in this water and had no equilibration time

Table 10. Metribuzin concentration (ppm) as a function of soil depth during the field experiment.

Depth (cm)	Metribuzin Concentration (ppm)							
	Initial	7/12	7/13	7/16	7/20	7/27	8/1	9/23
Vegetation								
0-5	T	3.9	4.6	2.4	2.3	1.2	0.8	0.2
5-10	T	0.7	1.2	0.6	0.6	0.3	0.1	T
10-15	T	0.6	0.7	0.5	0.6	0.4	0.1	T
15-23		0.8	0.6	0.5	1.1	0.1	T	T
23-30			0.2	0.1	0.5	T	T	T
30-46			0.2	0.3	0.5	0.1	T	T
46-61			0.1	T	0.1	T	0.1	0.1
61-91			T	T	T	T	T	T
91-122			T	T	T	T	T	T
No Vegetation								
0-5	T	0.55	0.56	0.53	0.33	0.18	0.16	0.06
5-10	T	0.17	0.18	0.20	0.13	0.11	0.08	0.03
10-15	T	0.17	0.34	0.20	0.17	0.15	0.08	0.03
15-23		0.20	0.32	0.19	0.20	0.16		
23-30								
30-46		0.11	0.31	0.20	0.22			
46-61		0.08	0.34	0.34	0.21			
61-91		0.04						
91-122		0.05						

Table 11. Metribuzin concentration ($\mu\text{g}/\text{cm}^3$) as a function of soil depth during the field experiment.

Depth (cm)	Metribuzin Concentration ($\mu\text{g}/\text{cm}^3$)							
	Initial	7/12	7/13	7/16	7/20	7/27	8/1	9/23
Vegetation								
0-5	T	5.85	6.90	3.60	3.45	1.80	1.20	0.30
5-10	T	1.09	1.87	0.94	0.94	0.47	0.16	T
10-15	T	0.94	1.09	0.78	0.94	0.62	0.16	T
15-23		1.24	0.94	0.78	1.72	0.16	T	T
23-30			0.30	0.15	0.75	T	T	T
30-46			0.29	0.43	0.71	0.14	T	T
46-61			0.15	T	0.15	T	0.15	0.15
61-91			T	T	T	T	T	T
91-122			T	T	T	T	T	T
No Vegetation								
0-5	T	0.83	0.84	0.80	0.50	0.27	0.24	0.09
5-10	T	0.26	0.28	0.31	0.20	0.17	0.12	0.05
10-15	T	0.26	0.53	0.31	0.27	0.23	0.13	0.05
15-23		0.31	0.50	0.30	0.31	0.25		
23-30								
30-46		0.16	0.44	0.29	0.32			
46-61		0.12	0.52	0.52	0.32			
61-91		0.06						
91-122		0.07						

Table 12. Metribuzin concentration ($\mu\text{g}/\text{cm}^2$) as a function of soil depth during the field experiment.

Depth (cm)	Metribuzin Concentration ($\mu\text{g}/\text{cm}^2$)							
	Initial	7/12	7/13	7/16	7/20	7/27	8/1	9/23
Vegetation								
0-5	T	29.72	35.05	18.29	17.53	9.14	6.10	1.52
5-10	T	5.54	9.50	4.78	4.78	2.39	0.81	T
10-15	T	4.78	5.54	3.96	4.78	3.15	0.81	T
15-23		9.53	7.16	5.94	13.11	1.22	T	T
23-30			2.29	1.14	5.71	T	T	T
30-46			4.42	6.55	10.82	2.13	T	T
46-61			2.29	T	2.29	T	2.29	2.29
61-91			T	T	T	T	T	T
91-122			T	T	T	T	T	T
No Vegetation								
0-5	T	4.19	4.27	4.04	2.51	1.37	1.22	0.46
5-10	T	1.33	1.41	1.56	1.02	0.86	0.62	0.23
10-15	T	1.31	2.69	1.58	1.35	1.19	0.64	0.23
15-23		2.38	3.80	2.26	2.38	1.91		
23-30								
30-46		2.39	6.74	4.36	4.80			
46-61		1.86	7.92	7.92	4.89			
61-91		1.92						
91-122		2.26						

Table 13. Amount and percentage recovery of metribuzin in the solute transport plot.

Plot	Sampling Date					
	7/13	7/16	7/20	7/27	8/1	9/23
Vegetation						
Amount added (g)	33.9	33.9	33.9	33.9	33.9	33.9
Amount recovered (g)	24.7	15.1	22.0	6.7	3.7	1.4
% recovered	72.6	44.6	64.7	19.8	11.0	4.2
No Vegetation						
Amount added (g)	33.9	33.9	33.9	33.9	33.9	33.9
Amount recovered (g)	11.4	9.0	7.2	2.0	0.9	0.3
% recovered	33.6	26.4	21.3	5.8	2.7	1.0

with soil surfaces, it obviously would move readily with the water, especially if no interaction with organic matter and clay surfaces occurred along the travel path. The higher recovery percentage in the vegetation plots can be attributed to a greater concentration in the surface 23 cm of soil. This higher concentration may be caused by the adsorptive effects of the grass which would retard metribuzin movement into the soil by "sorption" onto leaves, roots and stems. The grass in the vegetation plot presented a large surface area available for adsorption of the herbicide.

The relationship between the logarithm of the metribuzin residues and time in the two plots is shown in Figure 11. Assuming a first order degradation process, the rate coefficients were 0.0879 and 0.135 day⁻¹ of the vegetation and no-vegetation plots, respectively. The metribuzin half lives were calculated to be 7.88 and 5.13 days. The longer half life in the vegetation plot can be attributed to lower soil temperatures, especially in the surface horizon. The average half life of 6.51 days for the two plots agrees well with the half-life values published by Hyzak and Zimdahl (1974) of 16 days at 35°C in air-dry soil and Lay and Ilnicki (1974) of 6 days at 28°C in soil at 60% of "field capacity."

Comparison of Water and Solute Fluxes

Solutes such as Cl⁻ and metribuzin are shown by the foregoing data to move with water in the soil. It is of interest to compare the magnitudes of the transport rates of soil water, Cl⁻ and metribuzin during the monitoring period for the two moisture regimes. This comparison would give information on the interactions between the solutes and soil surfaces. Because transport of metribuzin in soil was

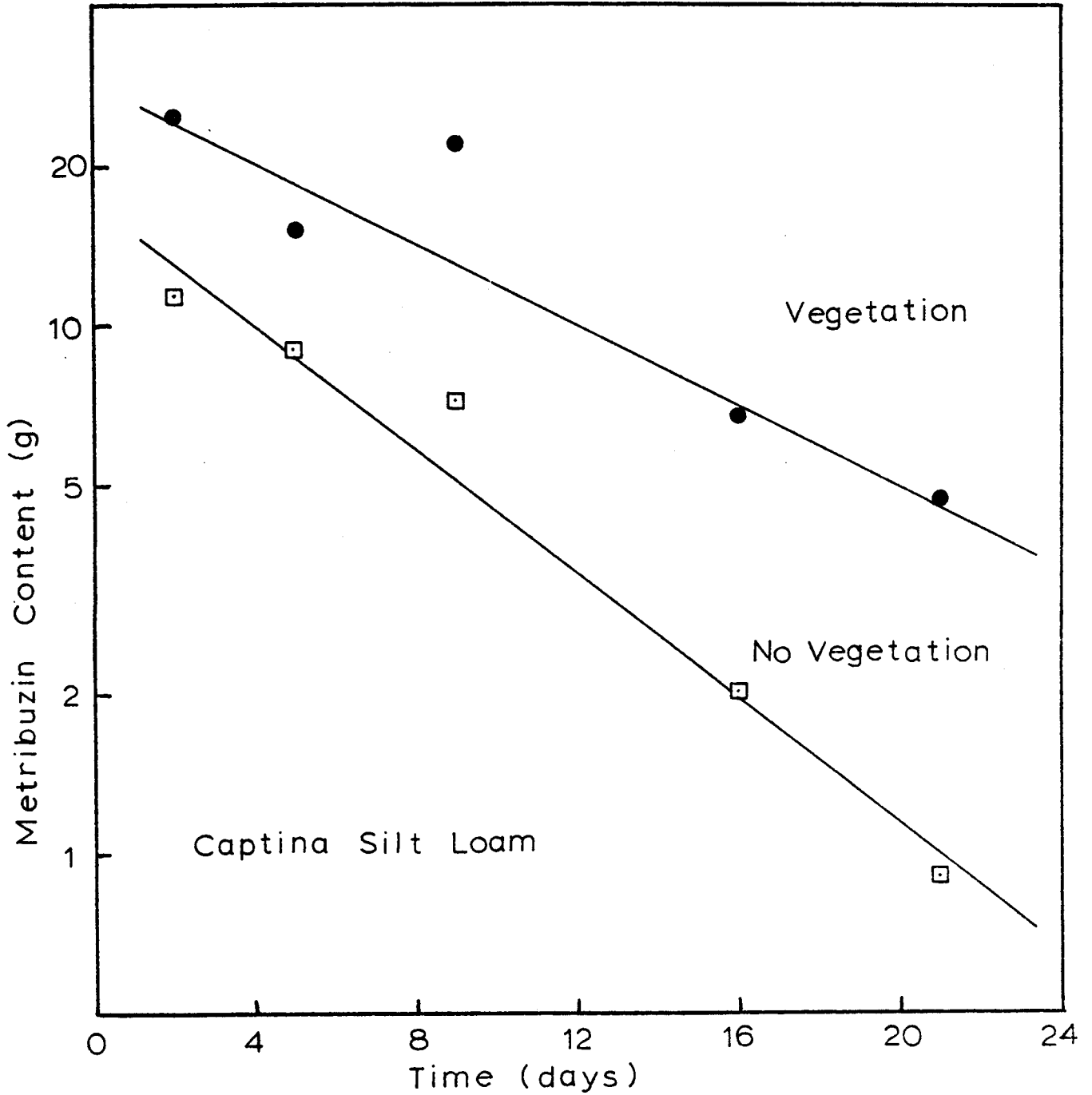


Figure 11. Relation between the logarithm of metribuzin concentration and time for vegetation and non-vegetation plots.

complicated by microbial degradation processes, most of the discussion centers on water and Cl^- fluxes.

Fluxes of water and Cl^- across the 15 cm depth are given for both plots in Figure 12. In both the vegetation and no-vegetation plots, water initially was moving upward whereas Cl^- was moving downward. It is postulated that water was moving in two directions simultaneously in response to thermal gradients, localized matric gradients caused by water extraction by plant roots, and the overall matric and gravitational gradients. It is thought that the downward movement of water occurred in the large pores and transported the Cl^- downward faster than the rate of Cl^- diffusion into the smaller pores. Upward movement of water may have occurred in the smaller pores where the Cl^- concentration was lower because of anion exclusion. In addition, some of the water may have moved upward in the vapor phase. Thus, the net water movement was in the upward direction whereas the net Cl^- movement was in the downward direction. After a few days, the flux curves of Cl^- and water were roughly parallel, both indicating upward movement of water and Cl^- . Rainfall during August and early September reversed the flow direction. After these rains the Cl^- concentration (Table 6) in the surface remained greater than that at any point in the profile. Thus, water, whether in the evaporation or infiltration process, affects but does not completely govern Cl^- movement in the Captina soil. Initial upward movement of water was greater in the vegetation covered plot. Because the greatest density of grass roots usually is in the surface 15 cm of soil, the extraction of soil water by the grass roots in the vegetation plot created hydraulic gradients and fluxes of greater magnitude than those caused by the evaporation from the no-vegetation plot. Later, as the

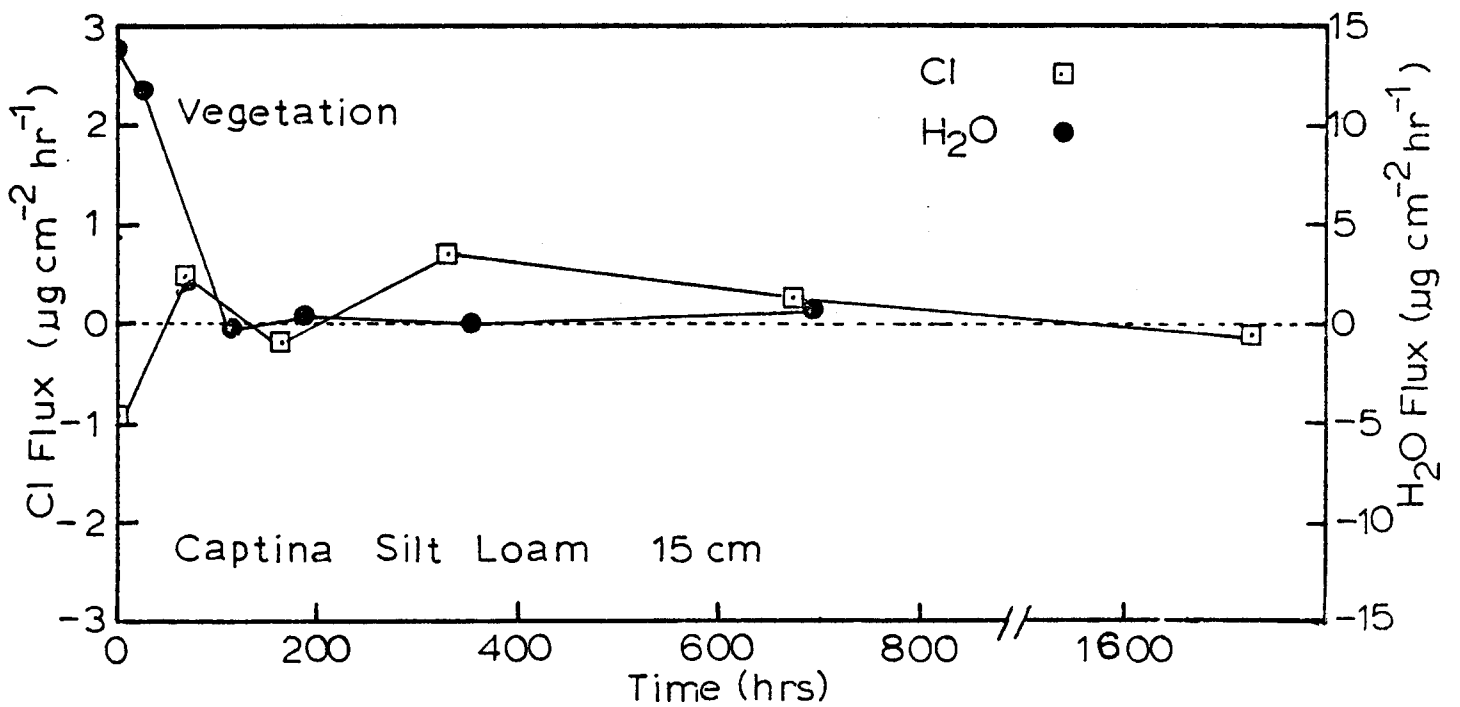
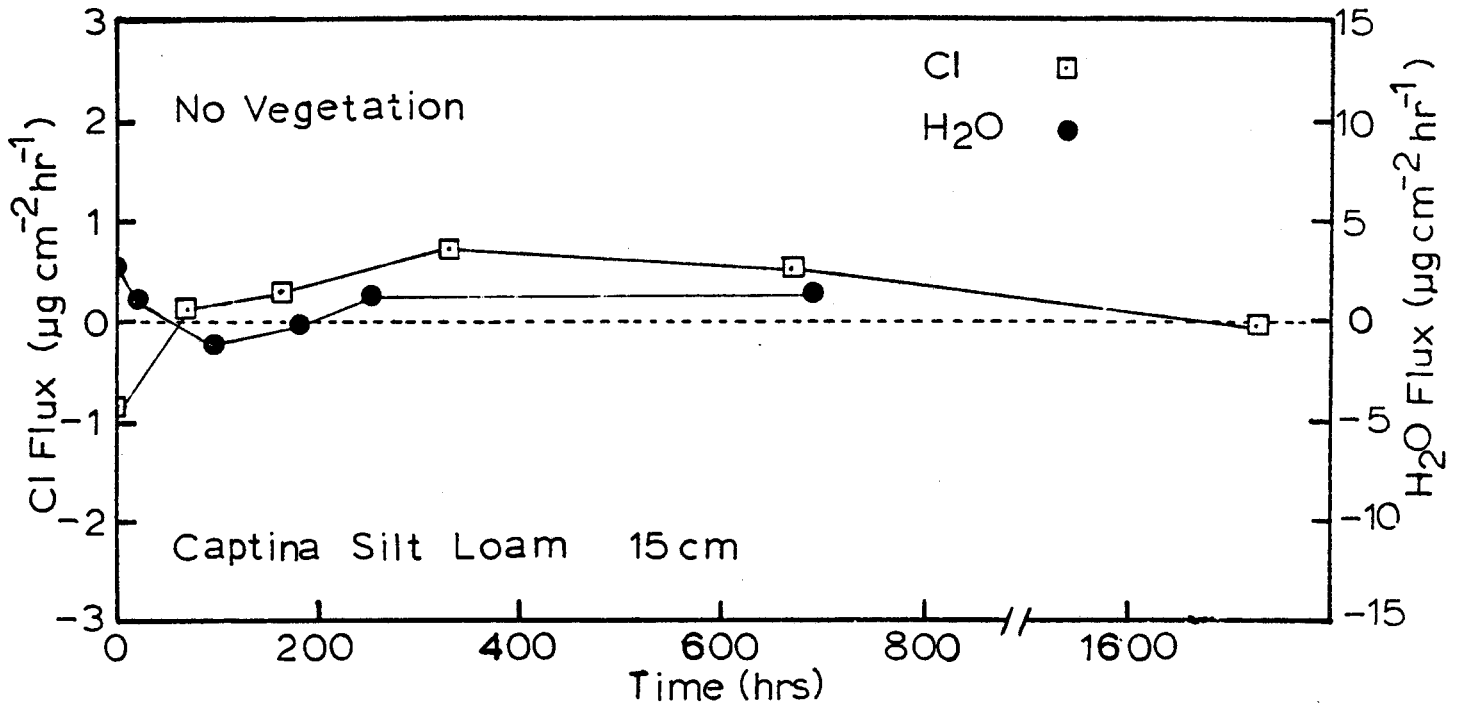


Figure 12. Fluxes of water and Cl^- across 15 cm depth in solute transport plot.

grass died, the gradients and fluxes of water were greater in the no-vegetation plot.

Fluxes of water and Cl^- across the 45 cm depth are given for both plots in Figure 13. The percolating water initially was moving downward in both plots and continued to flow downward at a greater rate for a longer period of time than at the 15 cm depth. The water changed direction sooner in the no-vegetation plot because of the influence of its greater evaporation rate. The fact that the Cl^- fluxes were roughly parallel with those of water indicated that a constant mass of Cl^- was transported across the 45 cm depth. The magnitudes of the water and Cl^- fluxes were greater across the 45 cm depth than across the 15 cm depth. For example, the water fluxes were as much as 50 times greater, whereas the Cl^- fluxes were only twice as great. This result points to the fact that water and Cl^- were not moving at the same rate, i.e. not in a 1:1 mass ratio.

Fluxes for water and Cl^- across the 122 cm depth are shown in Figure 14. Water was flowing downward past this depth for a longer time than at the shallower depths. The magnitudes of the water fluxes at this depth are for the most part lower than those observed across the 45 cm depth but are greater than those across the 15 cm depth. Chloride was observed to move upward during most of the monitoring period. Thus, the fluxes of Cl^- and water were not necessarily in the same direction or of the same magnitude at any given time during the experiment. These data seem to indicate that soil-water solute transport under field conditions is extremely complicated and that one cannot simply multiply the flux of water by the Cl^- concentration to determine the amount of Cl^- moved out of the Captina profile.

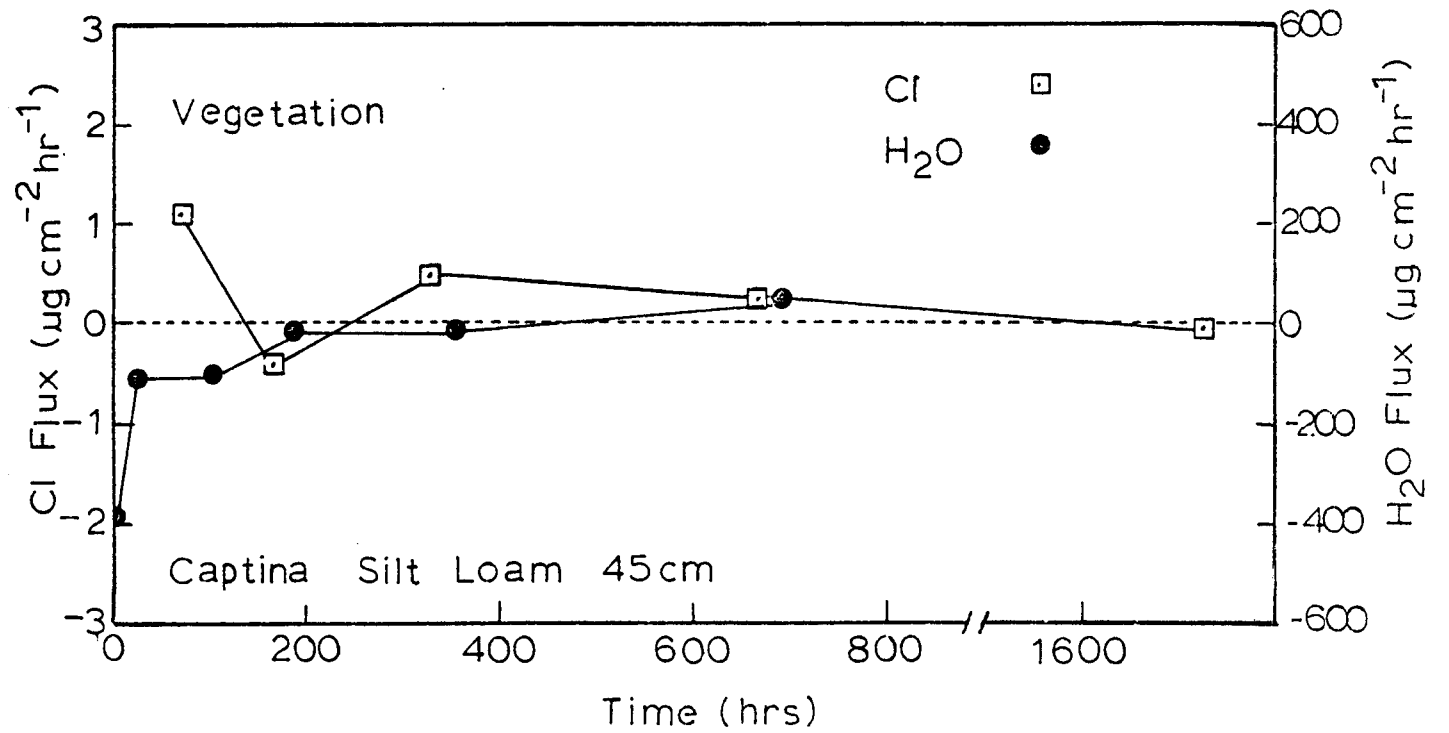
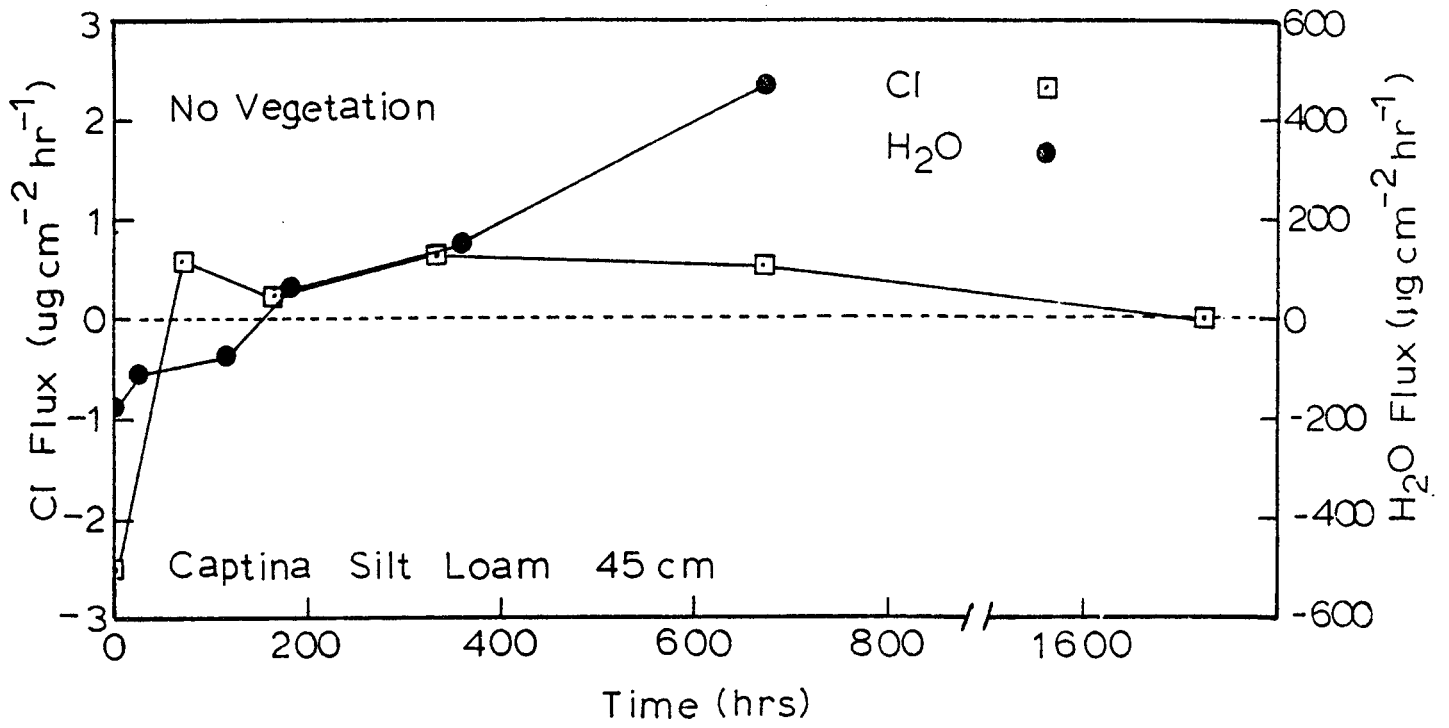


Figure 13. Fluxes of water and Cl⁻ across 45 cm depth in solute transport plot.

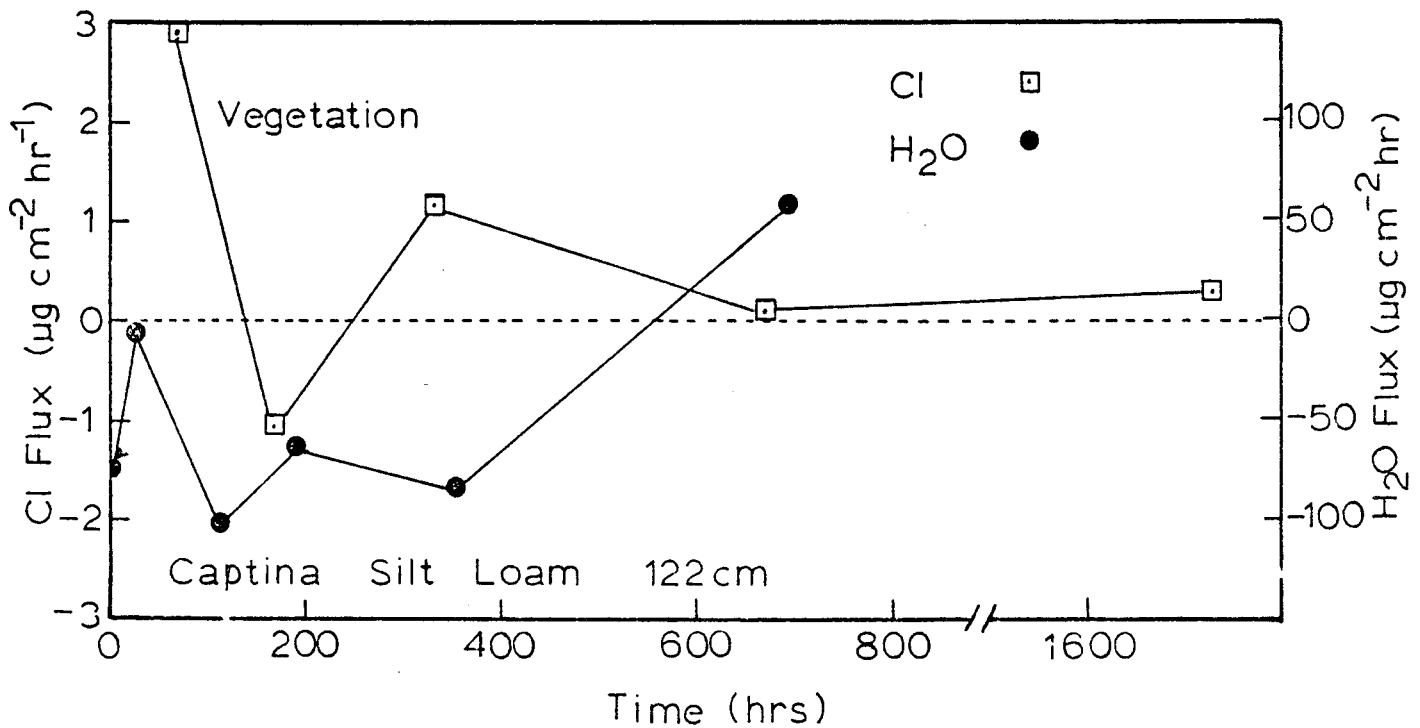
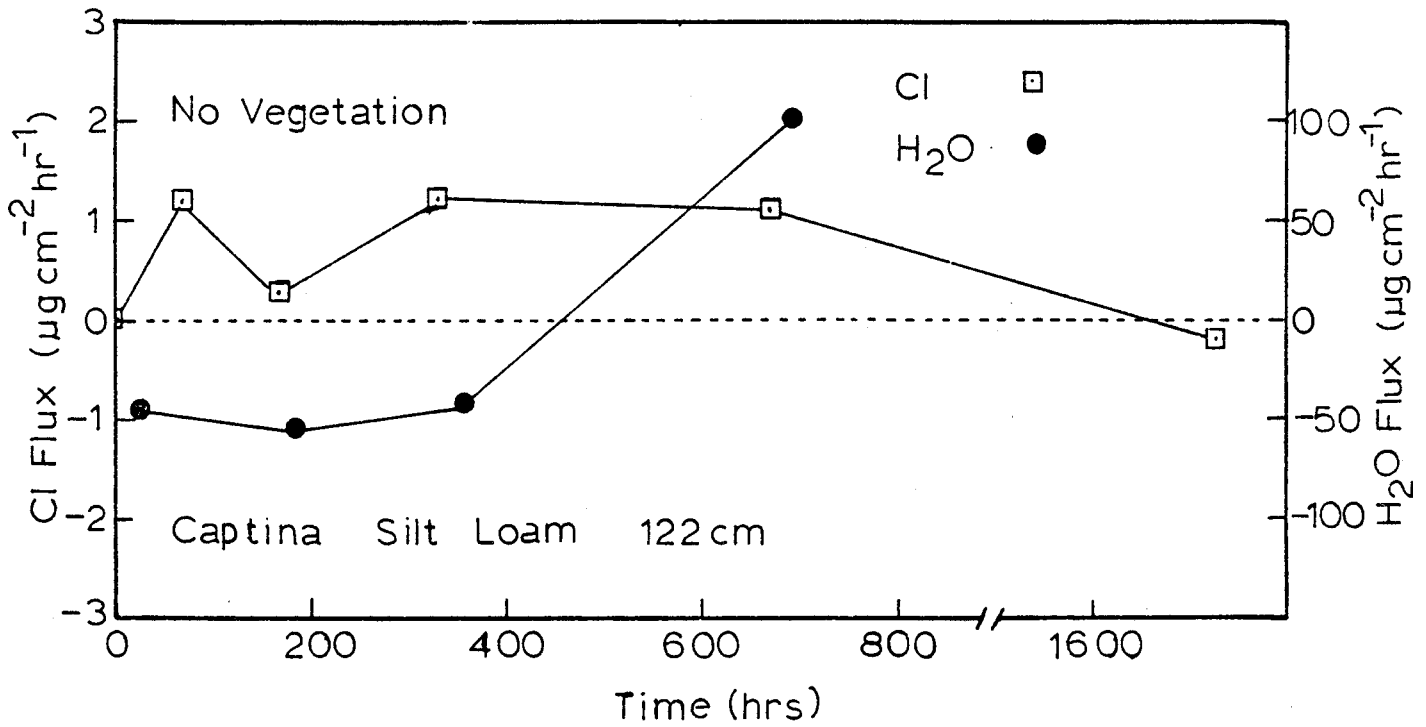


Figure 14. Fluxes of water and Cl⁻ across 122 cm depth in solute transport plot.

Laboratory Study

Adsorption-desorption of Metribuzin

Adsorption and desorption characteristics of metribuzin were determined as functions of concentration and equilibration time for two horizons (Ap and B2t) in the Captina and one horizon (Ap) in the Dubbs. The soil:water ratio in the Dubbs was 1:1 and the equilibration time was four hours. The soil:water ratio in the Captina was 1:2 and the equilibration time was 168 hours. Adsorption-desorption isotherms for the Dubbs Ap and Captina Ap and B2t horizons are given in Figures 15 through 17, respectively. Each data point represents the average of four or more determinations. The linear relationship between the amount adsorbed and the solution concentration suggests that under equilibrium conditions adsorption of metribuzin can be described adequately with the Freundlich equation where the exponent $1/n$ has a magnitude close to 1. Freundlich plots of the data (Figures 18 and 19) show the exponent $1/n$ for the Ap and B2t horizons of the Captina soil to be 1.04 and 0.85, respectively. Figures 20 and 21 show Freundlich model lines fitted to the data. Table 14 lists the Freundlich constants for the adsorption and desorption curves. A comparison of the amounts adsorbed by the two soils can be made by calculating the distribution coefficients, K_d , which are the slopes of the lines in Figures 15 through 17. The K_d values calculated from a least squares fit of the data for the Ap horizons of the Dubbs and Captina soils were 0.54 and 0.46, respectively. The K_d for the B2t horizon of the Captina soil was 0.18. These relatively low K_d values indicate that more herbicide was present in the solution phase than in the adsorbed phase and suggest that metribuzin

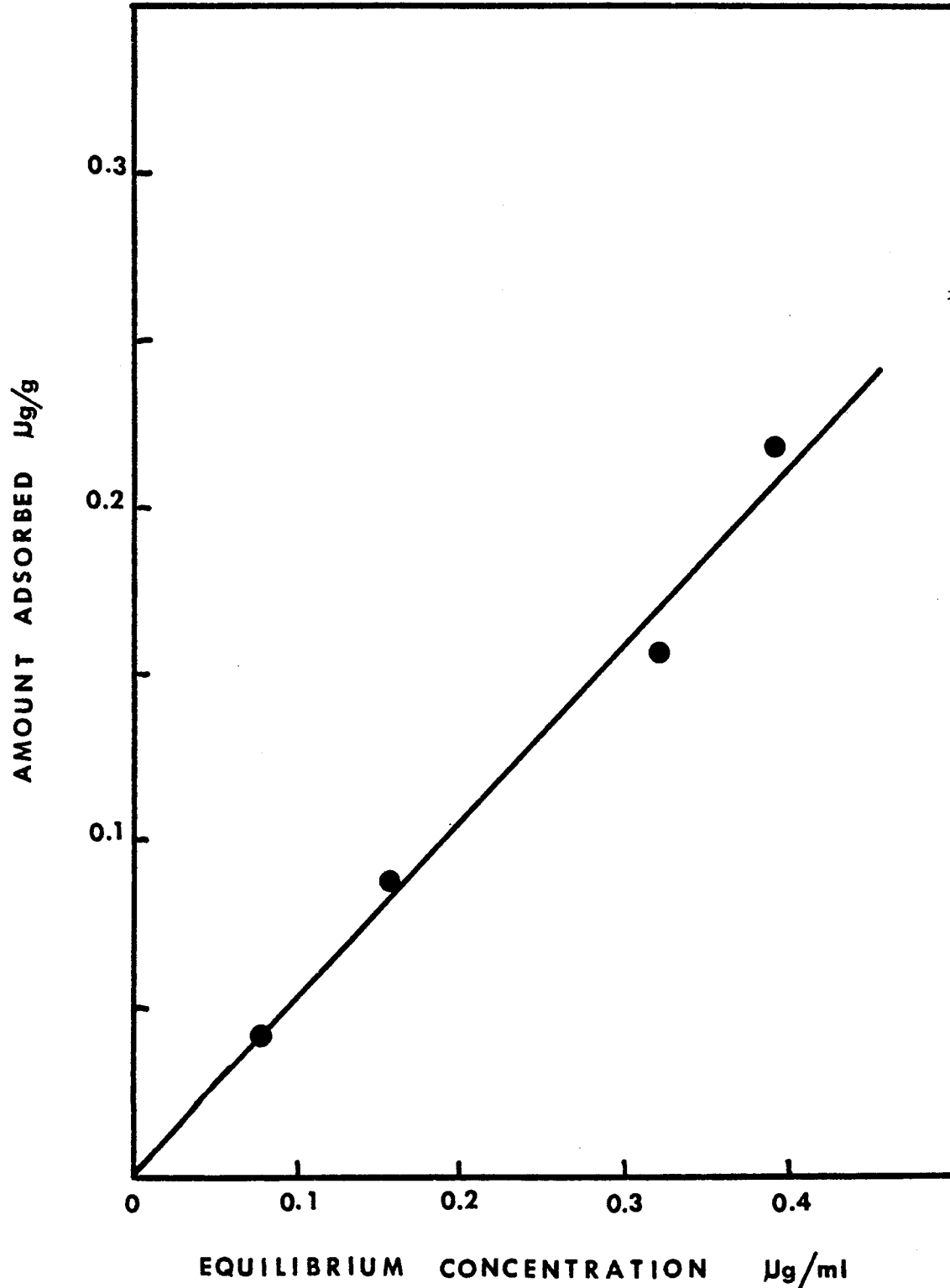


Figure 15. Adsorption of ^{14}C -metribuzin by Ap horizon of the Dubbs soil.

Figure 16. Adsorption-desorption of ^{14}C -metribuzin by Ap horizon of Captina soil.

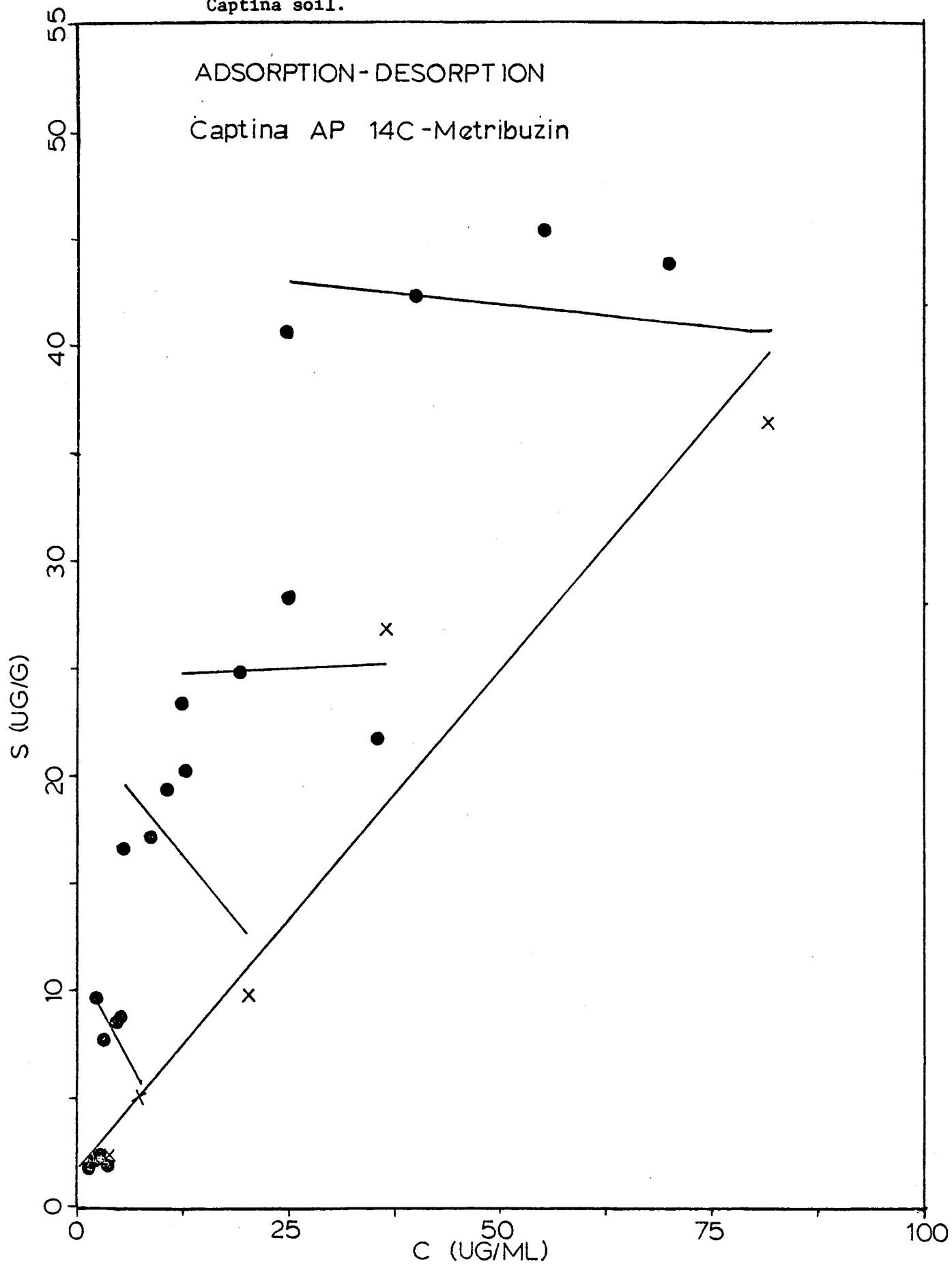
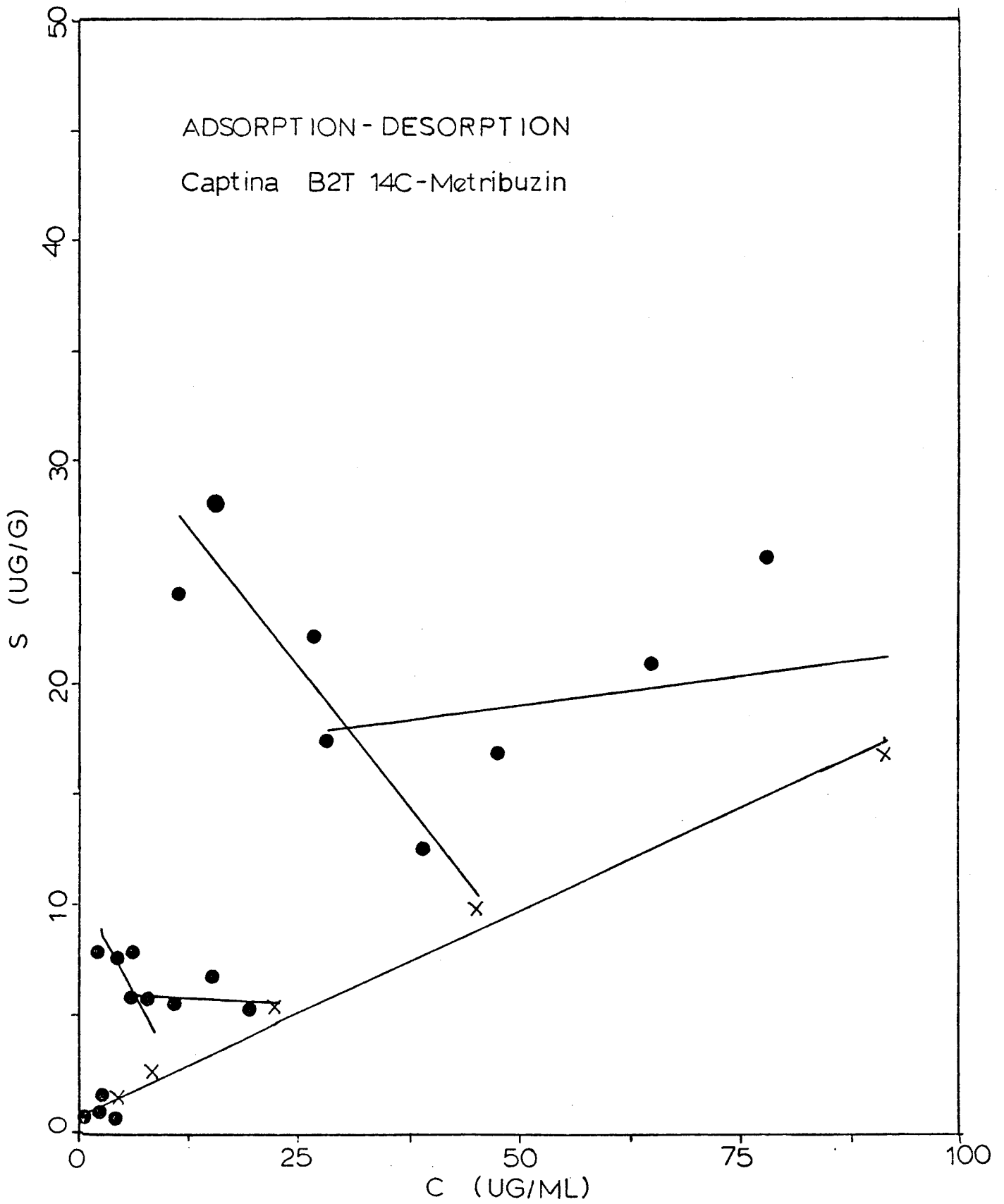


Figure 17. Adsorption-desorption of ^{14}C -metribuzin by B2t horizon of Captina soil.



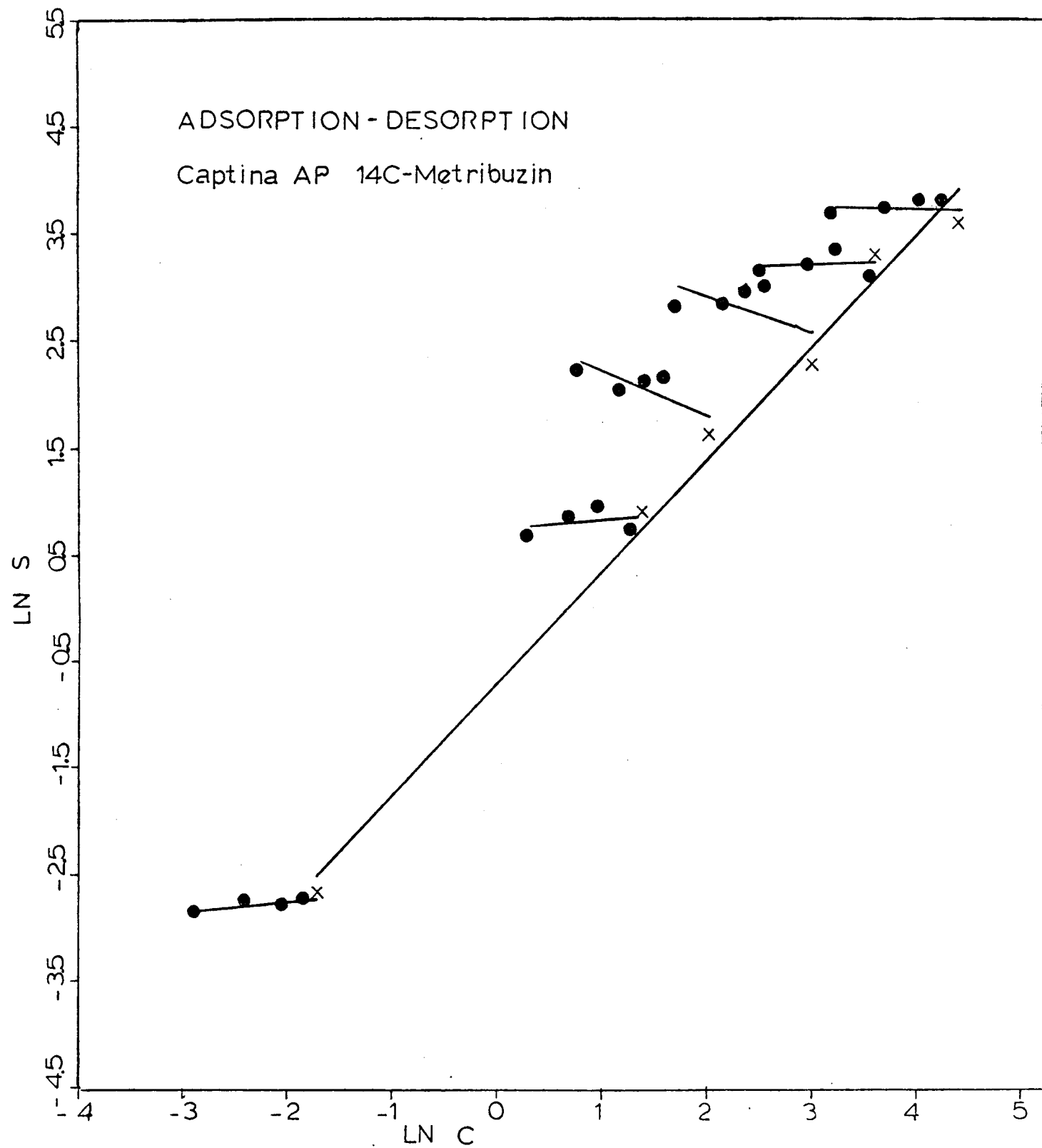


Figure 18. Freundlich plot of adsorption-desorption of ^{14}C -metribuzin by Ap horizon of Captina soil.

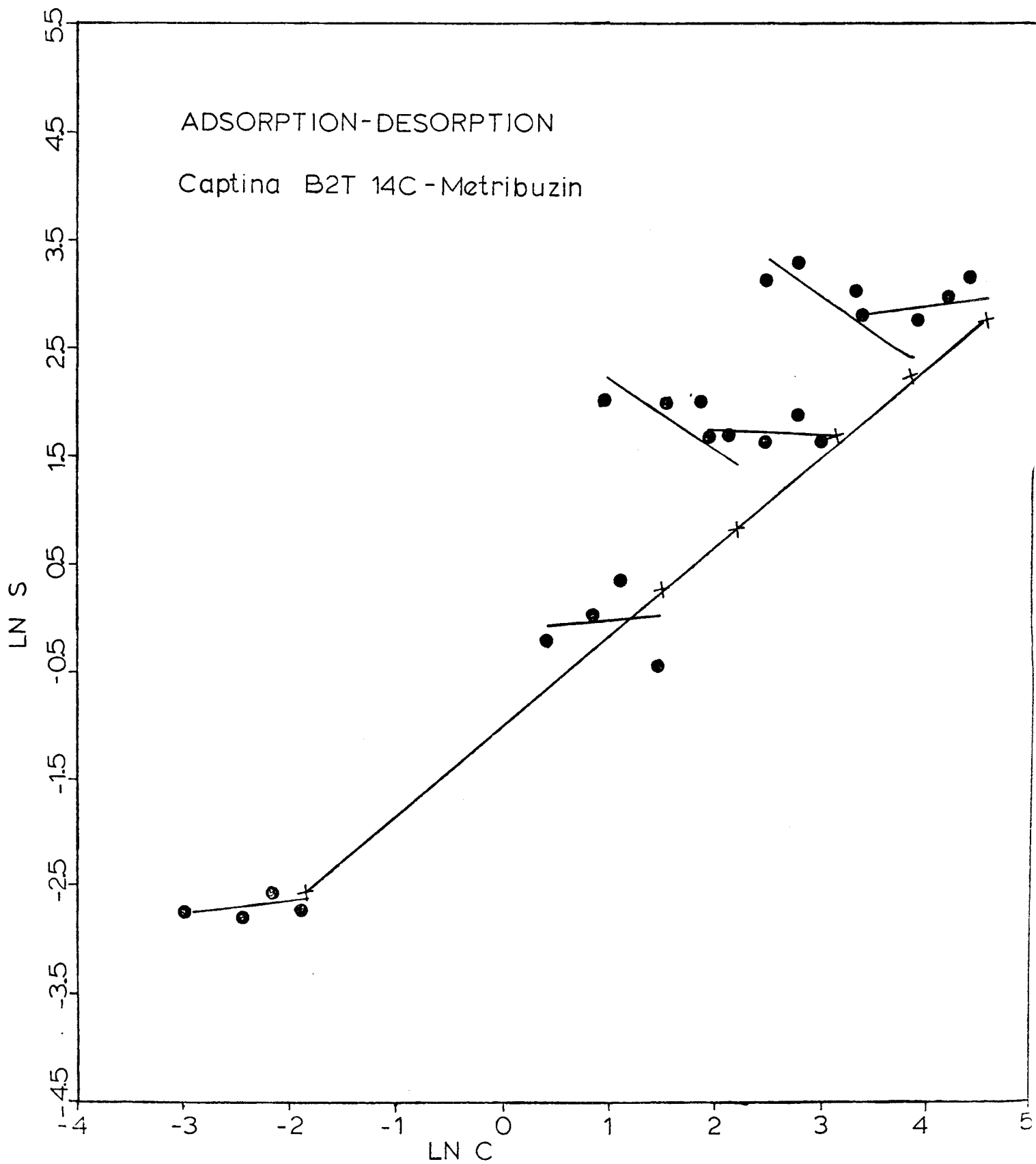


Figure 19. Freundlich plot of adsorption-desorption of ^{14}C -metribuzin by B2t horizon of Captina soil.

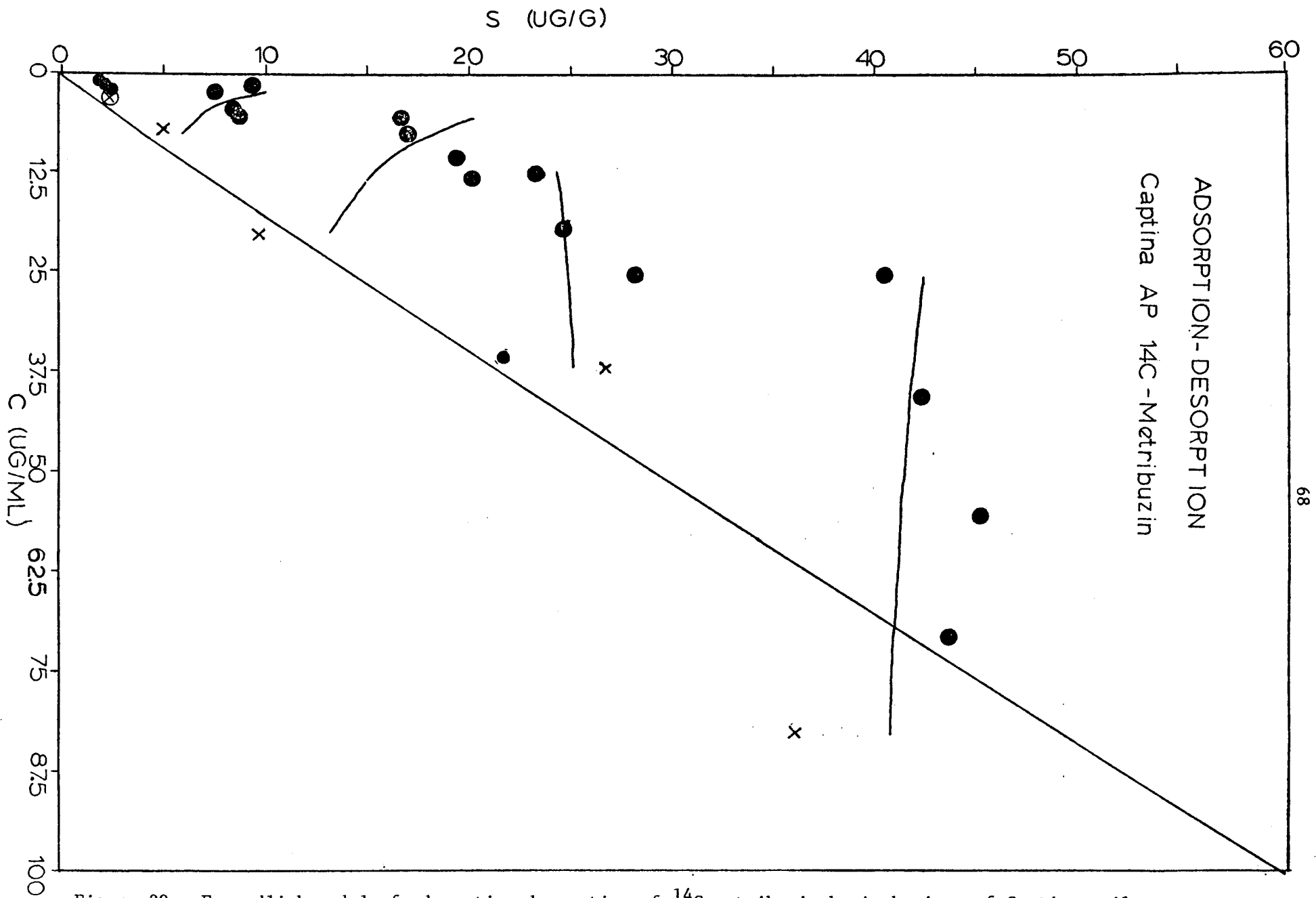


Figure 20. Freundlich model of adsorption-desorption of ^{14}C -metribuzin by Ap horizon of Captina soil.

Figure 21. Freundlich model of adsorption-desorption of ^{14}C -metribuzin by B2t horizon of Captina soil.

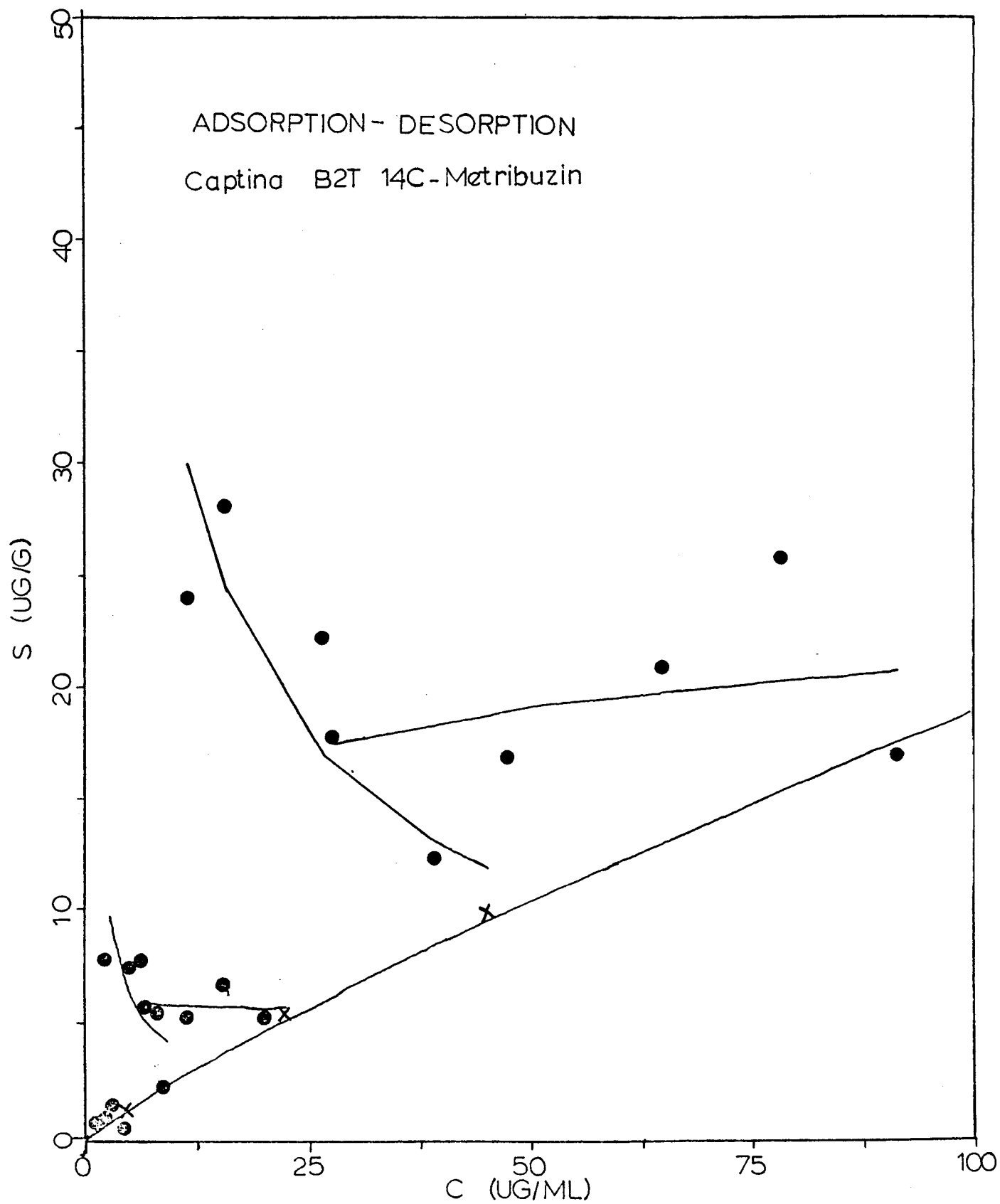


Table 14. Freundlich adsorption and desorption constants for metribuzin on a Captina silt loam.

Soil Horizon	k	n
Ap		
Adsorption	0.49	0.96
Desorption		
0.2 ppm	0.08	9.08
5.0 ppm	2.10	11.11
10.0 ppm	14.03	-2.33
25.0 ppm	35.06	-3.03
50.0 ppm	22.75	33.33
100.0 ppm	47.22	-33.33
B2t		
Adsorption	0.37	1.18
Desorption		
0.2 ppm	0.09	7.69
5.0 ppm	0.93	11.11
10.0 ppm	18.39	-1.47
25.0 ppm	6.42	-33.33
50.0 ppm	158.55	-1.47
100.0 ppm	10.72	6.67

should be relatively mobile in the soil. In the Captina soil the K_d value for the Ap horizon was observed to be twice as large as that for the B2t even though the latter horizon contained more clay and had a higher cation exchange capacity. The Ap horizon did contain approximately twice as much organic matter as the B2t (Table 15); distribution coefficients have been shown to be highly correlated with organic matter (Hamaker and Thompson, 1972). The Ap horizons in the Dubbs and Captina soils had approximately the same organic matter contents and had similar cation exchange capacities which account for the similar K_d values.

If the adsorption of metribuzin could be described with a first-order rate equation, a plot of $\ln(1/1-f)$, where f is the fraction adsorbed, versus equilibration (shaking) time, would yield a straight line with a slope proportional to the rate constant and an intercept of zero. This plot is shown in Figure 22 for the Ap horizon of the Captina soil. Each data point represents the average of four or more observations. The adsorption of metribuzin by the Captina soil is not a first-order process but consists of three stages. The first adsorption stage is rapid, the second is highly dependent on the shaking time, and in the third stage little additional metribuzin is adsorbed with time. The straight line obtained in a plot of K_d versus the logarithm of the shaking time (Figure 23) supports this hypothesis. In an attempt to determine whether metribuzin adsorption is a diffusion-controlled process in this soil, a plot was constructed showing the amount adsorbed versus the square root of the shaking time (Figure 24). For adsorption far from equilibrium, the amount of herbicide adsorbed is directly proportional to the square root of the shaking time if adsorption is diffusion controlled. Although straight lines can be drawn

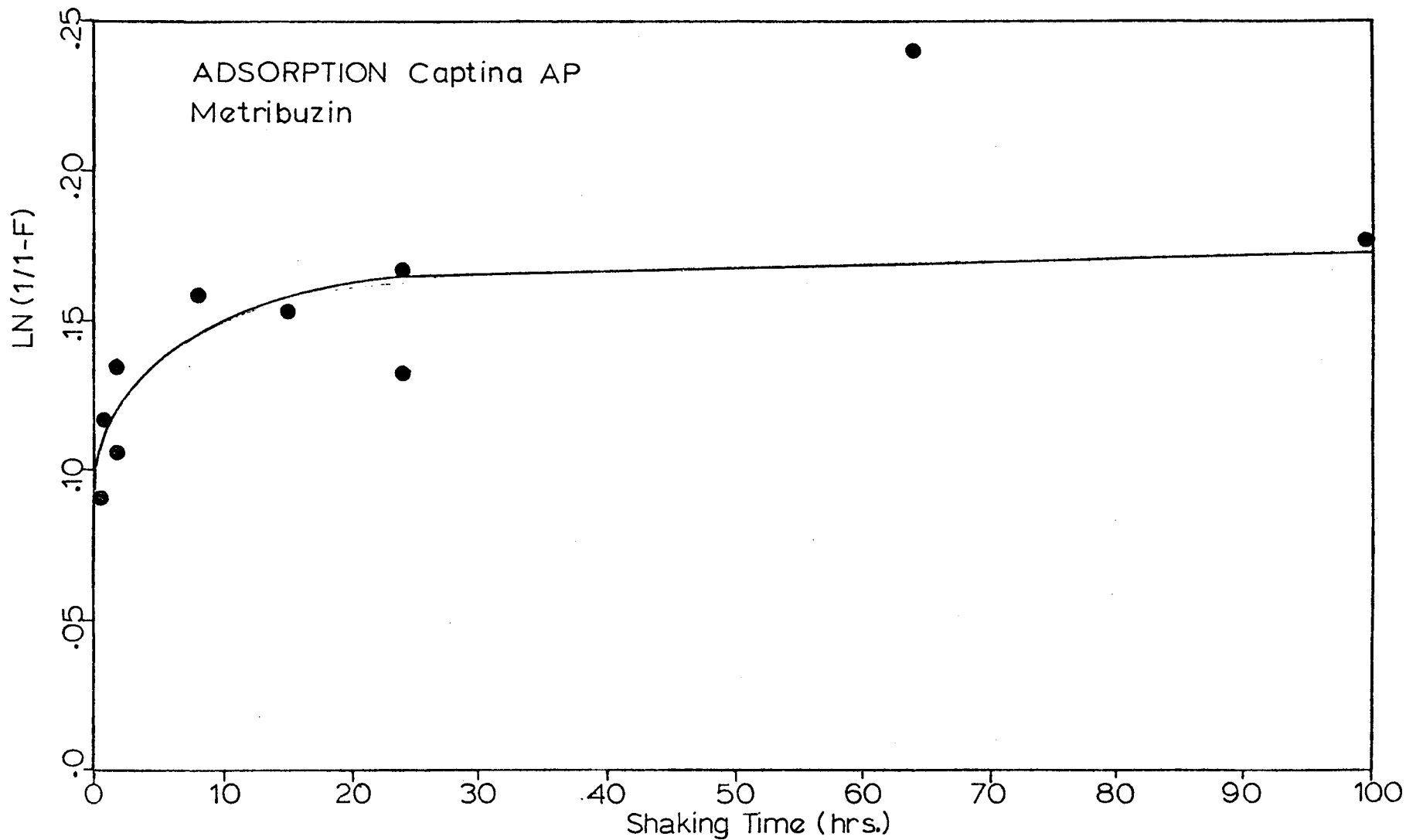


Figure 22. First order adsorption plot of adsorption of ^{14}C -metribuzin by Ap horizon of Captina soil.

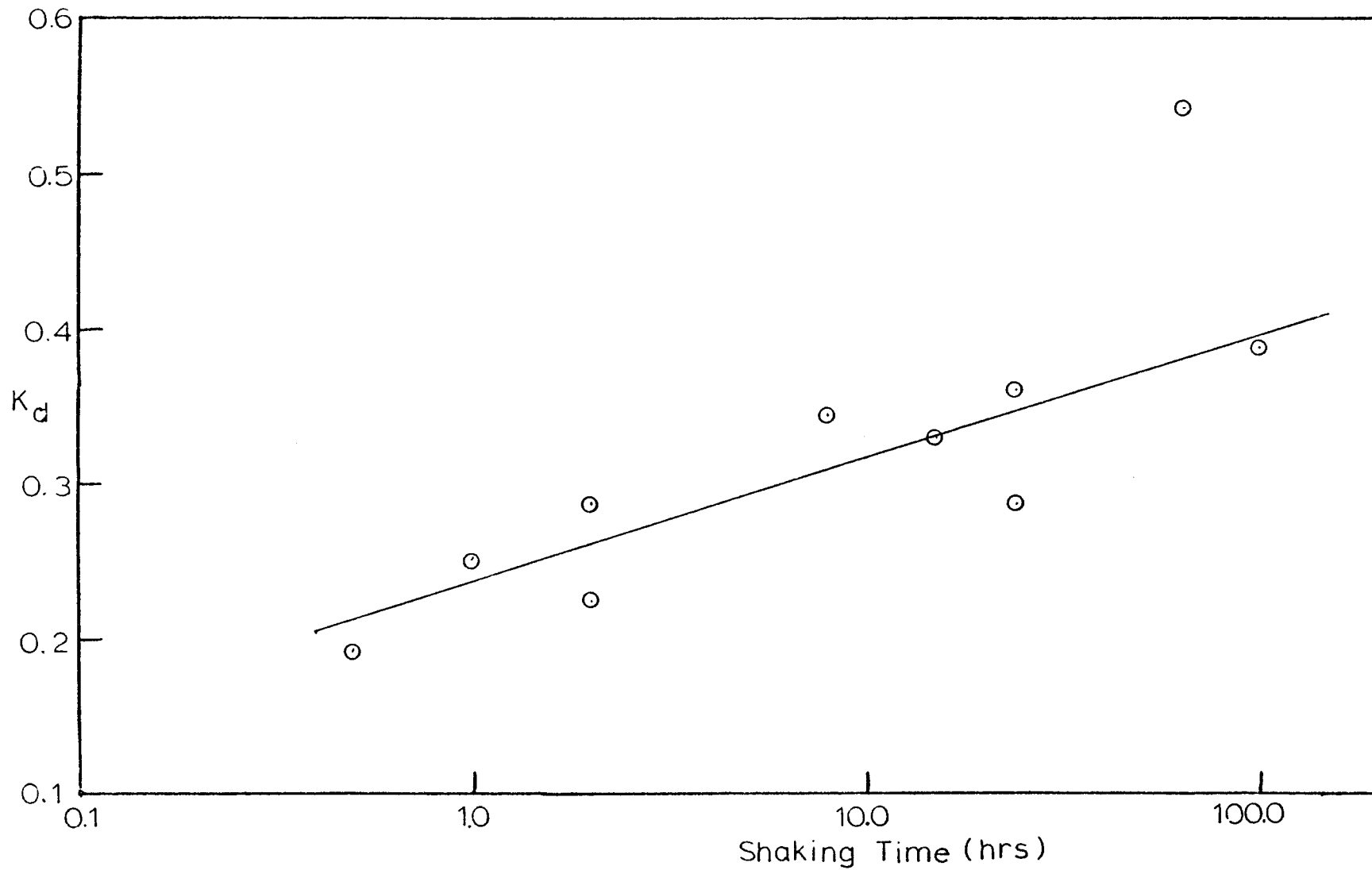


Figure 23. Relation between distribution coefficient (K_d) and the logarithm of shaking time.

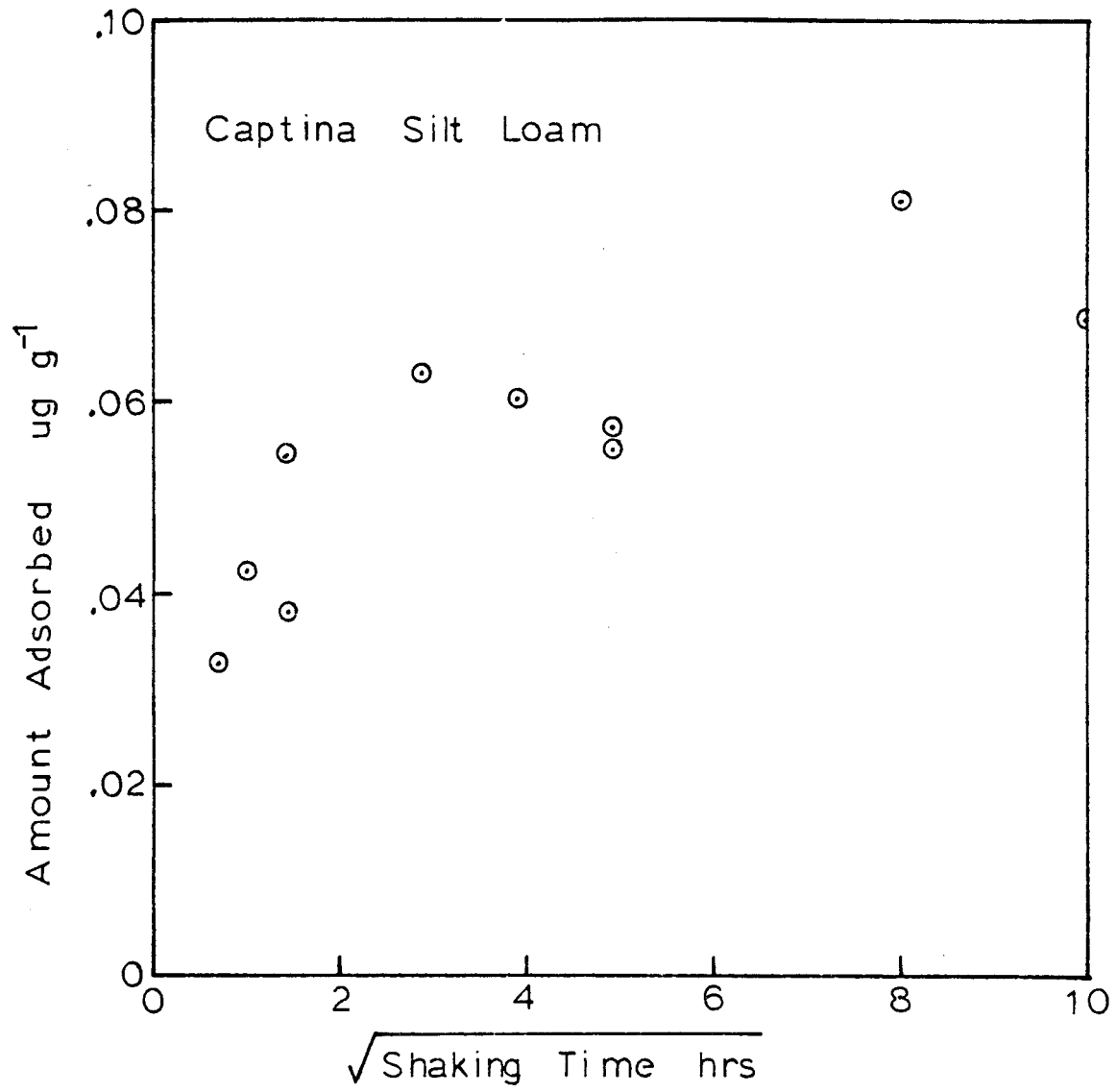


Figure 24. Relation between amount of metribuzin adsorbed and the $t^{1/2}$ for Captina silt loam.

through data points, a better overall fit can be obtained with a curved line.

The distribution coefficient (K_d) of the Dubbs soil is plotted against shaking time in Figure 25. As in the Captina soil, the results at short shaking times (less than 5 hours) show considerable variation which indicates that equilibrium has not been reached. No data are available for longer shaking times.

Although only a small fraction of the herbicide is absorbed by the Captina soil, the desorption data suggest that metribuzin is strongly adsorbed by soil surfaces. Most of the slopes of the desorption isotherms shown in Figures 16 through 19 are negative (Table 14) indicating that metribuzin was adsorbed during the desorption process. This result can be illustrated further by the data shown in Figures 26 and 27. They show that with successive extraction the amount of adsorbed metribuzin either remains approximately the same as that initially adsorbed or actually increases. The increase in adsorbed metribuzin is more pronounced in the Ap horizon of Captina than in the B2t as would be expected considering its higher K_d value. Possible explanations for this result include (1) a lack of equilibrium between the adsorbed and solution phases, or (2) a change in soil structure during the equilibration process which exposes more surfaces for adsorption. It is unclear from the data what the actual explanation is.

Self-Diffusion of $^3\text{H}\text{OH}$, ^{36}Cl , and ^{14}C -Metribuzin

Experiments were conducted to study the effects of several soil physical and chemical properties on the magnitude of the self-diffusion coefficients of $^3\text{H}\text{OH}$, ^{36}Cl , and ^{14}C -metribuzin.

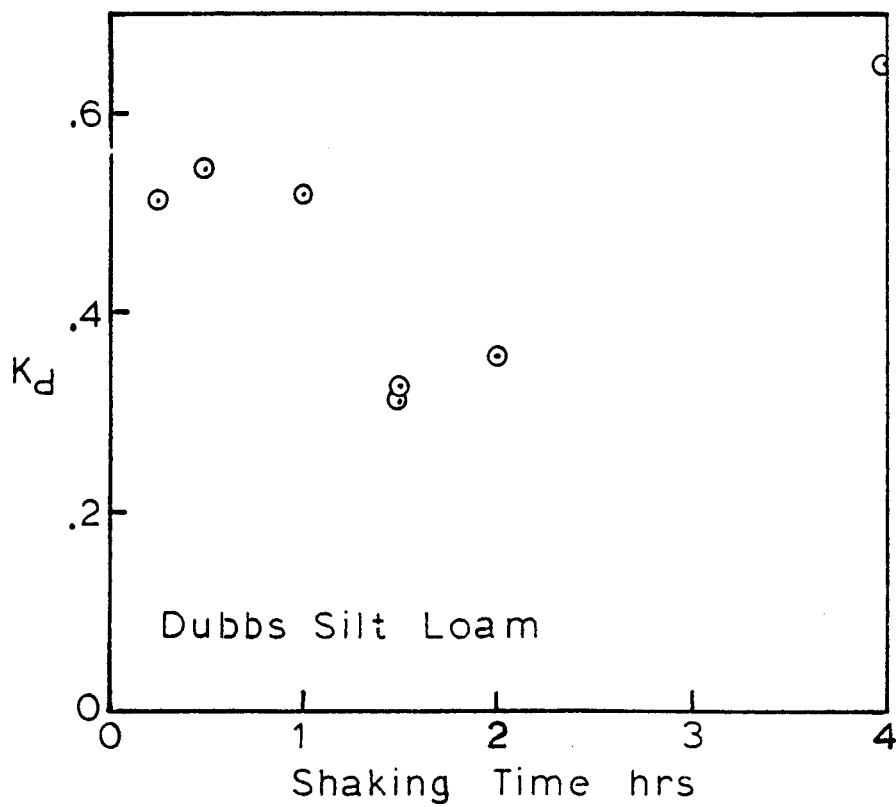


Figure 25. Relation between adsorption of metribuzin and shaking time for the Dubbs soil.

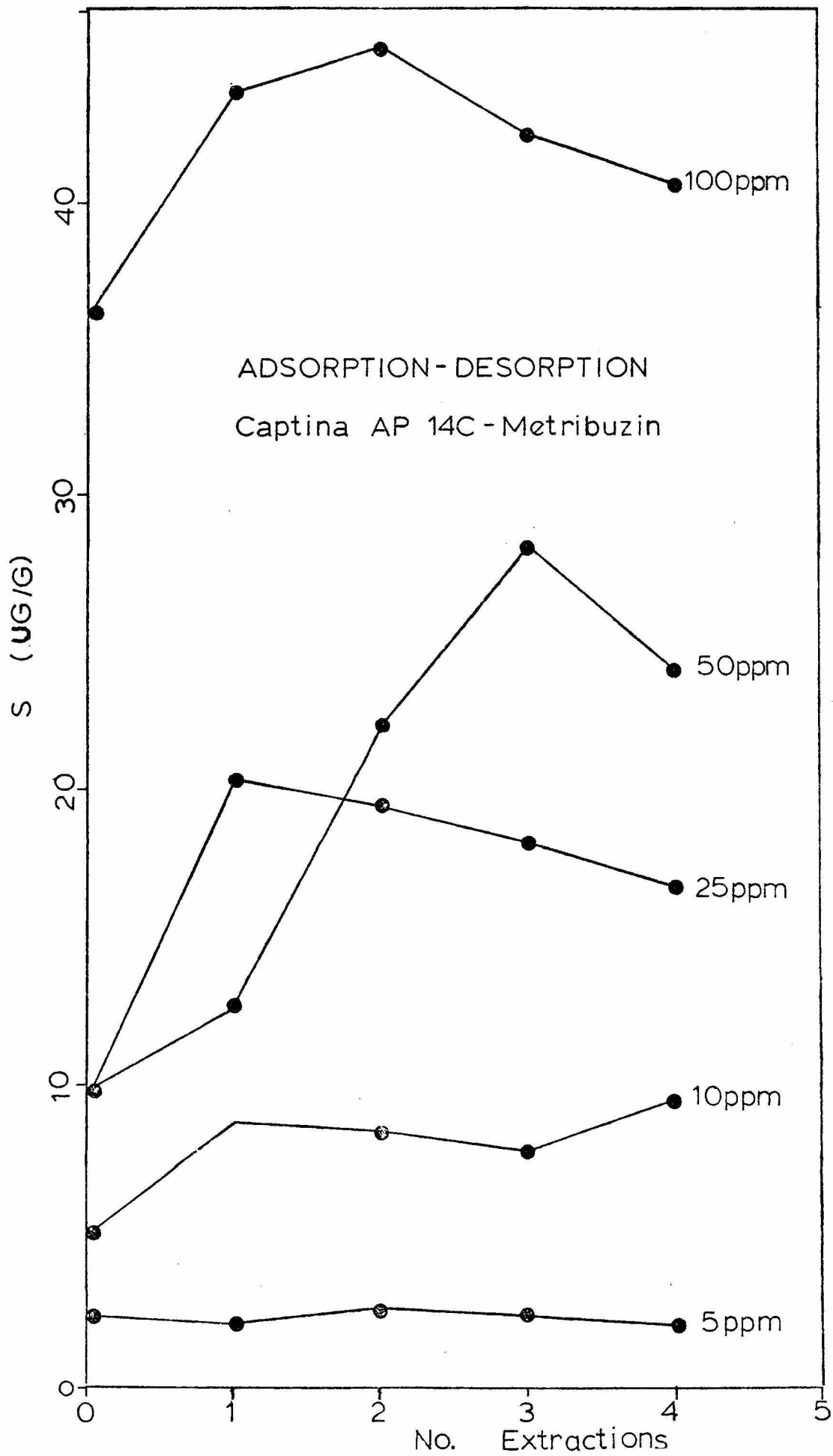


Figure 26. Relation between amount of metribuzin adsorbed and number of extractions for Captina Ap.

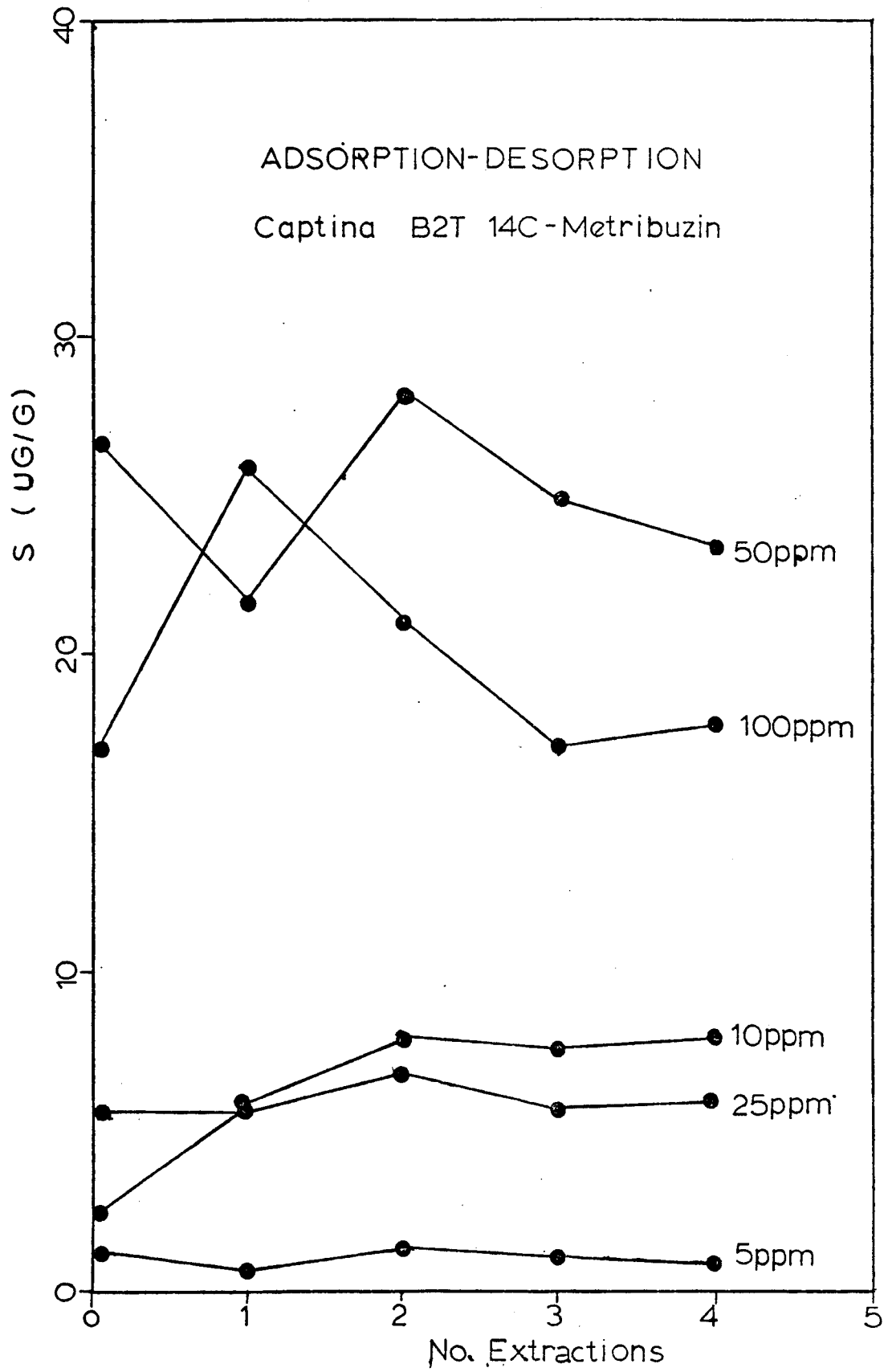


Figure 27. Relation between amount of metribuzin adsorbed and number of extractions for Captina B2t.

The initial experiments concerned the self-diffusion of ^3HOH in several soils, three of which are common in the Mississippi Delta. The physical and chemical properties of the three Delta soils are given in Table 15 and the relation between the self-diffusion coefficients of ^3HOH and volumetric soil water contents is shown in Figure 28. The resulting curves are similar in shape for each soil; however, the diffusion coefficients differ among water contents for the various soils. Each curve shows a rapid decrease in the self-diffusion coefficient as the water content decreases from near saturation to approximately 27 to 39 percent. At some water content for each soil, the diffusion coefficient begins to increase as the water content is further reduced. This increase continues until a water content of about 5 to 10 percent is reached. These curves are similar to those found by Quisenberry (1970) who studied the self-diffusion coefficients of ^3HOH in seven Kentucky soils. The three most important factors influencing the diffusion of a water molecule in a soil water system with water contents in the range of plant growth are (1) pathlength of the diffusing molecules, (2) the attraction of the soil surfaces for the polar water molecule, and (3) the viscosity of the soil water. Thus, the decrease in magnitude of the diffusivity from saturation to a minimum value probably can be attributed to an increase in tortuosity. The concurrent increase in diffusivity beyond this point is due to significant contributions from diffusion of ^3HOH in the vapor phase. Hartley (1964) pointed out that diffusion can be as much as 10,000 times faster in the vapor phase than in the liquid phase. Although no values were determined, it would be expected that the diffusivity would be at a maximum between 5 and 10 percent water content. Then the curves would decrease

Table 15. Physical and chemical properties of Ap horizon of three soils used in the laboratory studies.

Soil Property	Soil Series		
	Sharkey	Beulah	Dubbs
Texture, %			
Sand	3.1	90.4	32.2
Silt	48.7	5.3	58.5
Clay	48.2	4.3	9.2
Textural Class	sic	fs	sil
Water Retention, wt. %			
0.1 atm	36.3	5.7	31.2
0.3 atm	33.9	3.1	15.0
0.8 atm	28.9	2.8	9.0
1.0 atm	25.2	2.7	8.1
pH	6.3	5.3	6.8
CEC (meq/100 g)	37.2	3.3	10.1
% Base Saturation	69.0	36.0	71.0
% Carbon	2.11	0.57	1.03
E. G. Retention (mg/g)	96.0	9.6	21.0

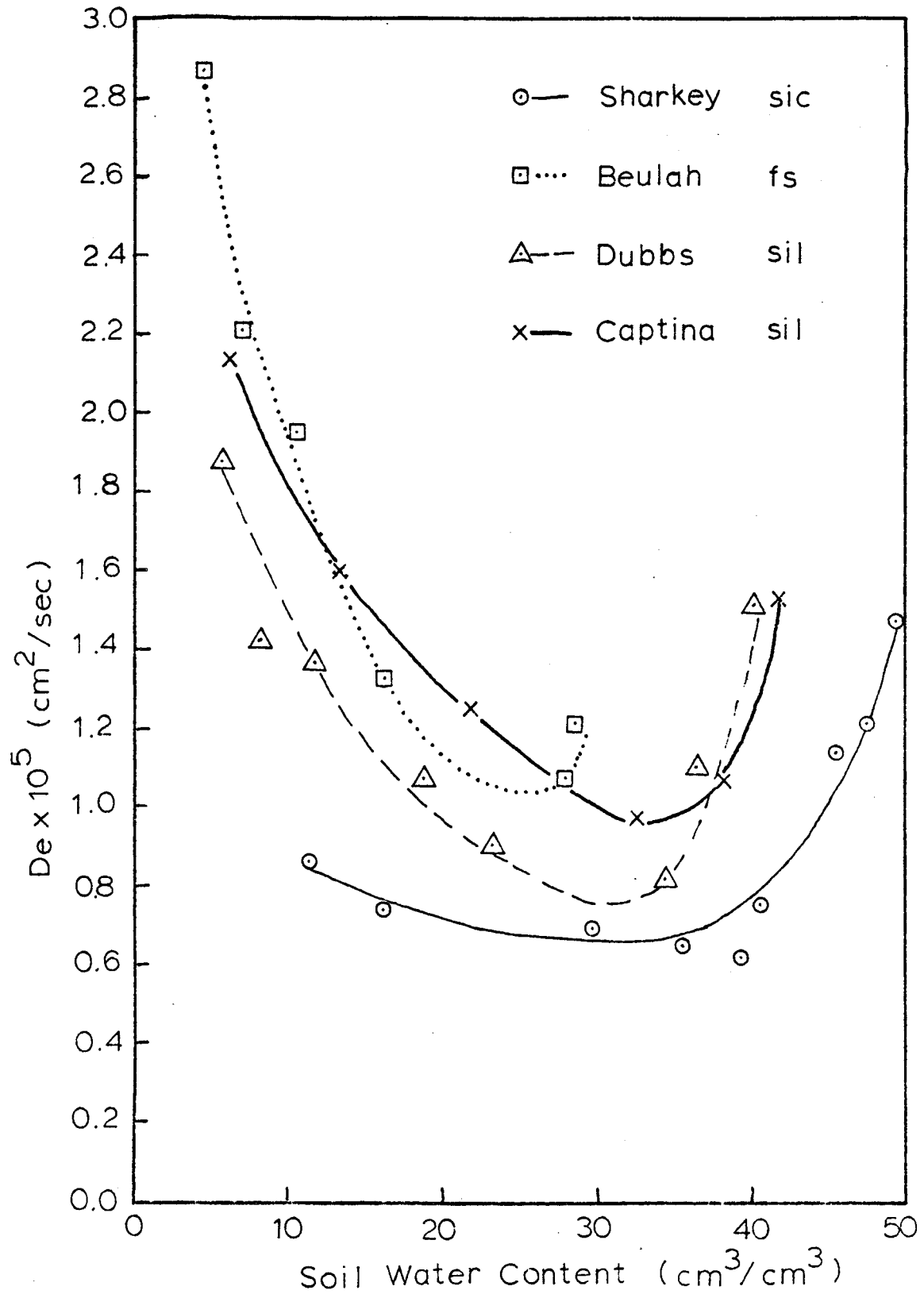


Figure 28. Relation between self-diffusion of ^3HOH and soil water contents of selected soils.

again with a further decrease in soil water content.

At a given water content the magnitude of the diffusivity of ^3HOH was generally highest in the most coarsely textured soil, intermediate in the silt loams, and lowest in the silty clay soil. Contributions from vapor phase movement were observed at a higher water content in the Sharkey silty clay than in the Dubbs (silt loam), Captina (silt loam), or Beulah (fine sand). This finding is misleading, however, because the tensions on the soil water were lower in the Beulah when vapor movement became significant. Soils of relatively low clay content such as the Beulah have a greater number of large and continuous pores at water contents and tensions just below saturation.

Self-diffusion coefficients were determined as functions of moisture content and temperature for ^3HOH , Cl^- and metribuzin in the Captina and Dubbs soils. The results for the Ap and B2t horizons of the Captina soil and for the Ap horizon of the Dubbs soil at 23°C are given in Figures 29, 30, and 31, respectively. Each data point represents the average of at least four determinations. At a given soil water content, the diffusion coefficients of ^3HOH have the highest values, those of Cl^- have intermediate values, and those of metribuzin have the lowest values. This pattern is to be expected because the self-diffusion coefficients of ^3HOH , Cl^- and metribuzin in aqueous solution are 2.44×10^{-5} (Wang et al., 1953), 1.85×10^{-5} (Porter et al., 1960), and $0.94 \times 10^{-5} \text{ cm}^2/\text{sec}$ (Brown, 1974), respectively. However, at low moisture contents the tortuosity of the soil dominates all factors affecting diffusion, and the self-diffusion coefficients exhibit values of similar magnitude, i.e. self-diffusion coefficients go to zero as the soil moisture content approaches zero. Tritiated water exhibited

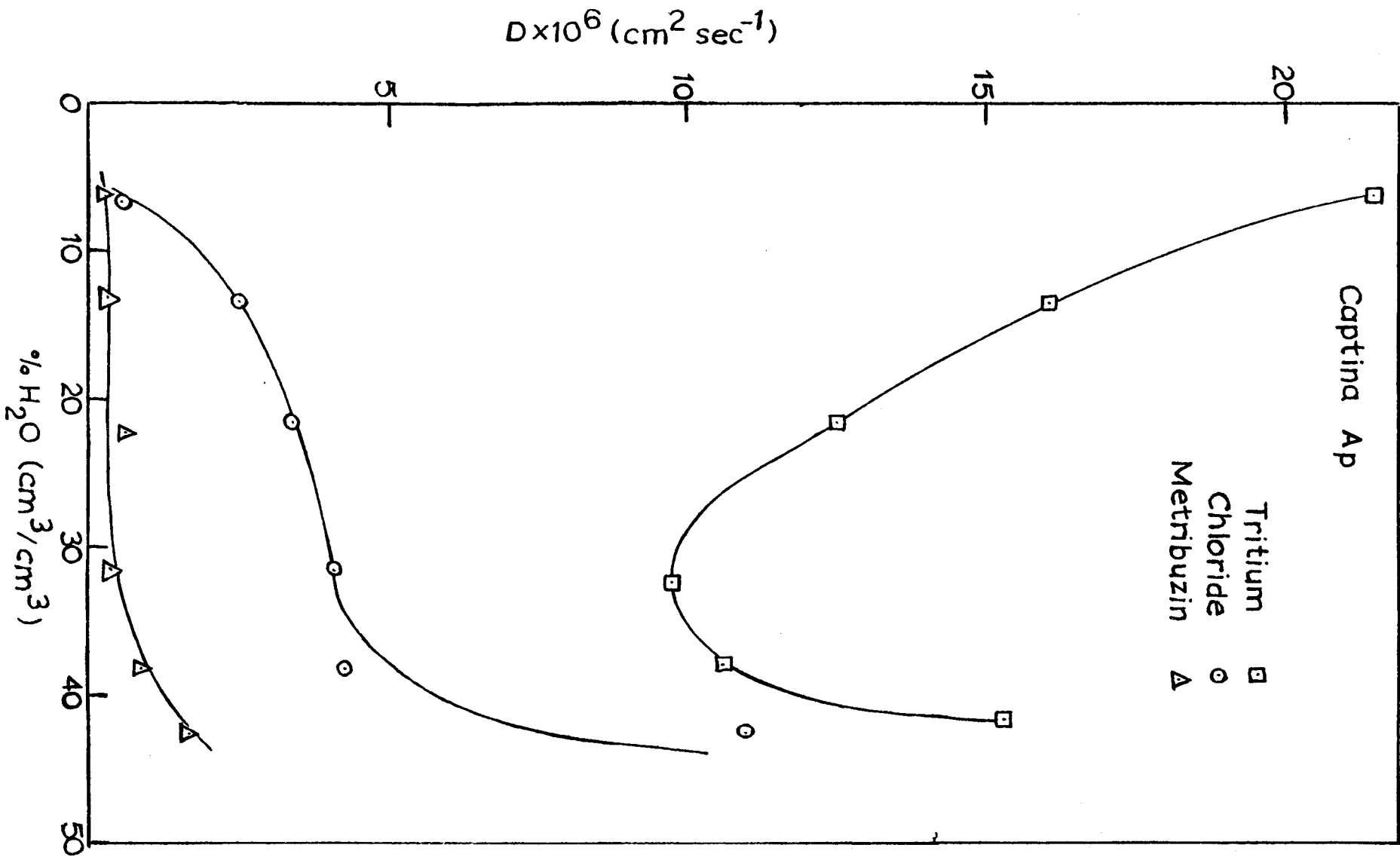


Figure 29. Relation between self-diffusion coefficients of ^3HOH , ^{36}Cl , and ^{14}C -metribuzin and soil water content of the Ap horizon of Captina soil.

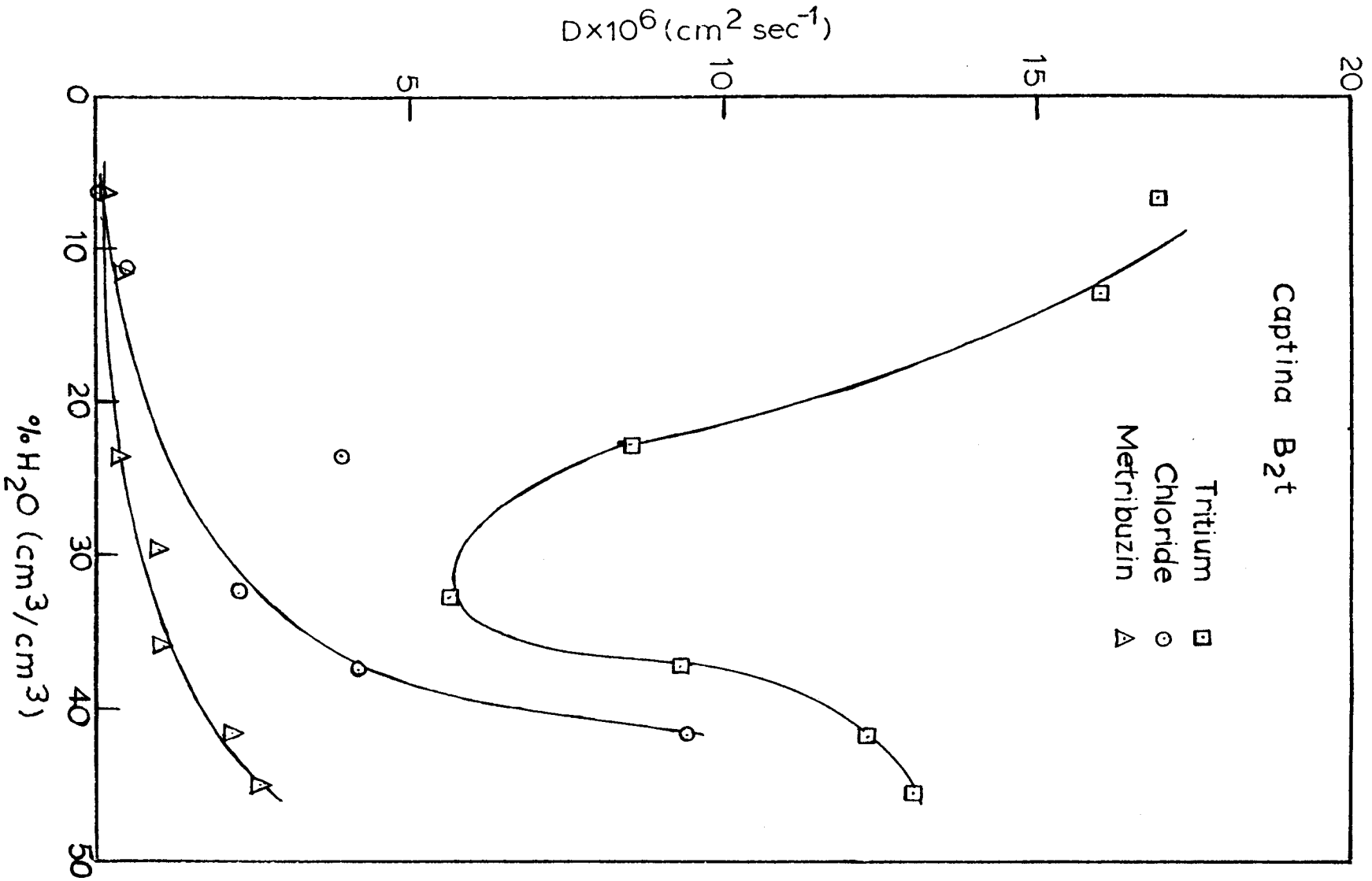


Figure 30. Relation between self-diffusion coefficient of ^3HOH , ^{36}Cl , and ^{14}C -metribuzin and soil water content of B2t horizon of Captina soil.

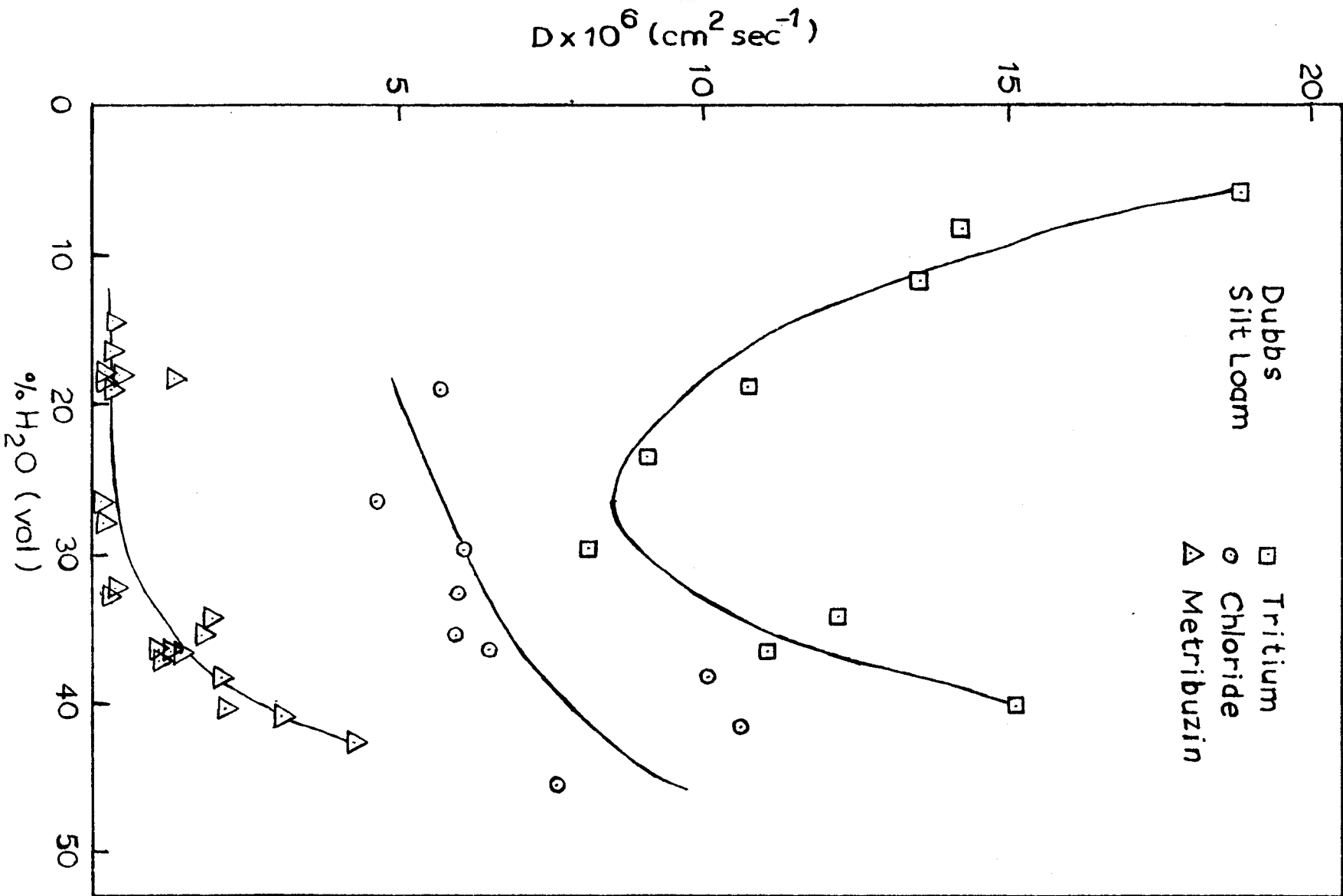


Figure 31. Relation between self-diffusion coefficient of ³H₂O, ³⁶Cl, and ¹⁴C-metribuzin and soil water content of Ap horizon of Dubbs soil.

diffusion in both vapor and liquid phases. The shapes of the self-diffusion curves indicate that little if any diffusion of Cl^- or metribuzin occurs in the vapor phase.

In the Captina soil, the diffusion coefficients of ^3HOH and Cl^- for any given moisture content are higher in the Ap than in the B2t horizon. This difference can be attributed to the lower tortuosity in the Ap horizon resulting from its coarser texture. A lower tortuosity implies that the actual path length a molecule must travel to move between two points in the soil is closer to the linear distance between the two points. A shorter actual distance traversed by a molecule results in a higher apparent self-diffusion coefficient. The self-diffusion coefficients of metribuzin are similar in the two horizons. Although the Ap horizon has a lower tortuosity, adsorption experiments have shown metribuzin to be adsorbed in the Ap horizon at approximately double the rate in the B2t horizon. Adsorption slows the overall diffusion rate resulting in lower self-diffusion coefficients. Apparently in these two horizons, the effects of tortuosity and adsorption are of the same magnitude. This would be expected of pesticides having low values of distribution coefficients (K_d), i.e., pesticides in which the distribution between phases is such that the concentration is higher in the solution than in the adsorbed phase. The self-diffusion curves for the Dubbs and Captina Ap horizons are similar. Variations can be attributed largely to differences in pore size distributions between the soils.

Self-diffusion coefficients also were determined at three temperatures for the Ap horizon of the Captina soil to evaluate thermodynamic constants for the materials. From the Arrhenius equation (equation [27]),

it follows that a plot of the natural logarithms of the self-diffusion coefficients (cm^2/sec) versus the reciprocal of the absolute temperature ($^{\circ}\text{K}$) will yield the activation energy values for diffusion from the slope and frequency factors from the intercept.

$$D = S e^{-\Delta H_a/RT} \quad [27]$$

where D is the self-diffusion coefficient (cm^2/sec) at the temperature T ($^{\circ}\text{K}$), S is the frequency factor (cm^2/sec), R is the gas constant (1.987 cal/mole deg.) and ΔH_a is the activation energy (cal/mole). Figure 32 gives this information for ^3HOH , ^{36}Cl , and ^{14}C -metribuzin. Values of activation energy and frequency factors are shown in Table 16. Figure 33 shows the activation energy values as functions of soil moisture content. As soil moisture content decreases, more energy is required for diffusion. A decrease in soil moisture also results in an increase in tortuosity and the molecules require more energy to travel over this increased path length. In the case of tritium, with diffusion occurring primarily in the vapor phase at low moisture contents, energy is required for evaporation also. Because activation energy values are generally higher for metribuzin than for tritium or chloride, additional energy must be supplied to counter the effects of adsorption. Chloride appears to require the least energy for diffusion. Because chloride is negatively charged, repulsion from negatively charged clay particles may supply some of the energy required for diffusion.

Dispersion

The dispersion coefficient, D , is a combination of the self-diffusion coefficient, D_e , and the hydrodynamic dispersion coefficient, D_2 .

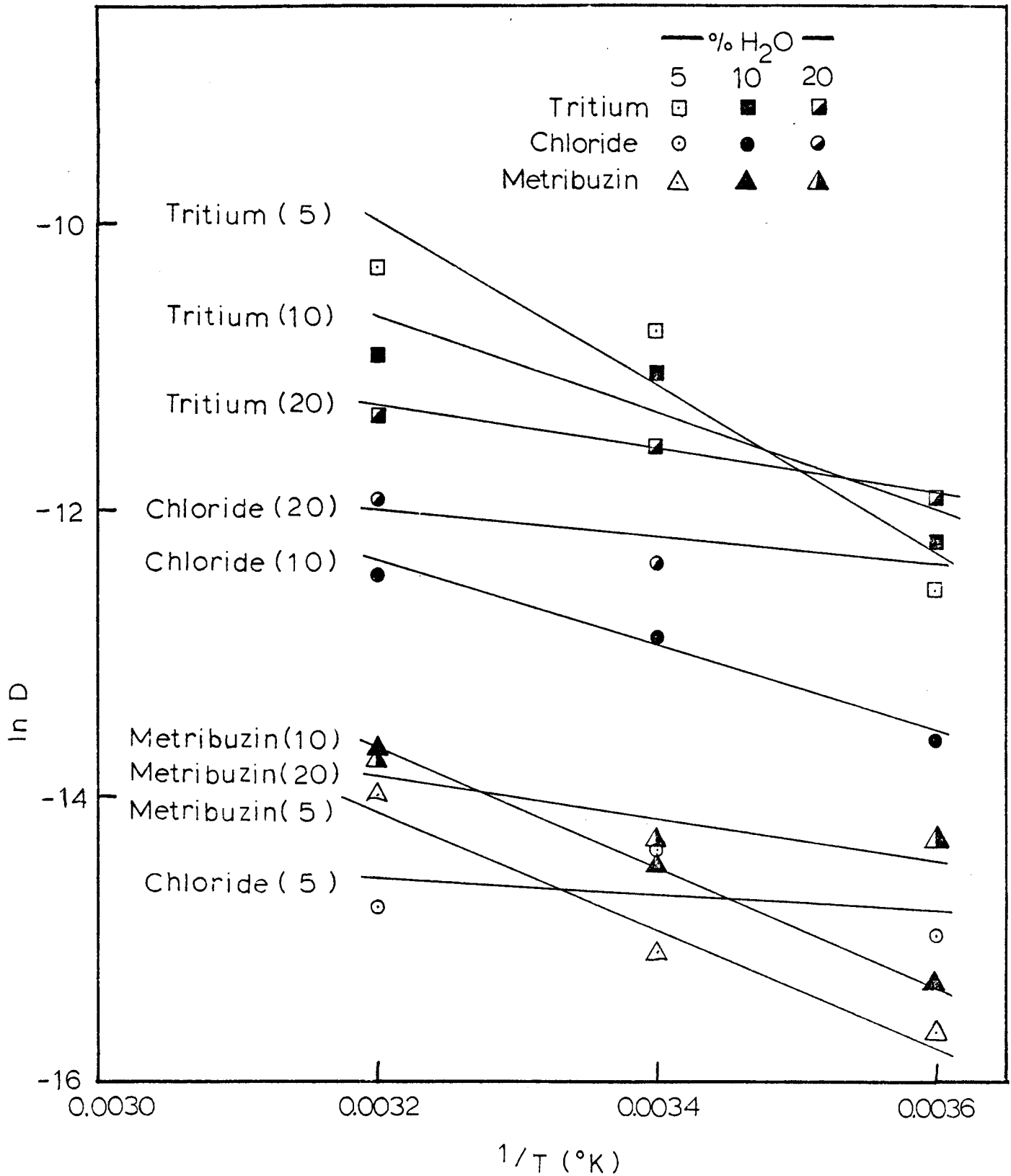


Figure 32. Arrhenius plot of diffusivity versus $1/T$.

Table 16. Thermodynamic constants for self-diffusion in Captina silt loam.

Isotope	% H ₂ O	Temperature (°C)	D x 10 ⁶ (cm ² /sec)	Δ H _a (cal/mole)	S (cm ² sec ⁻¹)
¹⁴ C - metribuzin	5	5	0.158	9357.9	3.1978
		23	0.277		
		35	0.850		
	10	5	0.219	8714.6	1.5842
		23	0.517		
		35	1.167		
	20	5	0.621	3658.2	4.0465 x 10 ⁻⁴
		23	0.613		
		35	1.111		
Tritium	5	5	3.443	10527.0	972.0331
		23	21.514		
		35	33.485		
	10	5	4.929	5791.9	0.2384
		23	16.070		
		35	18.218		
	20	5	6.654	2884.5	1.2941 x 10 ⁻³
		23	9.772		
		35	11.950		
Chloride - 36	5	5	0.308	81.1	4.8081 x 10 ⁻⁷
		23	0.567		
		35	0.379		
	10	5	1.209	5868.9	0.05423
		23	2.564		
		35	3.942		
	20	5	4.843	2288.5	2.6382 x 10 ⁻⁴
		23	4.198		
		35	6.674		

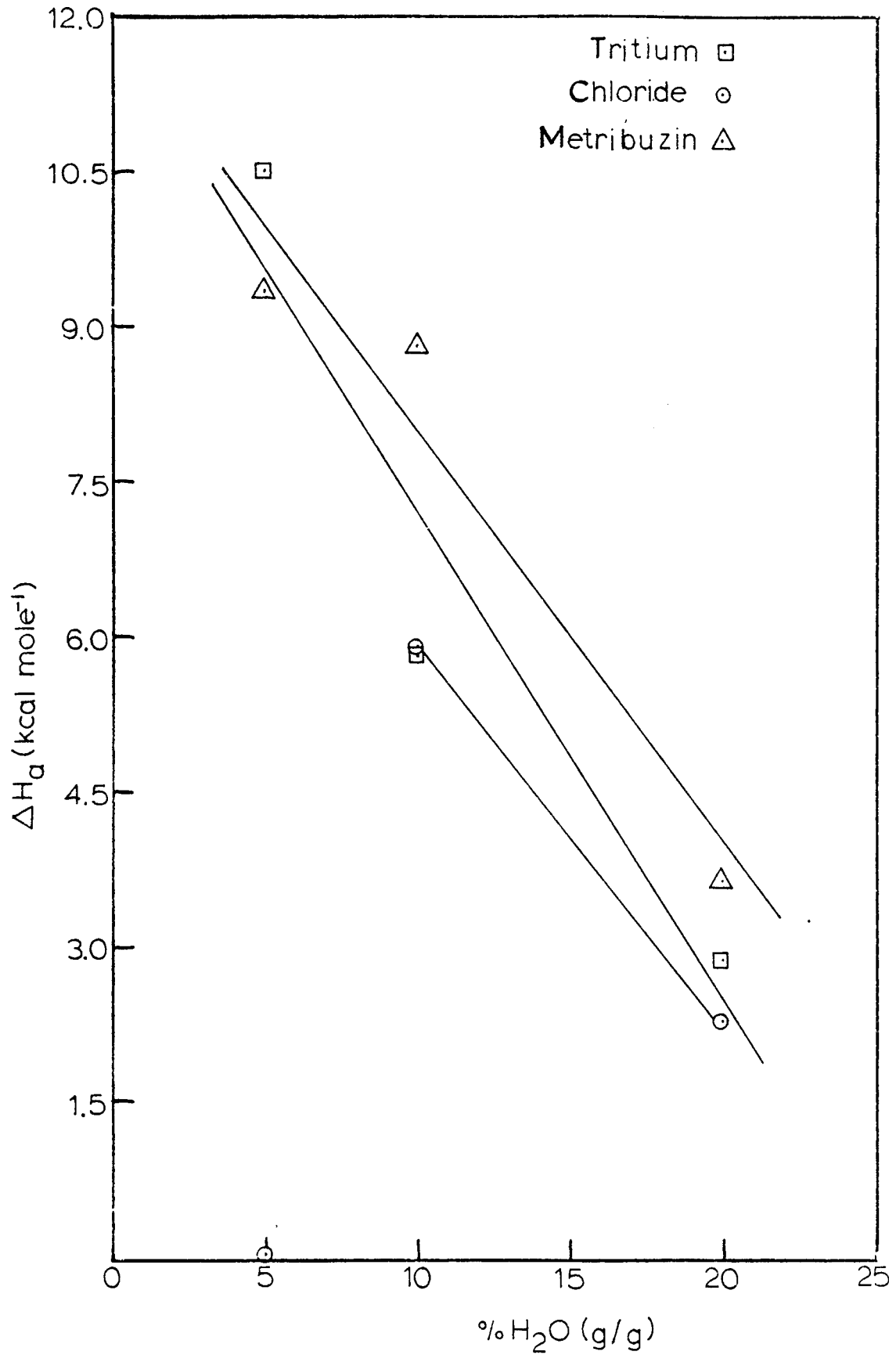


Figure 33. Activation energy values of radioactive isotopes as a function of soil water content.

The factors influencing self-diffusion have been discussed. Hydrodynamic dispersion depends primarily on the average pore velocity of the soil water. Separation of these coefficients will lead to a better understanding of solute movement processes in soils.

Most experiments designed to evaluate these coefficients have used miscible displacement techniques and/or steady-state conditions. The method reported herein permits the determination of dispersion at low soil moisture contents and under transient state conditions.

Experiments were performed with the Ap horizon of the Dubbs soil and the Ap and B2t horizons of the Captina soil. Representative breakthrough curves are given in Figures 34, 35, and 36. A 5 percent by weight moisture content difference initially was imposed on the soil and the half-cells were allowed to remain in contact for time periods ranging from 1 1/2 to 2 1/2 hours. Metribuzin was added to the half cell with the higher moisture content to determine its rate of flow with the soil water. In other instances, metribuzin was added to the low moisture side to determine whether it could move against the moisture gradient. Qualitatively, the curves show that metribuzin moves at a slower rate than the soil water; however, small quantities were able to move a significant distance against the soil moisture flow. The curves also indicate that the interface between the half cells offered little, if any, impedance to flow.

Dispersion coefficients ($\times 10^6$) calculated from the curves shown in Figures 34, 35, and 36 are 16.2, 22.9, and 34.1 for tritiated water and 3.52, 2.35, and 0.02 for metribuzin, respectively. The dispersion coefficients of tritiated water in soil with a 5 percent gradient range from 1.5 to 2.5 times as large as self-diffusion coefficients at similar

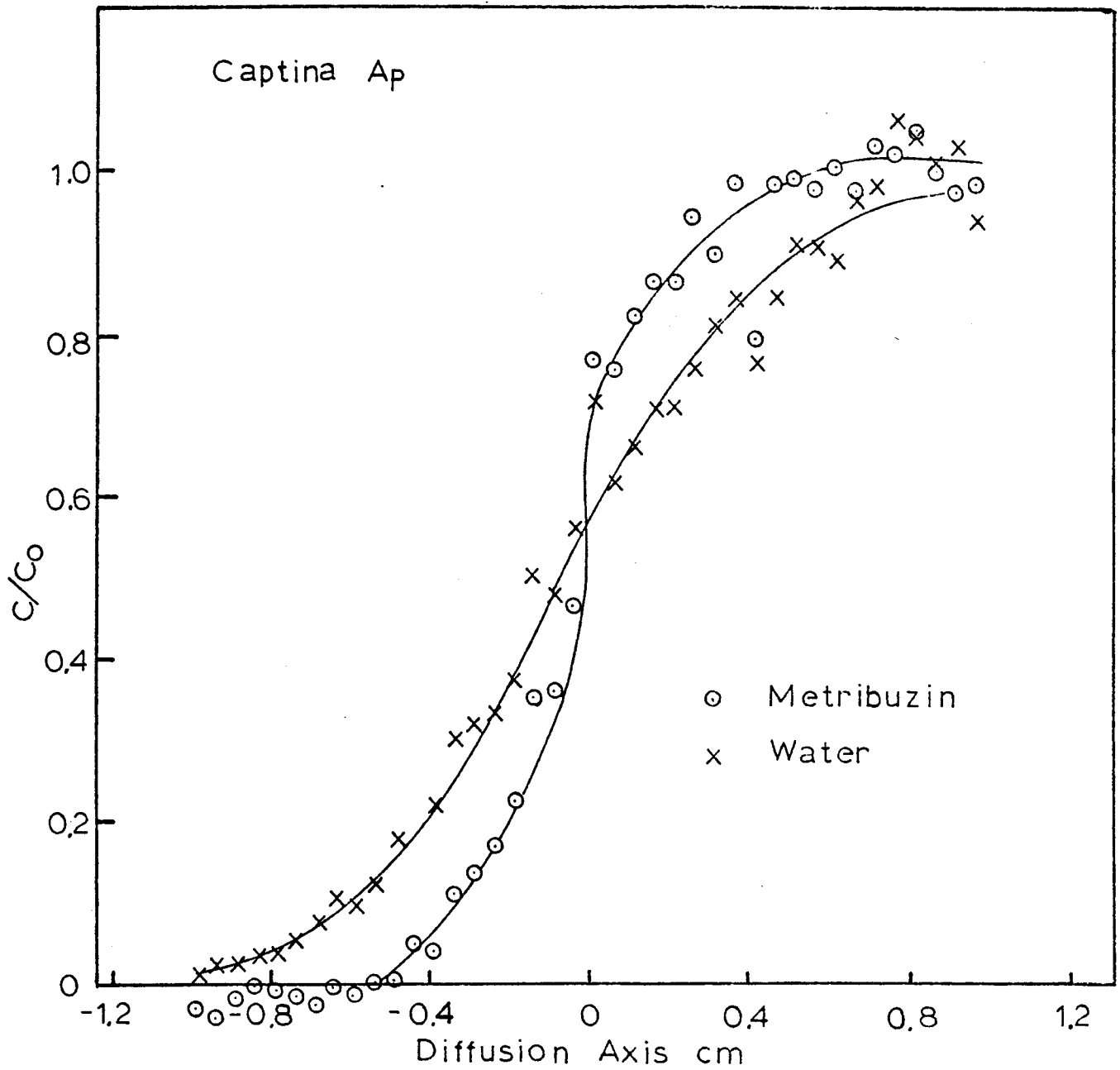


Figure 34. Dispersion break-through curve for metribuzin and water in Captina Ap. Moisture contents of half cells equal 20 and 25 percent. Two hour diffusion time.

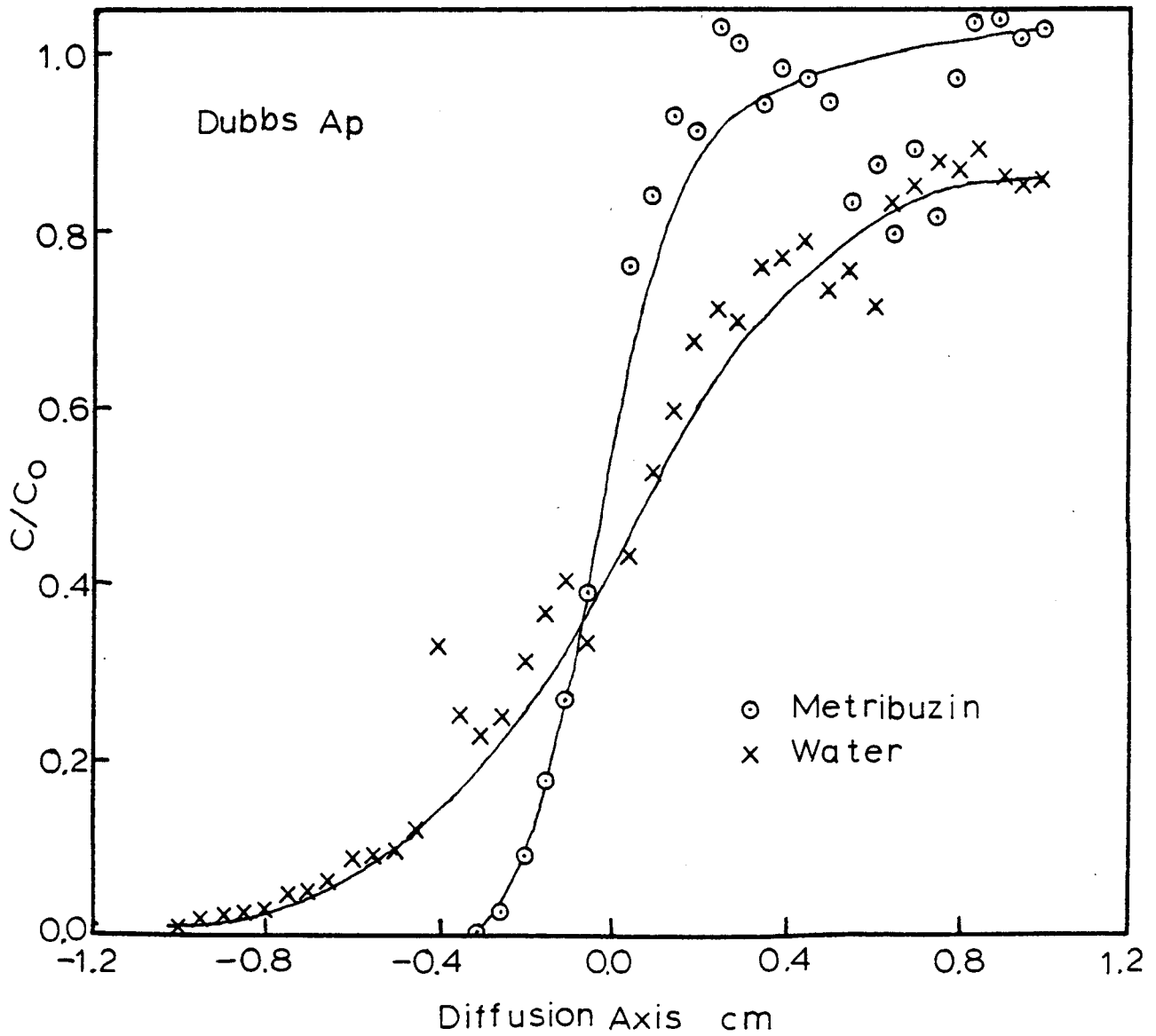


Figure 35. Dispersion break-through curve for metribuzin and water in Dubbs Ap. Moisture contents of half cells equal 15 and 20 percent. One and one half hour diffusion time.

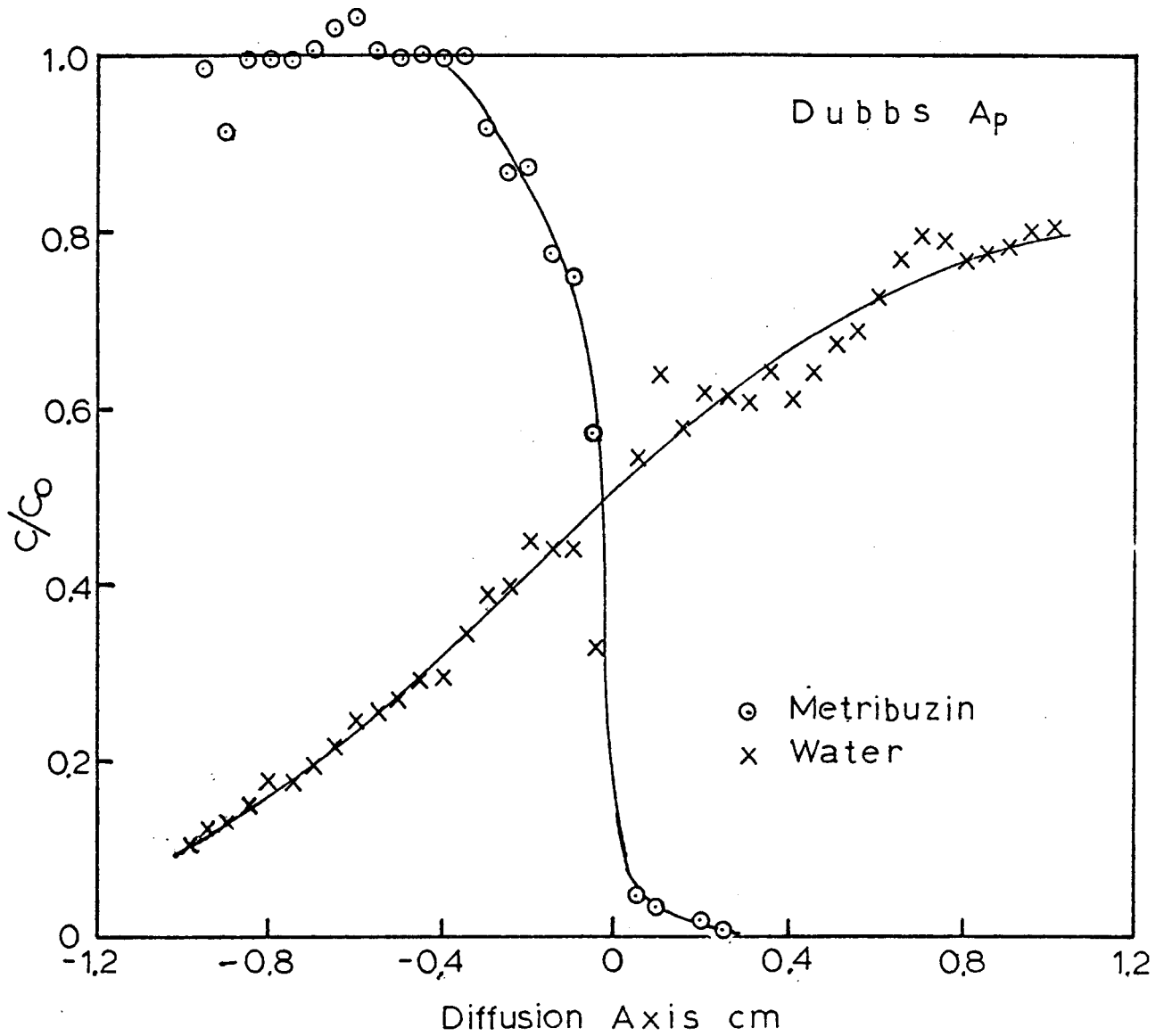


Figure 36. Dispersion break-through curve for metribuzin and water in Dubbs Ap. Moisture contents of half cells equal 15 and 20 percent. Metribuzin added to low moisture side. Two and one half hour diffusion time.

moisture contents. The dispersion coefficient of metribuzin ranges from 4 to 7 times as large as its corresponding self-diffusion coefficient. The dispersion coefficient of metribuzin moving against the flow of water is only about 1/30 of the self-diffusion coefficient. These data imply that the dispersion coefficient is not a linear combination of the hydrodynamic dispersion coefficient and the self-diffusion coefficient. When $D_2=0$ (no water flow), $D = D_e$ implying

$$D = mD_2 + D_e \quad [28]$$

if D is a linear combination of D_2 and D_e . With use of the data from the Dubbs soil, we find mD_2 for metribuzin transport with the water flow to be approximately 3 times mD_2 for its transport against the water flow. Obviously, diffusion is the major transport mechanism in small pores where water movement is much less than the average pore velocity. An acceptable model for D should incorporate a water velocity distribution as a function of the pore size distribution for a particular soil. D_2 and D_e could then be expressed as functions of the water velocity distribution.

With use of measured self-diffusion values, this procedure offers a method for determining the relative contributions of hydrodynamic dispersion and diffusion to the movement of solutes in soil-water systems. It is a new method and much work remains before it is perfected. Attention should be given primarily to the quantitative information which can be obtained from this method. Computer programs written by Fuqua et al. (1973) for calculation of counter diffusion coefficients were used to evaluate dispersion but, because of the nature of these

experiments, certain modifications of the programs will be necessary to obtain correct values. The method offers considerable promise as an aid in understanding soil-water solute transport systems.

Appendix Table 1. Water retention data for
three depths of Captina soil.

	Soil Water Content (cm^3/cm^3)						
	Soil Water Tension (bars)						
	1/3	1/2	1.0	3.0	5.0	10.0	15.0
22-30	21.97	14.39	13.95	8.12	7.89	7.36	5.43
61-91	24.15	19.53	18.95	14.01	12.93	12.18	11.11
91-122	24.52	19.71	18.54	14.45	14.31	13.73	12.03

Appendix Table 2. Self-diffusion of ^3HOH in selected soils.

Soil	θ_{wt} %	θ_{vol} %	Diffusion Coefficient $D_e \times 10^5 \text{ cm}^2/\text{sec}$
Sharkey (CT02)	8.99	11.55	0.867
	10.80	14.17	0.656
	12.34	16.16	0.746
	16.22	22.24	0.656
	20.70	29.76	0.692
	25.11	35.57	0.644
	39.31	29.73	0.622
	31.62	40.64	0.758
	38.84	45.53	1.146
	41.90	47.50	1.210
	46.28	49.58	1.474
Beulah	3.40	4.74	2.871
	4.79	6.97	2.216
	7.54	10.79	1.959
	11.46	16.31	1.323
	19.45	28.11	1.077
	20.69	28.80	1.213
Dubbs	4.43	5.90	1.888
	6.11	8.17	1.425
	8.60	11.72	1.362
	13.91	18.98	1.072
	16.16	23.33	0.903
	20.14	29.56	0.812
	22.82	34.01	1.221
	25.48	36.49	1.106
30.23	40.06	1.518	
Captina (Ap)	5	6.09	2.152
	10	13.38	1.607
	15	21.68	1.257
	20	32.47	0.977
	25	38.07	1.066
	30	41.72	1.531
Captina (B2t0)	5	6.46	1.687
	10	12.68	1.599
	15	22.83	0.859
	20	32.74	0.558
	25	37.38	0.929
	30	41.90	1.229
	35	45.53	1.306
40	48.72	1.148	

Literature Cited

1. Bailey, G.W., and J.L. White. 1970. Factors influencing the adsorption, desorption, and movement of pesticide in soil. *Residue Rev.* 32:29-92.
2. Boast, C.W. 1973. Modeling the movement of chemicals in soils by water. *Soil. Sci.* 115:224-230.
3. Bresler, E. 1973. Simultaneous transport of solutes and water under transient unsaturated flow conditions. *Water Resour. Res.* 9:975-986.
4. Brown, D.A. 1974. A capillary tube diffusion cell for measuring ion diffusion in aqueous solutions. *Soil Sci. Soc. Amer. Proc.* 38:533-535.
5. Carslaw, H.S., and J.C. Jaeger. 1959. Conduction of Heat in Solids. 2nd ed. Oxford University Press, Oxford, England.
6. Childs, E.C., and N. Collis-George. 1950. The permeability of porous materials. *Proc. Roy. Soc.* 201:392-405.
7. Crank, J. 1956. The Mathematics of Diffusion. Oxford University Press, Oxford, England.
8. de Boer, J.H. 1968. The Dynamical Character of Adsorption. 2nd ed. Oxford University Press, Oxford, England.
9. Fuqua, B.D., R.J. Dunn, and D.A. Brown. 1973. Computer procedure for calculating counter-diffusion coefficients. *Soil Sci. Soc. Amer. Proc.* 37:548-552.
10. Green, R.E. 1974. Pesticide - clay - water interactions. In Pesticides in Soil and Water. *Soil Sci. Soc. Amer.*, p. 3-37.
11. Green, R.E. and J.C. Corey. 1971. Calculation of hydraulic conductivity: A further evaluation of some predictive methods. *Soil Sci. Soc. Amer. Proc.* 35:3-8.
12. Hamaker, J.W. and J.M. Thompson. 1972. Adsorption. In Organic Chemicals in the Soil Environment. Marcel Dekker, Inc., New York, 1:49-149.
13. Hartley, G.S. 1964. Herbicide behavior in soil. In L.J. Audus, The Physiology and Biochemistry of Herbicides. Academic Press, New York, p. 111-161.
14. Hyzak, D.L., and R.L. Zeimdahl. 1974. The residual activity of metribuzin in soil. *Weed Res.* 14:289-291.

15. Kirkham, C., and W.L. Powers. 1972. Advanced Soil Physics. John Wiley and Sons, Inc., New York, p. 534.
16. Klute, A. 1965. Laboratory Measurement of Hydraulic Conductivity of Unsaturated Soil. In C.A. Black, ed. Methods of Soil Analysis. No. 9 Monograph Series, Amer. Soc. Agron., p. 253-261.
17. Klute, A. 1972. The determination of the hydraulic conductivity and diffusivity of unsaturated soils. *Soil Sci.* 113:264-276.
18. Lay, M.M., and R.D. Ilnicki. 1974. The residual activity of metribuzin in soil. *Weed Res.* 14:289-291.
19. Leistra, Minze. 1973. Computation models for the transport of pesticides in soil. *Residue Rev.* 49:87-130.
20. Lindstrom, F.T., and L. Boersma. 1970. Theory of chemical transport with simultaneous sorption in a water saturated porous medium. *Soil Sci.* 110:1.
21. Lindstrom, F.T., L. Boersma, and D. Stockard. 1971. A theory on the mass transport of previously distributed chemicals in a water saturated sorbing porous medium: isothermal cases. *Soil Sci.* 112:291-300.
22. Luxmoore, R.J. 1973. Application of the Green and Corey method for computing hydraulic conductivity in hydrologic modeling.
23. Marshall, T.J. 1958. A relation between permeability and size distribution of pores. *J. Soil Sci.* 9:1-8.
24. Nielsen, D.R., J.W. Biggar, and K.T. Erk. 1973. Spatial variability of field-measured soil-water properties. *Hilgardia* 42:215-260.
25. Nielsen, D.R., J.M. Davidson, J.W. Biggar, and R.J. Miller. 1964. Water movement through panoche clay loam soil. *Hilgardia* 35: 491-506.
26. Ogata, Gen, and L.A. Richards. 1957. Water content changes following irrigation of bare field soil that is protected from evaporation. *Soil Sci. Soc. Amer. Proc.* 21:355-356.
27. Olsen, S.R., and W.D. Kemper. 1968. Movement of nutrients to roots. *Adv. in Agron.* 20:91-151.
28. Philip, J.R. 1958. Physics of water movement in porous solids. *Natl. Acad. Sci. Natl. Res. Council Pub.* 629, Hwy. Res. Board Special Report. 40:147-162.
29. Phillips, R.E., and D.A. Brown. 1964. Ion diffusion: II. Comparison of apparent self- and counter-diffusion coefficients. *Soil Sci. Soc. Amer. Proc.* 28:758-763.

30. Popham, I.W., and S.J. Ursic. 1968. Computer program for converting neutron probe readings to soil water equivalents. *Soil Sci.* 107:302.
31. Porter, L.K., W.D. Kemper, R.D. Jackson, and B.A. Stewart. 1960. Chloride diffusion in soils as influenced by moisture content. *Soil Sci. Soc. Amer. Proc.* 24:460-463.
32. Quisenberry, V. 1970. Capillary-diffusion and self-diffusion of liquid water in unsaturated soils. M.S. thesis. University of Kentucky, Lexington. 77 p.
33. Quisenberry, V. 1974. Soil-water percolation and displacement relative to initial water content under field and laboratory conditions. Ph.D. dissertation. University of Kentucky, Lexington. 206 p.
34. Richards, L.A. 1936. Capillary conductivity data for three soils. *Agron. J.* 28:297-300.
35. Richards, L.A., W.R. Gardner, and G. Ogata. 1956. Physical processes determining water loss from soil. *Soil Sci. Soc. Amer. Proc.* 20:310-314.
36. Rose, D.W., W.R. Stern, and J.E. Drummond. 1965. Determination of hydraulic conductivity as a function of depth and water content for soil in situ. *Aust. J. Soil Res.* 3:1-9.
37. Scott, H.D. 1975. The diffusion of herbicides in soils. Submitted to Encyclopedia of Pedology and Applied Geology.
38. Scott, H.D., R.E. Phillips, and R.F. Paetzold. 1974. Diffusion of herbicides in the adsorbed phase. *Soil Sci. Soc. Amer. Proc.* 38:558-562.
39. van Bavel, C.H.M., G.B. Stirk, and K.J. Brust. 1968. Hydraulic properties of a clay loam soil and the field measurement of water uptake by roots: I. Interpretation of water content and pressure profiles. *Soil Sci. Soc. Amer. Proc.* 32:310-317.
40. van Genuchten, M.T. and P.J. Wierenga. 1974. Simulation of one-dimensional solute transfer in porous media. *N. M. Agri. Exp. Sta. Bull.* 628., p. 1-40.
41. Wang, J.H., C.V. Robinson, and I.S. Edelman. 1953. Self-diffusion and structure of liquid water. III. Measurement of the self-diffusion of liquid water with H², H³, and O¹⁸ as tracers. *J. Am. Chem. Soc.* 75:466-470.
42. Warrick, A.W., J.W. Biggar, and D.R. Nielsen. 1971. Simultaneous solute and water transfer for an unsaturated soil. *Water Resources Res.* 7: 1216-1225.
43. Weed, S.B., and J.B. Weber. 1974. Pesticide-organic matter interactions. In *Pesticides in Soil and Water*. *Soil Sci. Soc. of Amer.*, p. 39-66.